

VRL6267

ELECTRICAL



(NASA-CR-150021) A FREQUENCY RESPONSE
METHOD FOR THE ANALYSIS AND DESIGN OF
MULTIRATE SAMPLED-DATA SYSTEMS Technical
Summary Progress Report (Auburn Univ.)
164 p

N76-79037

Unclas
07268

00/98

ENGINEERING EXPERIMENT STATION
AUBURN UNIVERSITY
AUBURN, ALABAMA

A FREQUENCY RESPONSE METHOD FOR THE ANALYSIS
AND DESIGN OF MULTIRATE SAMPLED-DATA SYSTEMS

C. L. Phillips, Project Leader

Twentieth Technical Report

October, 1971


Contract NAS8-11274

George C. Marshall Space Flight Center


National Aeronautics and Space Administration

Huntsville, Alabama

Approved by:


C. C. Carroll
Professor and Head of
Electrical Engineering

Submitted by:


C. L. Phillips
Professor of
Electrical Engineering

FOREWORD

This document is a technical summary of progress made since May, 1970, by the Auburn University Electrical Engineering Department toward fulfillment of contract NAS8-11274. This contract was granted to the Engineering Experiment Station, Auburn, Alabama, by the George C. Marshall Space Flight Center, National Aeronautics and Space Administration, Huntsville, Alabama.

A FREQUENCY RESPONSE METHOD FOR THE ANALYSIS
AND DESIGN OF MULTIRATE SAMPLED-DATA SYSTEMS

C. L. Phillips and H. E. Crisp

ABSTRACT

Single-loop, linear, multirate sampled-data systems and multiple input-multiple output, linear, multirate sampled-data systems are both considered. For the single-loop case, a Bode plot design technique based on a bilinear transformation is presented. From the Bode plot procedure, an upper bound for the choice of the multirate n is determined. A procedure for obtaining the Bode plot for the uncompensated multirate open-loop transfer function from the equivalent slow single rate transfer function is also developed.

For the multiple input-multiple output case, a known technique for continuous systems is extended to multirate sampled-data systems. An open-loop frequency response design technique is then developed. Initially, two input-two output systems are considered. The technique is then extended to the general m input- m output case.

TABLE OF CONTENTS

LIST OF TABLES	vi
LIST OF FIGURES	vii
I. INTRODUCTION	1
II. LITERATURE SURVEY	4
Frequency Response Design Technique for Multirate Digital Controllers	
Multiple Input-Multiple Output Systems	
III. A FREQUENCY RESPONSE DESIGN TECHNIQUE FOR SINGLE INPUT-SINGLE OUTPUT, MULTIRATE SAMPLED-DATA SYSTEMS	11
The Bilinear Transformation	
Bode Plot Design Technique	
Digital Computation of the Multirate System Frequency Response	
A Multirate System Identity	
IV. AN OPEN-LOOP FREQUENCY RESPONSE DESIGN TECHNIQUE FOR MULTIPLE INPUT-MULTIPLE OUTPUT SYSTEMS	41
Extension of the Method of Povejsil and Fuchs	
Development of the Open-Loop Technique for Two Channel, Continuous-Data Systems	
Extension of the Open-Loop Technique to Two Channel, Sampled-Data Systems	
V. THE OPEN-LOOP DESIGN TECHNIQUE FOR SYSTEMS WITH MORE THAN TWO INPUTS AND OUTPUTS	94
Procedure for Obtaining Open-Loop Transfer Functions	

Procedure for Obtaining Open-Loop Poles

The Design Procedure

VI. CONCLUSIONS	128
REFERENCES	132
APPENDIX A	134
APPENDIX B	137
APPENDIX C	139
APPENDIX D	142
APPENDIX E	147
APPENDIX F	150

LIST OF TABLES

IV-1. Design Test for Decoupling	59
IV-2. Design Test for Decoupling	89

LIST OF FIGURES

III-1.	Basic multirate sampled-data system	12
III-2.	Transformation of the region of stability from the z_n -plane to the w_n -plane	15
III-3.	Multirate system with zero-order hold inserted after the error sampler	21
III-4.	$\log_{10} \tan(\theta)$ vs. θ template	25
III-5.	Illustration of graphical technique for determining multirate frequency response	26
III-6.	Gain and phase characteristics for $G(w)$, $0 \leq w_3 \leq j\infty$. . .	28
III-7.	Multirate input to a continuous plant	35
III-8.	Multirate system with quantization disturbance at digital controller output accumulator	37
III-9.	System of Figure III-8 rearranged ($r(t) = 0$)	38
IV-1.	Three input-three output, multirate sampled-data system . .	42
IV-2.	Two input-two output, continuous-data system	49
IV-3.	Signal flow graph for Figure IV-2	50
IV-4.	Figure IV-3 opened after E_1 node	51
IV-5.	Figure IV-3 opened after E_2 node	53
IV-6.	Figure IV-3 opened after X_1 node in G_{21} branch	55
IV-7.	Uncompensated Nyquist diagram	57
IV-8.	Nichols chart determination of $D_2 G_{22} / (1 + D_2 G_{22})$	60
IV-9.	Compensated Nyquist diagram	62
IV-10.	System time-response for $r_1(t) = u(t)$, $r_2(t) = 0$	63

IV-11.	Two channel, cross-coupled, sampled-data system	65
IV-12.	Single rate system opened at $E_1(z)$	66
IV-13.	Single rate system opened after cross-coupling transfer function block	68
IV-14.	Two input-two output, multirate system opened at $E_1(z)$. . .	72
IV-15.	Uncompensated Nyquist diagram for $-E'_1(w_2)/E_1(w_2)$	78
IV-16.	Uncompensated Nyquist diagram for $-E'_2(w_4)/E_2(w_4)$	80
IV-17.	Uncompensated system time-response, $r_1(t) = u(t)$, $r_2(t) = 0$	81
IV-18.	Db magnitude vs. $\log_{10}(w_2)$	83
IV-19.	Phase angle vs. $\log_{10}(w_2)$	84
IV-20.	Nichols chart determination of $D_1(w_2)G_{11}(w_2)/(2$ $+ D_1(w_2)G_{11}(w_2)$	85
IV-21.	Compensated Nyquist diagram for $-E'_1(w_2)/E_1(w_2)$	90
IV-22.	Compensated Nyquist diagram for $-E'_2(w_4)/E_2(w_4)$	91
IV-23.	Compensated system response, $r_1(t) = u(t)$, $r_2(t) = 0$	92
IV-24.	Compensated system response, $r_2(t) = u(t)$, $r_1(t) = 0$	93
V-1.	Multirate sampled-data system with n-inputs and n-outputs .	96
V-2.	Nyquist diagram to determine right half plane poles	109
V-3.	Uncompensated Nyquist diagram for $-E'_1(w_2)/E_1(w_2)$	112
V-4.	Uncompensated Nyquist diagram for $-E'_2(w_4)/E_2(w_2)$	113
V-5.	Uncompensated Nyquist diagram for $-E'_3(w_8)/E_3(w_8)$	114
V-6.	Uncompensated system outputs for step input at $r_1(t)$	116
V-7.	Magnitude characteristics	117
V-8.	Phase angle characteristics	118

V-9.	Cross-coupling transfer function db magnitudes vs. $\log_{10}(w_2)$	119
V-10.	Cross-coupling transfer function phase angles vs. $\log_{10}(w_2)$	120
V-11.	Nichols chart determination of $(1/2)D_1(w_2)G_{11}(w_2)/(1$ $+ (1/2)D_1(w_2)G_{11}(w_2)$	122
V-12.	Compensated Nyquist diagram for $-E'_1(w_2)/E_1(w_2)$	126
V-13.	Compensated system outputs for step input at $r_1(t)$	127
F-1.	Signal flow graph for three input-three output system opened at $E_1(z)$	152

I. Introduction

Analysis and design techniques for single input-single output, single rate sampled-data systems are well defined [1]. These techniques are based either on a z-transform representation of the system or a difference equation representation and range from the root-locus and frequency domain approaches to the optimal approach. Of these various approaches, the frequency domain technique for digital controller design has proved extremely effective for linear sampled-data systems.

It is the objective of Chapter III to present a frequency response design technique for single input-single output, multirate sampled-data systems. Such systems occur when the digital controller provides output information at a rate different from the basic system sampling rate. The design technique which is presented is applicable to linear systems for which the sampling operation is represented by an impulse modulator followed by a zero-order hold [1]. Also, the fast-rate sampling must be an integer multiple of the slow-rate sampling frequency. The technique utilizes a bilinear transformation which enables one to employ a Bode plot design procedure. Also, an upper bound for the selection of the ratio of sampling frequencies, n , is developed.

In conjunction with the development of the frequency response design technique, the digital computation of the multirate system frequency response is discussed. The infinite series form of the s-domain multirate system transfer function is developed for this purpose. Finally, a

multirate system identity is presented to assist in determining the z_n -form of the multirate system transfer function. This identity is utilized to determine the multirate system output for a quantization disturbance at the digital controller output accumulator.

The subject of multiple input-multiple output systems is considered in Chapter IV. It is the objective of this chapter to investigate primarily the case of two and three inputs and outputs. Initially, the method of Povejsil and Fuchs [11] for continuous-data systems is extended to multirate, three input-three output systems. The disadvantages of this technique are discussed. An open-loop frequency response design technique is then developed for two input-two output, continuous-data systems. This technique provides for approximately decoupling the system, as well as meeting the usual design specifications. The analytical basis for the technique which is presented is the Nyquist criterion [16]. After presenting an example to illustrate the open-loop technique, an extension is made to single-rate, and then multirate, two input-two output, sampled-data systems. A second example is presented to illustrate the open-loop frequency response technique for multirate, two input-two output, sampled-data systems.

The open-loop technique is extended in Chapter V to systems having more than two inputs and two outputs. This extension sets forth procedures for obtaining open-loop transfer functions, for determining the open-loop poles which lie outside the unit circle in the multirate z -plane, and for determining the compensation in each channel of the

general n input- n output system. These procedures are illustrated by application to a three input-three output, multirate sampled-data system.

Preliminary to Chapters III, IV, and V, Chapter II contains a literature survey. This survey covers multirate sampled-data systems and multiple input-multiple output systems.

II. LITERATURE SURVEY

It is the intent of this literature survey to discuss the important contributions to the frequency response design technique for multirate digital controllers and, also, to discuss the more important developments in the analysis and design of multiple input-multiple output systems.

A. Frequency Response Design Technique for Multirate Digital Controllers

The design of a multirate digital controller was first considered by Kranc [2]. Kranc argued the case for utilizing a multirate controller on the basis of reducing ripple error between sampling instants and improving the settling time for a step input. The improvement in ripple performance is based on the assumption of zero steady-state error being desired at the sample instants. Kranc showed that, generally, these advantages could be gained at no increase in the number of storage elements in the controller. The improvement in ripple performance was shown to hold for inputs whose Laplace transforms are of the type $1/s^k$.

Kranc's work was based on a single loop linear system with a digital controller having a slow-rate input and a fast-rate output. The desired digital controller transfer function was determined according to

$$D(z_n) = \frac{1}{G(z_n)} \cdot \frac{K(z_n)}{1 - K(z_n)} \quad , \quad (\text{II-1})$$

where $G(z_n)$ is the plant transfer function, $K(z_n)$ is the system transfer function from input to output, and z_n is $e^{sT/n}$. Kranc developed a table of "minimum settling time prototypes" which assured a zero steady-state error for inputs of the type $1/s^k$. The disadvantage of Kranc's technique is that for inputs other than the design input, the system performance is generally unsatisfactory [6].

Shortly after this first article, Kranc introduced his switch decomposition technique for input-output analysis of multirate sampled-data systems. This technique replaces each switch in the system which operates at an integer multiple of the basic system sampling frequency by a set of switches operating at the basic system sampling frequency, each switch having advance and delay elements. The disadvantage of this technique is that it is extremely unwieldy for complex systems.

Kalman and Bertram introduced a state space approach to the theory of sampled-data systems [4]. Their approach provides a means for analyzing nonconventional as well as conventional sampled-data systems. This is done by obtaining a discrete state transition matrix for the entire system. The disadvantage of this method for multirate sampled-data systems is that the discrete state variable description of multirate systems is extremely complex.

A possible frequency domain design technique for multirate digital controllers was first proposed by Phillips and Johnson [5]. The basic

system considered by Phillips and Johnson is the single loop, linear system for which the output sampling rate of the digital controller is an integer multiple of the input sampling rate. For such a system, a z_n -form open-loop transfer function is developed. This transfer function is of the form

$$\frac{C(z_n)}{E(z_n)} = \frac{1}{n} \sum_{p=0}^{n-1} D(z_n \epsilon^{j\phi_p}) G(z_n \epsilon^{j\phi_p}) \quad , \quad (\text{II-2})$$

where $C(z_n)$ is the multirate system output, $E(z_n)$ is multirate error, $G(z_n)$ is the plant transfer function, and $D(z_n)$ is the digital controller. Also, n is the integer ratio of the fast-rate sampling frequency to the slow-rate sampling frequency, ϕ_p is $2\pi p/n$, and z_n is $\epsilon^{Ts/n}$. The Nyquist diagram [16] is obtained for (II-2) by allowing z_n to vary along the unit circle in the z_n -plane [1]. For the multirate system, it is shown that the Nyquist criterion becomes

$$Z = n(N + P) \quad , \quad (\text{II-3})$$

where Z is the number of zeroes of the system characteristic equation that lie outside the unit circle in the z_n -plane, P is the number of poles that lie outside the unit circle, and N is the number of encirclements of the -1 point made by the Nyquist diagram. It is noted that one problem associated with the open-loop transfer function of (II-2) is that it is not possible to factor out the compensation function.

Knowles and Edwards also considered the single loop, linear sampled-data system in terms of comparing the multirate system ripple error and quantization error performance against the single rate system performance. Knowles and Edwards developed a frequency-domain closed-loop system transfer function, for which the open-loop transfer function is equivalent to (II-2). An approximate transfer function was then developed which consisted of the first term of (II-2). This approximate transfer function was justified on the basis of the necessity in actual practice of making the open-loop transfer function low-pass with respect to the system slow-rate sampling frequency in order to attenuate the frequency sidebands inherently present in the sampled output of the computer at frequency multiples of $2\pi/T$ rad/sec. Using the approximate transfer function, Knowles and Edwards were able to show that for a phase-lead compensation and a sinusoidal input, the multirate system ripple error performance was inferior to that of the single rate system. No conclusions could be made concerning quantization error performance.

Phillips presented a frequency response design technique for multirate digital controllers for the case that the system is not low-pass with respect to the slow-rate sampling frequency [7]. This technique is based on the observation that each term of the sum of (II-2) is only the first term, $D(z_n)G(z_n)$, for z_n shifted along the unit circle. Hence, if $G(z_n)$ contains resonant modes for frequencies greater than one-half the slow-rate sampling frequency, the manner in which these resonant modes affect the multirate system's frequency response may be observed. If

compensation is required in a frequency range greater than one-half the slow-rate sampling frequency, the manner in which the compensator affects each term of (II-2) may be seen and the compensator is designed accordingly.

B. Multiple Input-Multiple Output Systems.

An effective design procedure for multiple input-multiple output systems was first presented by Povejsil and Fuchs [11]. The procedure of Povejsil and Fuchs is presented for linear, continuous systems, for which the system is characterized by n integro-differential equations relating each of the controlled variables to the input forcing functions. Given a set of performance specifications, it is assumed that the desired s -domain characteristic equation for the controlled system is given or may be deduced. The determinant of the uncontrolled system is then obtained from the given system equations and expanded to give a characteristic equation of the form of the desired characteristic equation. Povejsil and Fuchs then set forth a synthesis procedure whereby the coefficients of the uncontrolled system characteristic equation are compared with the coefficients of the desired system characteristic equation. Where these coefficients differ, the original system equations are examined to determine the compensation form which will establish the desired value of the coefficient.

The advantage of the above technique is that the cross-coupling terms do not complicate the design, but rather, may be helpful in

achieving the desired control. However, the procedure becomes extremely complex for large systems. Also, in determining the desired form of the compensations, conflicting requirements may be encountered.

Newman introduced a frequency-domain procedure for analyzing the effects of cross-coupling terms in two input-two output, continuous systems [10]. Newman's analysis showed the manner in which the introduction of cross-coupling into an unstable system could stabilize the system. Since Newman's design procedure assumes that the cross-coupling terms can be manipulated, its usefulness is limited.

Chen, Mathias, and Sauter developed a Bode plot design procedure for multiple input-multiple output systems which resulted in a decoupled system. It is pointed out that by decoupling the system, the response and dynamic characteristics of the system may be designed one loop at a time. The design procedure is based on a matrix definition of the system, for which the net forward signal path matrix, N , is defined by

$$N = PG \quad , \quad (II-4)$$

where P is the plant matrix and G is the controller matrix. It is then assumed that the compensated system is decoupled, in which case N is a diagonal matrix. The design specifications such as steady-state error, per cent overshoot, and bandwidth are then translated into equivalent Bode diagrams, from which the diagonal elements of N may be specified. The controller G is then computed according to

$$G = P^{-1}N \quad .$$

(II-5)

The disadvantage of the above technique is that the elements of the controller matrix must be computed, which if done purely on the basis of control specifications, may lead to elements of G having more zeroes than poles. Further, the procedure in general leads to a controller containing cross-channel control elements.

The state-space approach to the design of multivariable systems was considerably enhanced by Falb and Wolovich, who first proved the necessary and sufficient conditions for decoupling multivariable systems by state feedback and by output feedback [13]. These conditions were later proved in a more compact manner by Gilbert [14]. As has been previously noted, the immediate difficulty in applying state space techniques to multirate sampled-data systems is that the discrete state variable description of such a system is extremely complex.

Decoupling multivariable systems by state feedback is not a generally practical approach, since the method requires that all the system states be available. Whereas decoupling by output feedback is generally more practical, Falb and Wolovich show that the class of systems for which this is possible is considerably smaller than the class which may be decoupled by state feedback.

III. A FREQUENCY RESPONSE DESIGN TECHNIQUE FOR SINGLE INPUT-SINGLE OUTPUT, MULTIRATE SAMPLED-DATA SYSTEMS.

Recently, some interest has arisen in the multirate (more than one sampling rate present in the system) sampled-data system frequency response design technique [5] - [7]. Such systems arise where data is being received by the digital controller at one rate and processed at a different rate. The afore-mentioned references have discussed the frequency response design technique for multirate digital controllers in terms of the z_n -form of the multirate sampled-data system transfer function. The basic system discussed in these references is shown in Figure III-1. The z_n -form transfer function for this system is [5] - [7]:

$$\frac{C(z_n)}{R(z_n)} = \frac{\frac{1}{n} \sum_{p=0}^{n-1} D(z_n \exp(j\phi_p)) G(z_n \exp(j\phi_p))}{1 + \frac{1}{n} \sum_{p=0}^{n-1} D(z_n \exp(j\phi_p)) G(z_n \exp(j\phi_p))}, \quad (\text{III-1})$$

where

$$z_n = z^{\frac{1}{n}}, \quad (\text{III-2})$$

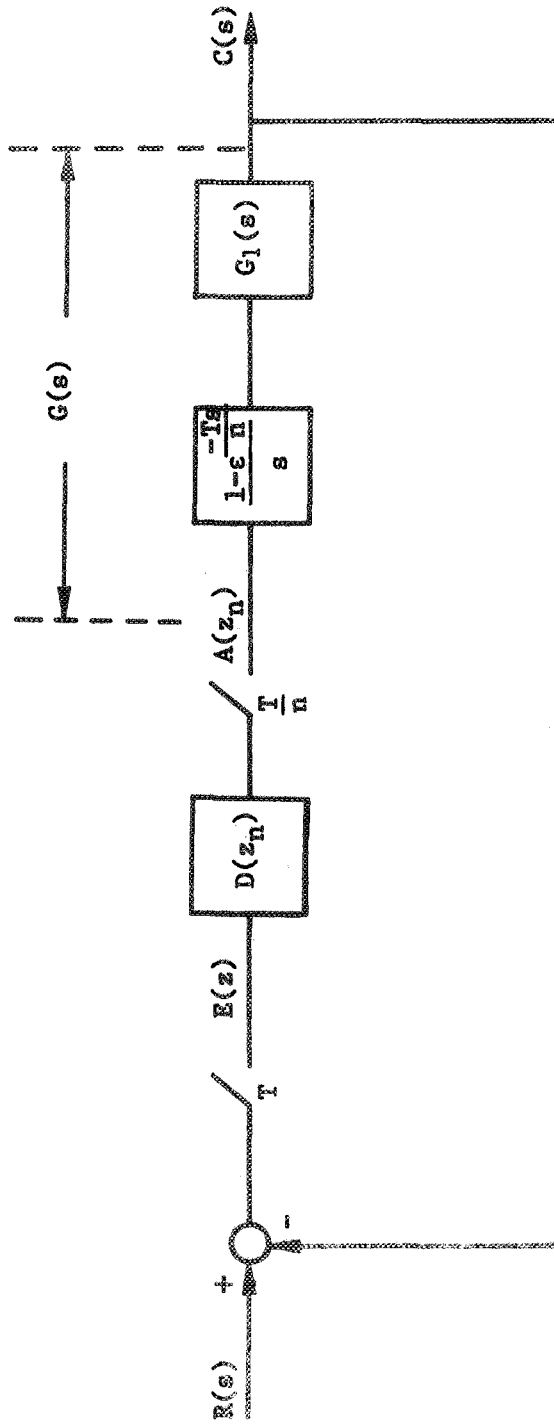


Figure III-1. Basic multirate sampled-data system.

$$\phi_p = \frac{2\pi p}{n}, \quad (III-3)$$

and

$$D(z_n \exp(j\phi_p))G(z_n \exp(j\phi_p)) = D(z)G(z) \Big|_{\substack{T = T/n \\ z = z_n \exp(j\phi_p)}} \quad (III-4)$$

In this chapter, a Bode plot design procedure for the system of Figure III-1 is presented. This procedure allows for the observation of the affect of the digital controller, $D(z_n)$, on each term of the n -term summation in (III-1) from the Bode plot of the first term. In addition, a technique is presented for obtaining the Bode plot for the multirate open-loop transfer function from the Bode plot of the single-rate open-loop transfer function. Also, an upper bound for the choice of the multirate n is developed.

A. The Bilinear Transformation.

The basis of the design technique which will be presented is the bilinear transformation from the z_n -plane to a w_n -plane by means of the relation [1]

$$z_n = \frac{1 + w_n}{1 - w_n} \quad (III-5)$$

The result of this transformation is to take the region of stability from the interior of the unit circle in the z_n -plane to the entire left-half of the w_n -plane, as shown in Figure III-2.

In order to apply the transformation, it is necessary to obtain the w_n -form of the multirate system characteristic equation. The Nyquist criterion may then be applied to the characteristic equation to determine the stability of the system. The w_n -form characteristic equation may be obtained by first deriving the z_n -form and utilizing (III-5). However, additional insight is gained by developing an identity to determine the w_n -form characteristic equation directly.

It may be stated, from (III-5), that

$$G(w_n) = G(z_n) \bigg|_{z_n = \frac{1 + w_n}{1 - w_n}} \quad (III-6)$$

Also [1],

$$G(z_n) = G(z) \bigg|_{\substack{z = z_n \\ T = T/n}} \quad (III-7)$$

and

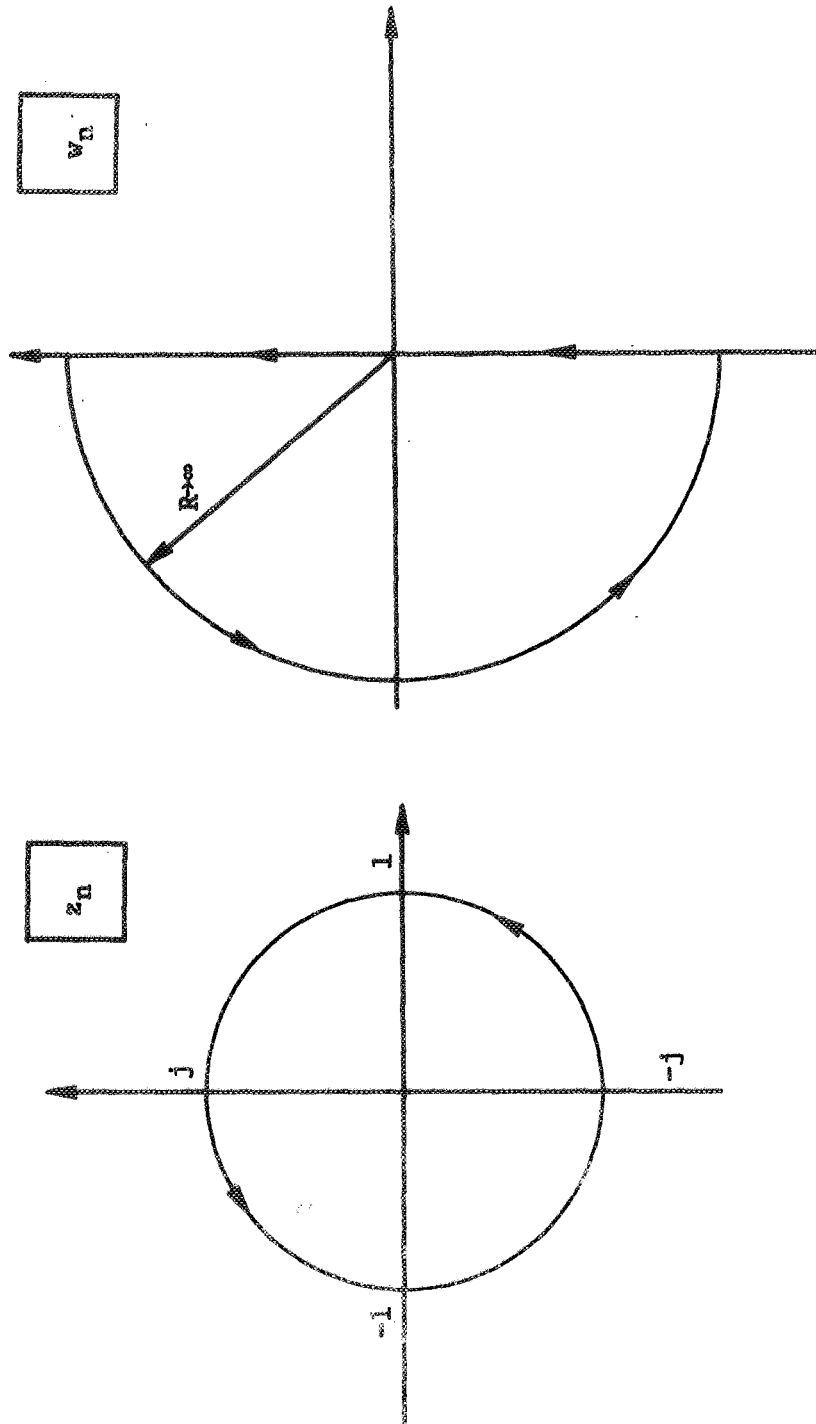


Figure III-2. Transformation of the region of stability from the z_n -plane to the w_n -plane.

$$G(z) = \sum_{\substack{\text{Res of } G(\lambda) \\ \text{at poles} \\ \text{of } G(\lambda)}} \frac{1}{1 - \exp(T\lambda)z^{-1}} \quad (III-8)$$

Hence, (III-6) may be written as

$$G(w_n) = \sum_{\substack{\text{Res of } G(\lambda) \\ \text{at poles} \\ \text{of } G(\lambda)}} \frac{w_n^{+1}}{w_n[1 + \exp(T\lambda/n)] + 1 - \exp(T\lambda/n)} \quad (III-9)$$

The z_n -form characteristic equation for the uncompensated system of Figure III-1 is

$$1 + (1/n) \sum_{p=0}^{n-1} G(z_n \exp(j\phi_p)) = 0, \quad (III-10)$$

which, from (III-4) and (III-8), may be expressed

$$1 + (1/n) \sum_{p=0}^{n-1} G(z_n) \Big|_{\exp(T\lambda_i/n) = \exp(T\lambda_i/n - j\phi_p)} = 0, \quad (III-11)$$

where the λ_i are the poles of $G(\lambda)$.

The w_n -form of (III-11) is, from (III-5),

$$1 + (1/n) \sum_{p=0}^{n-1} G(w_n) \Big|_{\exp(T\lambda_i/n) = \exp(T\lambda_i/n - j\phi_p)} = 0 \quad (III-12)$$

In application of the Nyquist criterion to (III-12), one must determine the number of poles of the summation in (III-12) which lie in the right-half w_n -plane. This is facilitated by observing from (III-12) and (III-9) that the poles of each term of the summation are determined by

$$w_n = \frac{\exp(T\lambda_i/n - j\phi_p) - 1}{\exp(T\lambda_i/n - j\phi_p) + 1} \quad (\text{III-13})$$

at each of the poles, λ_i , of $G(\lambda)$. These λ_i may be complex; let

$$\lambda_i = \alpha_i + j\beta_i \quad (\text{III-14})$$

Then (III-13) may be written

$$w_n = \frac{\exp(\alpha_i T/n + j\theta_i) - 1}{\exp(\alpha_i T/n + j\theta_i) + 1}, \quad (\text{III-15})$$

where θ_i is $\beta_i T/n - \phi_p$. Re-arranging and rationalizing, we obtain

$$w_n = \frac{\exp(2\alpha_i T/n) - 1 + j2\exp(\alpha_i T/n)\sin(\theta_i)}{[\exp(\alpha_i T/n)\cos(\theta_i) + 1]^2 + \exp(2\alpha_i T/n)\sin^2(\theta_i)} \quad (\text{III-16})$$

Whether the poles of (III-12) are located in the right or left half w_n -plane depends on the real part of (III-16). For stability, the

requirement is

$$\exp(2\alpha_1 T/n) - 1 < 0, \quad (\text{III-17})$$

which results in

$$\frac{2\alpha_1 T}{n} < 0. \quad (\text{III-18})$$

Hence, α_1 , the real part of the λ_1 pole of $G(\lambda)$, must be less than zero. We may also observe that for any λ_1 for which α_1 is greater than zero, there will be n poles in the right half plane, since there are n terms in the summation contained in the characteristic equation and the location of the poles of each are dependent upon θ_1 . Thus, one need only determine the number of poles of $G(w_n)$ which lie in the right half w_n -plane and multiply this number by n to obtain the total.

It has been shown [7] that is only necessary to compute the frequency response for $-\pi/n \leq \theta \leq \pi/n$ along the unit circle in the z_n -plane. This range of θ corresponds to the frequency range $-\omega_s/2 \leq \omega \leq \omega_s/2$ in the s -plane, where ω_s is the slow-rate sampling frequency. The corresponding range in the w_n -plane is determined as follows.

From (III-5), we may write

$$\left. \begin{array}{l} z_n \\ s = j\omega \end{array} \right| = \exp(j\omega T/n) = \frac{1 + w_n}{1 - w_n}, \quad (\text{III-19})$$

which may be re-arranged and reduced to obtain

$$w_n = \frac{j \sin (\omega T/n)}{1 + \cos (\omega T/n)} , \quad (\text{III-20})$$

or

$$w_n = j \tan (\omega T/2n) . \quad (\text{III-21})$$

The range on w_n for the frequency-response is determined by evaluating (III-21) for ω at $-\omega_s/2$ and $\omega_s/2$ and is

$$-j \tan (\pi/2n) \leq w_n \leq j \tan (\pi/2n) . \quad (\text{III-22})$$

B. Bode Plot Design Technique

When computed over the range indicated in (III-22), the total frequency-response for (III-12) is the sum of the following n terms:

$$(1/n)G(w_n), -j \tan (\pi/2n) \leq w_n \leq j \tan (\pi/2n)$$

$$(1/n)G(w_n), j \tan (\pi/2n) \leq w_n \leq j \tan (3\pi/2n)$$

.

.

.

$$(1/n)G(w_n), -j \tan (3\pi/2n) \leq w_n \leq -j \tan (\pi/2n)$$

It is noted that the n^{th} term can be observed from the complex conjugate of the 2^{nd} term, assuming $n > 2$. Likewise, assuming $n > 3$, the $n-1^{\text{st}}$ term can be observed from the complex conjugate of the 3^{rd} term. Hence, each term of the n -term summation can be observed by making a Bode plot of $G(w_n)$ for the range $0 \leq w_n \leq j \infty$ and marking off the appropriate ranges of w_n , where certain terms are observed as the complex conjugate of $G(w_n)$ in the appropriate ranges on the Bode plot. From the Bode plot, one may observe directly how many terms of the n -term summation need be considered in the design problem. The effect of the proposed digital controller on $G(w_n)$ may be determined over the entire range of w_n , from which the effect on each term of the summation may be observed.

It is noted that, in effect, the action of a multirate digital controller is to clamp its input at a constant level for a period of T seconds, while operating on this input and providing an output every T/n seconds. This clamping effect may be approximated by inserting a zero-order hold after the slow-rate error sampler in Figure III-1 and sampling the output of this zero-order hold every T/n seconds [5]. This procedure is illustrated in Figure III-3, where the z_n -form transfer function for the zero-order hold is [5]

$$H(z_n) = [1 + z_n^{-1} + \dots + z_n^{-(n-1)}] = \frac{1 - z_n^{-n}}{1 - z_n^{-1}} \quad (\text{III-23})$$

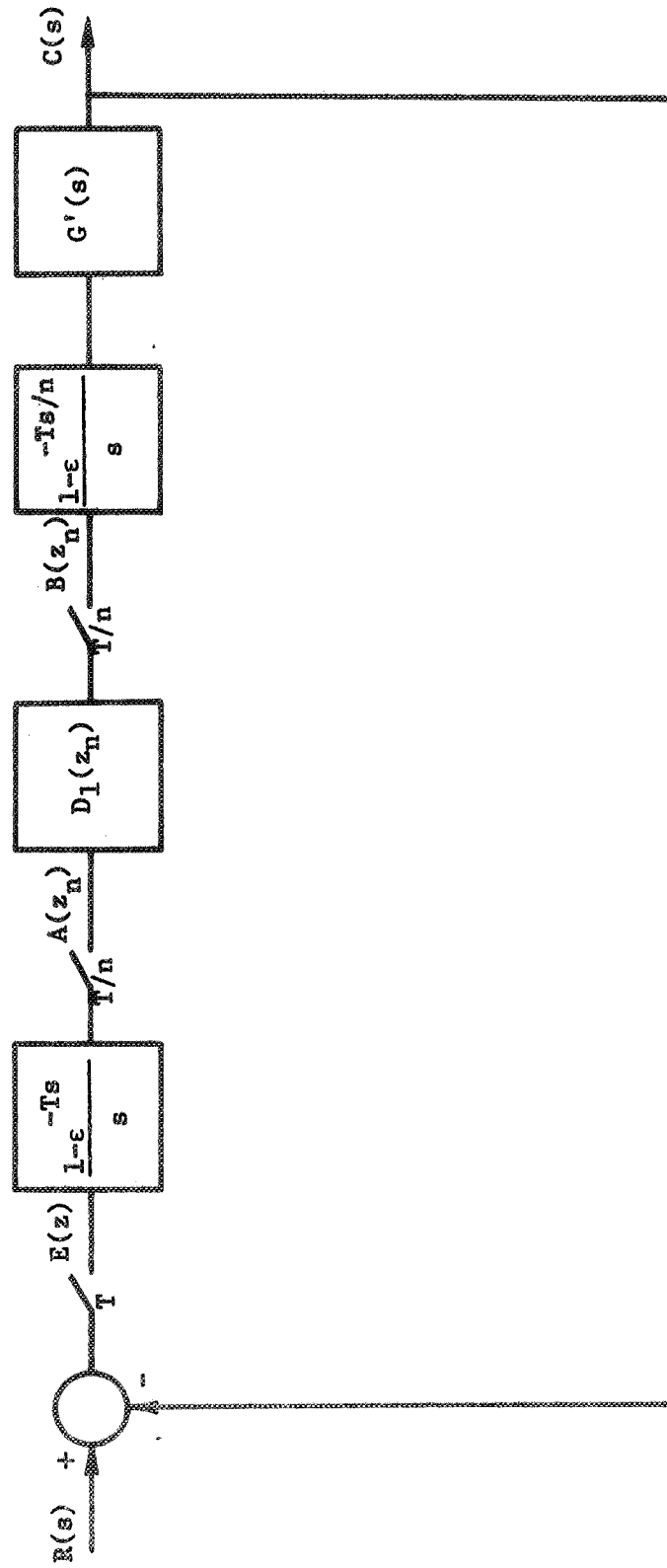


Figure III-3. Multirate system with zero-order hold inserted after the error sampler.

The comparison of Figures III-1 and III-3 shows that

$$D(z_n) = D_1(z_n)H(z_n) \quad . \quad (\text{III-24})$$

If (III-24) is substituted into (III-1), the characteristic equation for the system becomes

$$1 + (1/n) \sum_{p=0}^{n-1} D_1(z_n \exp(j\phi_p))H(z_n \exp(j\phi_p))G(z_n \exp(j\phi_p)) = 0 \quad . \quad (\text{III-25})$$

For the uncompensated case, $D_1(z_n \exp(j\phi_p))$ is unity. Let

$$G'(z_n \exp(j\phi_p)) = H(z_n \exp(j\phi_p))G(z_n \exp(j\phi_p)) \quad . \quad (\text{III-26})$$

The uncompensated system characteristic equation is

$$1 + (1/n) \sum_{p=0}^{n-1} G'(z_n \exp(j\phi_p)) = 0 \quad . \quad (\text{III-27})$$

We may also write [5]

$$(1/n) \sum_{p=0}^{n-1} G'(z_n \exp(j\phi_p)) = G'(z) \quad (\text{III-28})$$

where

$$G'(z) = H(z)G(z) \quad . \quad (\text{III-29})$$

However, from (III-23),

$$H(z) \Big|_{z = e^{j\omega T}} = 1 \quad . \quad (\text{III-30})$$

Hence,

$$(1/n) \sum_{p=0}^{n-1} G'(z_n \exp(j\phi_p)) = G(z) \quad . \quad (\text{III-31})$$

The w_n -form of (III-31) is

$$(1/n) \sum_{p=0}^{n-1} G'_p(w_n) = G(w) \quad , \quad (\text{III-32})$$

where

$$G'_p(w_n) = G'(w_n) \Big|_{\exp(T\lambda_1/n) = \exp(T\lambda_1/n - j\phi_p)} \quad . \quad (\text{III-33})$$

We may conclude from (III-32) that, for the system of Figure III-3, the uncompensated multirate open-loop frequency response may be obtained from the single-rate open-loop frequency response. It is only necessary to transform each value of w to the corresponding value of w_n . This may be done by utilizing (III-21). The procedure may be facilitated by means

of the $\log_{10} \tan(\theta)$ vs. θ template shown in Figure III-4. To use the template, one enters along the abscissa to the particular value of w , projects vertically to the $\log_{10} \tan(\theta)$ vs. θ characteristic, then horizontally to the corresponding value of θ , where, from (III-21),

$$\theta = \frac{\omega T}{2} \quad (III-34)$$

This value of θ is then divided by n and the corresponding value of $\log_{10} \tan(\theta/n)$ is determined from the template, yielding the value of w_n .

The use of the template of Figure III-4 is illustrated by the example of Figure III-5, where

$$G(s) = \frac{1 - \exp(-Ts)}{s} \cdot \frac{100}{s(s + 10)} \quad (III-35)$$

the slow-rate sampling period, T , is .1 seconds, and n is 3. The computer program of Appendix A was utilized to compute single rate and multirate frequency responses. The single rate db magnitude was then plotted against $\log_{10}(w)$. To determine the multirate db gain characteristic, the template of Figure III-4 was overlayed on Figure III-5. At each of the selected points on the $G(w)$ plot, the value of $\log_{10}(w_3)$ was determined according to the procedure stated in the previous paragraph. The point from the $G(w)$ plot is then transferred from its

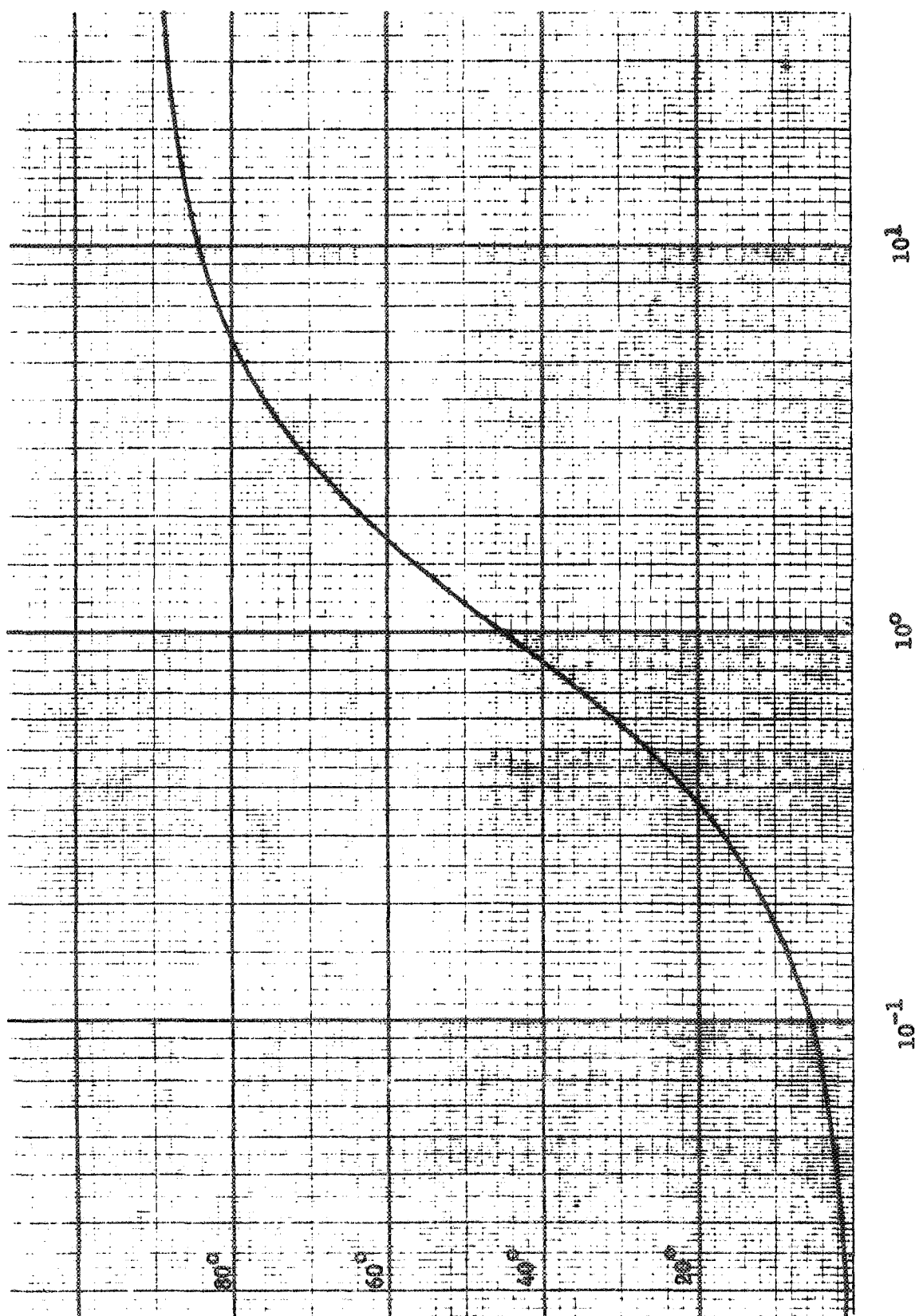


Figure III-4. $\log_{10} \tan(\theta)$ vs. θ template.

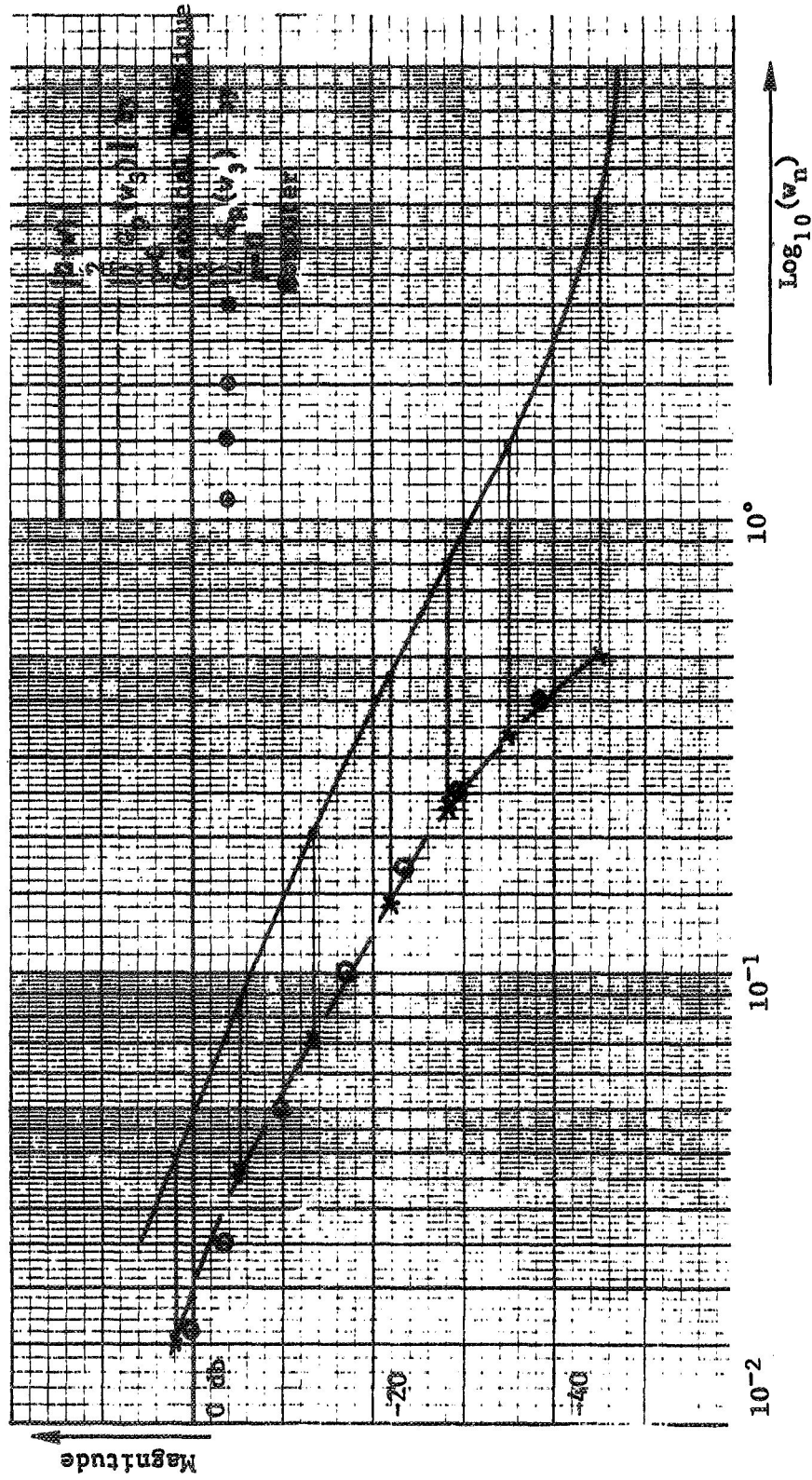


Figure III-5. Illustration of graphical technique for determining multirate frequency response.

$\log_{10}(w)$ position to the corresponding $\log_{10}(w_3)$ position. It is observed that the graphically determined multirate frequency response corresponds closely with the computed frequency response.

In practice, one of the design requirements on the multirate digital controller is that the compensated open-loop transfer function for the system of Figure III-1 must be low-pass with respect to the system slow-rate sampling frequency. By this, it is meant that the system slow-rate sampling frequency must be at least twice that of the highest frequency present in the frequency response of the compensated open-loop transfer function [1]. If this condition is met, it can be shown that the n -term summation constituting the open-loop transfer function can be approximated by its first term [6]. That is,

$$(1/n) \sum_{p=0}^{n-1} D(z_n \exp(j\phi_p)) G(z_n \exp(j\phi_p)) \approx (1/n) D(z_n) G(z_n) \quad . \quad (\text{III-36})$$

If it can be shown that the uncompensated system is low-pass, then the design requirement for the digital controller may be alleviated. It is noted that the effect of the multirate n on the low-pass nature of the uncompensated open-loop multirate transfer function can be observed from the Bode plot of the single-rate transfer function. This effect depends on the magnitude and phase angle of $G(w_n)$ for $w_n > j \tan(\pi/2n)$, the upper limit for the w_n frequency range of the first term. This is illustrated in Figure III-6, which is a Bode plot of $(1/n)G(w_n)$ for

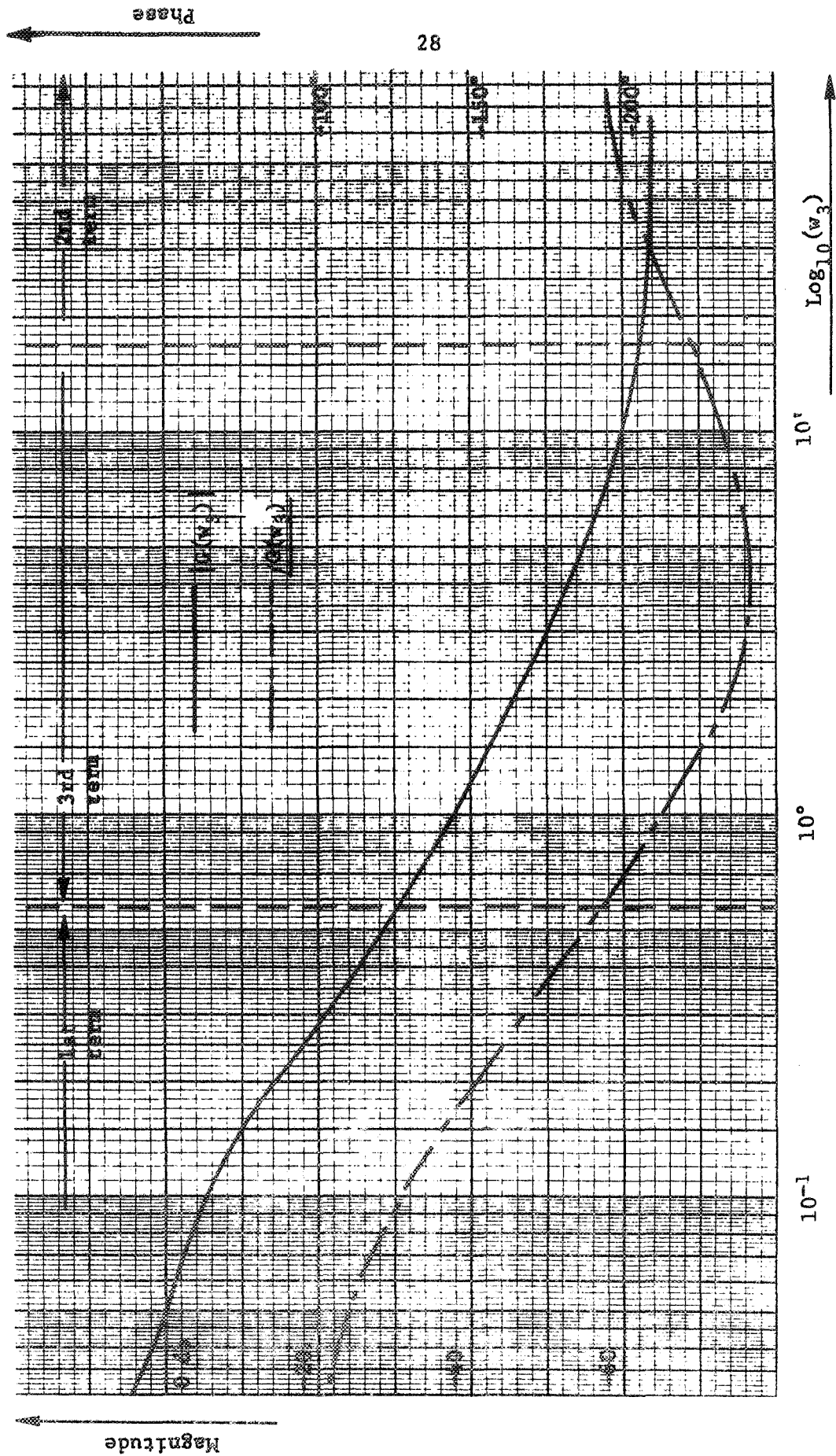


Figure III-6. Gain and phase characteristics for $G(w_3)$, $0 < w_3 < j\infty$.

$0 \leq w_n \leq j\infty$, where

$$G(s) = \frac{1 - \exp(-Ts/n)}{s} \cdot \frac{10}{s(s + 10)} \quad , \quad (\text{III-37})$$

T is .1 seconds, and n is 3. The regions for each of the terms of the summation constituting the total multirate transfer function are marked off on the frequency scale. The third term of the summation is determined from the complex conjugate of the second term at the same s -plane frequency values. With respect to the magnitude of $G(w_3)$ within its -3 db bandwidth, the magnitude of both the 2nd and 3rd terms is seen to be negligible. Hence, the complex sum of the three terms is accurately approximated by the first term within the -3 db bandwidth of $G(w_3)$.

An upper bound for the choice of n such that the uncompensated open-loop transfer function is low-pass may be obtained by assuming that the remaining terms beyond the first term add directly. For this case, the effect of the remaining terms on the total sum may be judged from their effect on the -3 db bandwidth of the total multirate transfer function. At the -3 db cutoff frequency,

$$\left| (1/n) \sum_{p=0}^{n-1} G_p'(w_n) \right| = .707 \quad , \quad (\text{III-38})$$

Assuming no high frequency resonant modes, the $n-1$ terms beyond the first term can be said not to significantly influence the value of the

total sum if

$$(n-1) \left| (1/n) G'(w_n) \right|_{w_n = j \tan(\pi/2n)} \leq .1(.707) \quad (III-39)$$

Now, if

$$(1/n) \sum_{p=0}^{n-1} G'_p(w_n) \approx (1/n) G'(w_n) \quad (III-40)$$

then, from (III-32),

$$(1/n) G'(w_n) \approx G(w) \quad (III-41)$$

at the same s-plane frequency values. Hence,

$$\left| (1/n) G'(w_n) \right|_{w_n = j \tan(\pi/2n)} \approx \left| G(w) \right|_{w \rightarrow j\infty} \quad (III-42)$$

Then, from (III-39), we may write

$$(n-1) \left| G(w) \right|_{w \rightarrow j\infty} \leq .0707 \quad (III-43)$$

and the limiting relation for n is

$$n \leq 1 + \frac{.0707}{|G(w)|} \quad (III-44)$$

$w \rightarrow j\infty$

The above relation provides a possible basis for the choice of n . The procedure would be to plot the gain characteristic of $G(w)$ and observe the low-pass nature of the plot as w approaches $j\infty$. If the magnitude of $G(w)$ is not significantly less than 1 as w approaches $j\infty$, the selection of n will not matter, since the total uncompensated multirate transfer function will not be low-pass whatever the value of n . The digital controller must then be designed to effect a low-pass system. If the magnitude of $G(w)$ is significantly less than 1 as w approaches $j\infty$, the choice of n may influence whether or not the summation may be approximated by the first term. Then (III-44) may be used to determine a maximum value of n to provide a low-pass uncompensated open-loop transfer function. It would not be necessary then to specifically designate the digital controller so as to effect a low-pass system, if it is possible to select n less than the maximum calculated value.

C. Digital Computation of the Multirate System Frequency-Response.

The computation of the frequency-response for (III-12), if performed on the digital computer, may lead to numerical inaccuracies if two or more poles of the continuous plant are nearly coincident [8]. The following development provides a means for avoiding these inaccuracies.

The multirate signal $e_n^*(t)$ may be expressed [1]

$$e_n^*(t) = e(t) \delta_n(t), \quad (\text{III-45})$$

where

$$\delta_n(t) = \sum_{k=0}^{\infty} \delta(t - kT/n) \quad . \quad (\text{III-46})$$

The Laplace transform of (III-45) is

$$E_n^*(s) = E(s) \circledast \Delta_n(s) \quad , \quad (\text{III-47})$$

where \circledast denotes complex convolution and $\Delta_n(s)$ is the Laplace transform of $\delta_n(t)$. (III-47) may also be written [1]

$$E_n^*(s) = \frac{1}{2\pi j} \int_{c-j\infty}^{c+j\infty} E(\lambda) \Delta_n(s-\lambda) d\lambda \quad . \quad (\text{III-48})$$

If $\lim_{\lambda \rightarrow \infty} \lambda E(\lambda) = 0$, (III-48) becomes

$$E_n^*(s) = - \sum_{\substack{\text{poles of} \\ \Delta_n(s-\lambda)}} \text{Res } E(\lambda) \Delta_n(s-\lambda) \quad , \quad (\text{III-49})$$

where

$$\Delta_n(s-\lambda) = \frac{1}{1-\exp(-\frac{T}{n}(s-\lambda))} = \frac{N_n(\lambda)}{D_n(\lambda)} \quad (III-50)$$

The poles of $\Delta_n(s-\lambda)$ are located such that

$$\lambda_m = s + jm(n\omega_s), \quad m = 0, \pm 1, \pm 2, \dots \quad (III-51)$$

where ω_s is the slow-rate sampling frequency. Since $\Delta_n(s-\lambda)$ has only simple poles, (III-48) may be written as [1]

$$E_n^*(s) = \sum_{m=-\infty}^{\infty} \frac{N_n(\lambda_m)}{D_n'(\lambda_m)} \cdot E(\lambda_m) \quad (III-52)$$

where

$$D_n'(\lambda_m) = -\frac{T}{n} \quad (III-53)$$

Then

$$E_n^*(s) = (n/T) \sum_{m=-\infty}^{\infty} E(s + jmn\omega_s) \quad (III-54)$$

Application of (III-54) to the system of Figure III-1 results in

$$(1/T) \sum_{m=-\infty}^{\infty} \sum_{p=0}^{n-1} G(j[\omega^*(mn+p)\omega_s]) \quad (III-55)$$

for the uncompensated multirate system open-loop transfer function. Since the frequency response is unique whether evaluated in the s , z , or w -plane, the w_n -plane Bode plot of the uncompensated open-loop transfer function may be obtained by evaluating (III-55) for various values of ω in the s -plane, then plotting db gain and phase angle against the corresponding values of $\log_{10}(w_n)$, according to (III-21). Only as many terms of the infinite summation as are required for accuracy need be used. The computer program of Appendix A incorporates (III-54) in computing the frequency-response for the open-loop transfer function of the multirate sampled-data system.

D. A Multirate System Identity

In determining the z_n -form of the multirate system output for inputs at various points in the system, difficulties may be encountered in obtaining a z_n -form transfer function. These difficulties arise due to the occurrence of terms involving the z -transform of the product of a multirate signal with a continuous plant s -domain transfer function. This problem is alleviated by an identity which expresses such a term in z_n -form.

Consider the configuration of Figure III-7. The signal $C(z)$ is described by

$$C(z) = Z\{E(z)_n G(s)\} . \quad (\text{III-56})$$

The signal $C(z)_n$ is given by

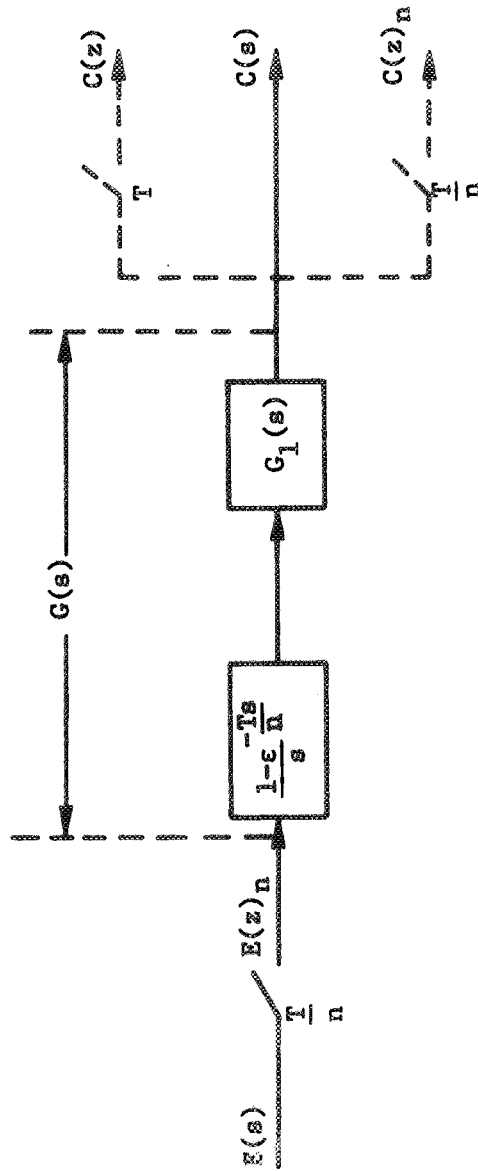


Figure III-7. Multirate input to a continuous plant.

$$C(z)_n = E(z)_n G(z)_n \quad (\text{III-57})$$

$C(z)$ may also be written [5]

$$C(z) = (1/n) \sum_{p=0}^{n-1} C[z \exp(j2p\pi)]_n \quad (\text{III-58})$$

Substituting (III-56) and (III-57) into (III-58),

$$Z\{E(z)_n G(s)\} = (1/n) \sum_{p=0}^{n-1} E[z \exp(j2p\pi)]_n \cdot G[z \exp(j2p\pi)]_n \quad (\text{III-59})$$

(III-59) will now be applied to the system of Figure III-8, where it is desired to determine the output of the system in terms of the quantization disturbance input at the digital controller output accumulator. Figure III-9 shows the system re-arranged for this purpose, with $r(t)$ set to zero. From Figure III-9,

$$C(z) = Z\{M(z)_n G(s)\} \quad (\text{III-60})$$

However,

$$M(z)_n = Q(z)_n - B(z)_n \quad (\text{III-61})$$

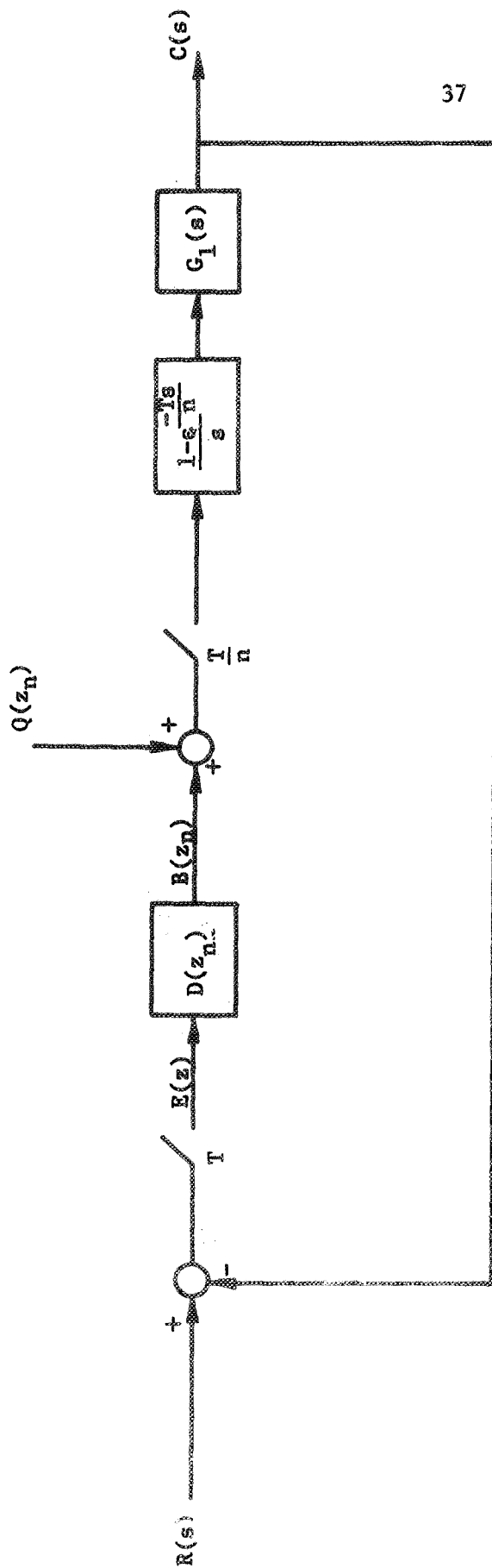


Figure III-8. Multirate system with quantization disturbance at digital controller output accumulator.

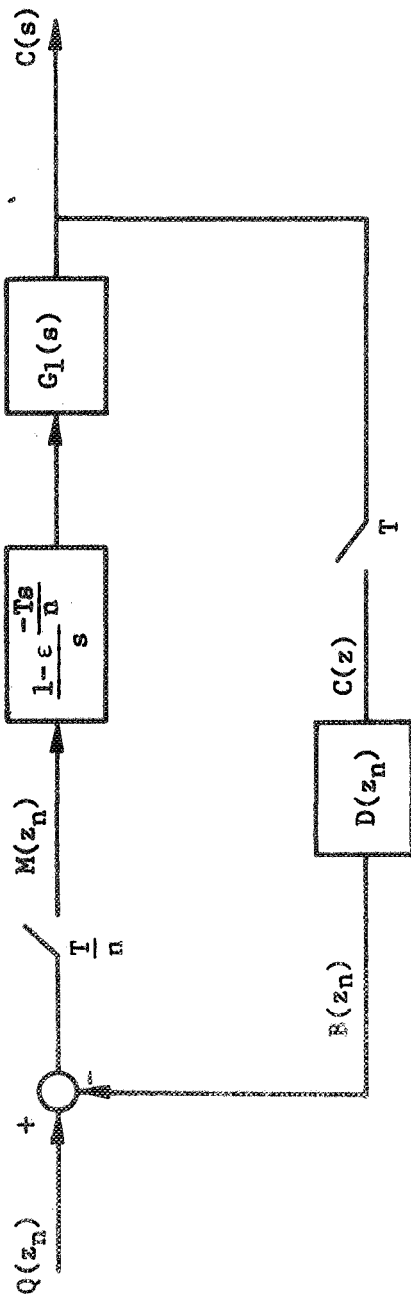


Figure III-9. System of Figure III-8 rearranged ($r(t) = 0$).

and

$$B(z)_n = D(z)_n C(z) \quad (\text{III-62})$$

Substituting (III-61) and (III-62) into (III-60) yields

$$C(z) = \frac{Z\{Q(z)_n G(s)\}}{1 + Z\{D(z)_n G(s)\}} \quad (\text{III-63})$$

Application of the results of (III-59) to (III-63) obtains

$$C(z)_n = \frac{(1/n) \sum_{p=0}^{n-1} Q[z \exp(j2p\pi)]_n G[z \exp(j2p\pi)]_n}{1 + (1/n) \sum_{p=0}^{n-1} D[z \exp(j2p\pi)]_n G[z \exp(j2p\pi)]_n} \quad (\text{III-64})$$

If $G(z)_n$ can be said to be low-pass with respect to the slow-rate sampling frequency, (III-64) may be written

$$\frac{C(z)_n}{Q(z)_n} = \frac{(1/n)G(z)_n}{1 + (1/n)D(z)_n G(z)_n} \quad (\text{III-65})$$

The z_n -form of (III-65) is

$$\frac{C(z_n)}{Q(z_n)} = \frac{(1/n)G(z_n)}{1 + (1/n)D(z_n)G(z_n)}, \quad (\text{III-66})$$

which is the desired result.

IV. AN OPEN-LOOP FREQUENCY RESPONSE DESIGN TECHNIQUE FOR MULTIPLE INPUT-MULTIPLE OUTPUT SYSTEMS

Multiple input-multiple output systems have received significant attention in the literature in recent years [10] - [15]. Whereas most of the research has been oriented towards developing analysis and design techniques for the general n -input, n -output case, techniques will be developed in this chapter specifically for two and three inputs and outputs. The case of three inputs-three outputs is of particular interest in the design of non-symmetric aerospace vehicles for significant flight in the atmosphere, such as the proposed NASA space shuttle. Such vehicles have significant coupling between the pitch, yaw, and roll axes. Initially, a known design technique for multiple input-multiple output continuous systems such as the above will be extended to the sampled-data case. A new technique will then be presented.

A. Extension of the Method of Povejsil and Fuchs [11].

This method has previously been discussed in Chapter II. It will now be shown that the method may also be applied to sampled-data systems.

Consider the system of Figure IV-1 with k , l , and m all equal to n , an integer. Each of the system outputs may be written in the form

$$Y_h(z) = E_1(z) \cdot (1/n) \sum_{p=0}^{n-1} D_1(z \exp(j\phi_p^{(1)})) \cdot G_{h1}(z \exp(j\phi_p^{(1)}))_n$$

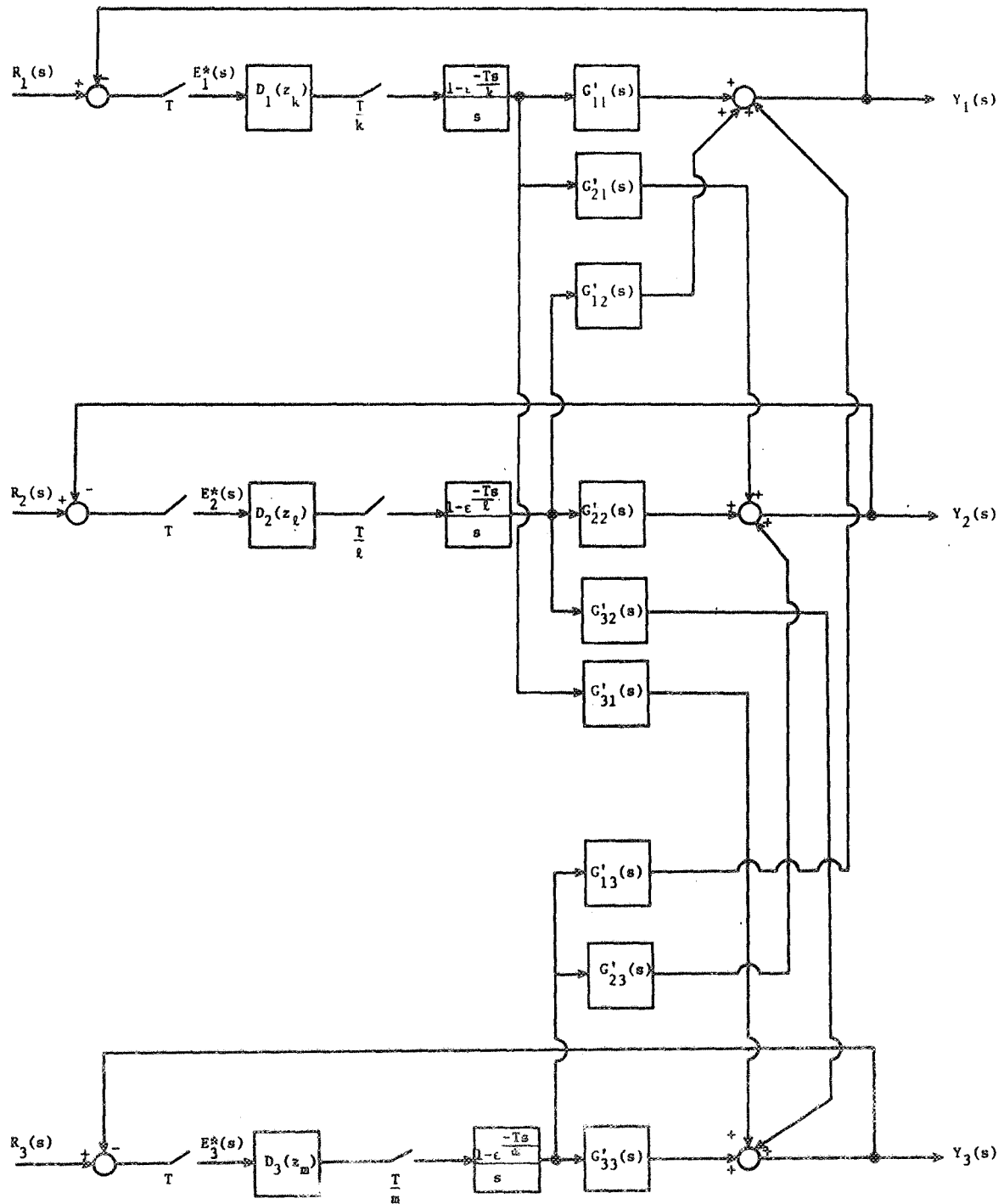


Figure IV-1. Three input-three output, multirate sampled-data system.

$$\begin{aligned}
& +E_2(z) \cdot (1/n) \sum_{p=0}^{n-1} D_2(z \exp(j\phi_p'))_n G_{h2}(z \exp(j\phi_p'))_n \\
& +E_3(z) \cdot (1/n) \sum_{p=0}^{n-1} D_3(z \exp(j\phi_p'))_n G_{h3}(z \exp(j\phi_p'))_n, \quad (IV-1)
\end{aligned}$$

where

$$G_{hg}(z) = z \left\{ \frac{1 - \exp(-Ts/n)}{s} \cdot G_{hg}(s) \right\}, \quad (IV-2)$$

$$E_g(z) = R_g(z) - Y_g(z), \quad (IV-3)$$

and

$$\phi_p' = 2\pi p. \quad (IV-4)$$

If (IV-3) is substituted into (IV-1) and h is set to 1, 2, and 3, the following matrix equation may be written:

$$[M(z)_n] \cdot \underline{Y}(z) = [N(z)_n] \cdot \underline{R}(z). \quad (IV-5)$$

The elements of $[M(z)_n]$ are, for row g and column h ,

$$\frac{1}{n} \sum_{p=0}^{n-1} D_h(z \exp(j\phi_p'))_n G_{gh}(z \exp(j\phi_p'))_n, \quad g \neq h, \quad (IV-6)$$

and

$$1 + \frac{1}{n} \sum_{p=0}^{n-1} D_h(z \exp(j\phi_p'))_n G_{gh}(z \exp(j\phi_p'))_n, \quad g = h. \quad (\text{IV-7})$$

The elements of $[N(z)_n]$ are given by (IV-6) for all g and h .

If it is assumed that the determinant of $[M(z)_n]$ is non-zero, we may write

$$\underline{Y}(z) = [M(z)_n]^{-1} \cdot [N(z)_n] \cdot \underline{R}(z). \quad (\text{IV-8})$$

Equation (IV-8) may be expressed as a function of z_n by substituting z_n for $z^{1/n}$ and $\exp(j\phi_p)$ for $\exp(j\phi_p')$. Then

$$\underline{Y}(z_n) = [M(z_n)]^{-1} \cdot [N(z_n)] \cdot \underline{R}(z_n). \quad (\text{IV-9})$$

The characteristic equation for the system, from (IV-9), is

$$|M(z_n)| = 0. \quad (\text{IV-10})$$

In order to apply the method of Povejsil and Fuchs, it is necessary to determine a specific z_n -form characteristic equation to achieve a desired system performance. It is noted that this desired system performance generally will be such that the system is regarded as being "low-pass"

with respect to the slow-rate sampling frequency, as was previously discussed in Chapter III. Hence, the summation terms indicated in (IV-6) and (IV-7) may be approximated by the first term in each case.

After establishing a desired system characteristic equation, the form of a proposed compensated system characteristic equation is examined to establish equations by which the coefficients can be calculated for the proposed compensators. Several disadvantages are noted in this procedure. The desired system characteristic equation is not necessarily easily established, especially in the case of high-order systems. Further, the form of the compensation must be assumed, hopefully by observation of the system characteristics. Finally, in calculating the coefficients for the assumed form of the compensation, conflicting requirements may be encountered.

Certain observations can also be made concerning multirate sampled-data systems for which the fast-rate sampling in each channel is at a different rate. For the system of Figure (IV-1), let $k \neq l \neq m$, but the ratios of l to k and m to l be integers, where k , l , and m are each integers. Then, for output h ,

$$\begin{aligned}
 Y_h(z) = & E_1(z) \cdot (1/k) \sum_{p=0}^{k-1} D_1(z \exp(j\phi_p^i))_k G_{h1}(z \exp(j\phi_p^i))_k \\
 & + E_2(z) \cdot (1/l) \sum_{p=0}^{l-1} D_2(z \exp(j\phi_p^i))_l G_{h2}(z \exp(j\phi_p^i))_l \\
 & + E_3(z) \cdot (1/m) \sum_{p=0}^{m-1} D_3(z \exp(j\phi_p^i))_m G_{h3}(z \exp(j\phi_p^i))_m . \quad (IV-11)
 \end{aligned}$$

In the same manner as for the previous case, the following matrix equation may be written:

$$[M(z)_{k,l,m}] \cdot \underline{Y}(z) = [N(z)_{k,l,m}] \cdot \underline{R}(z) \quad . \quad (\text{IV-12})$$

The elements of $[M(z)_{k,l,m}]$, for row g and column h , are

$$\frac{1}{r} \sum_{p=0}^{r-1} D_h(z \exp(j\phi_p'))_r G_{gh}(z \exp(j\phi_p'))_r, \quad g \neq h, \quad (\text{IV-13})$$

and

$$1 + \frac{1}{r} \sum_{p=0}^{r-1} D_h(z \exp(j\phi_p'))_r G_{gh}(z \exp(j\phi_p'))_r, \quad g = h, \quad (\text{IV-14})$$

where r may be k , l , or m . The elements of $[N(z)_{k,l,m}]$ are given by (IV-13) for all g and h . Then

$$\underline{Y}(z) = [M(z)_{k,l,m}]^{-1} [N(z)_{k,l,m}] \underline{R}(z), \quad (\text{IV-15})$$

assuming that the determinant of $[M(z)_{k,l,m}]$ is nonsingular.

The application of the method of Povejsil and Fuchs is somewhat more restricted in this case, since expression of (IV-15) in terms of z_k , for example, results in terms such as

$$\frac{1}{l} \sum_{p=0}^{l-1} D_2(z_k \exp(j\phi_p'/k))_u G_{g2}(z_k \exp(j\phi_p'/k))_u, \quad (\text{IV-16})$$

where u is the integer ratio of l to k , and

$$\begin{aligned}
 D_2(z_k \exp(j\phi_p^i/k))_u G_{g2}(z_k \exp(j\phi_p^i/k))_u \\
 = D_2(z \exp(j\phi_p^i))_l G_{g2}(z \exp(j\phi_p^i))_l \bigg|_{z^{(1/l)} = z_k^{(1/u)}} \cdot \quad (IV-17) \\
 \exp(j\phi_p^i)^{(1/l)} = \exp(j\phi_p^i/k)^{(1/u)}
 \end{aligned}$$

Similar terms result if (IV-15) is expressed in terms of z_l . Since the desired form of the compensated system characteristic equation must be pre-determined and the form of the digital controller transfer function must be assumed beforehand, terms which include fractional powers of a multirate variable, such as the above, would cause considerable difficulty. If (IV-15) is expressed in terms of z_m , terms involving $D_1(z_m)_{\frac{1}{u}}$ and $D_2(z_m)_{\frac{1}{v}}$ result, where

$$D_1(z_m)_{\frac{1}{u}} = D_1(z)_k \bigg|_{z^{(1/k)} = z_m^{1/(1/u)}} \cdot \quad (IV-18)$$

and

$$D_2(z_m)_{\frac{1}{v}} = D_2(z)_l \bigg|_{z^{(1/l)} = z_m^{1/(1/v)}} \cdot \quad (IV-19)$$

Such terms would cause difficulty in determining a desired form for a proposed digital controller. Hence, the method of Povejsil and Fuchs could be used for the case of (IV-15) only with considerable effort.

B. Development of the Open-Loop Technique for Two-Channel, Continuous-Data Systems.

Consider the two-channel, continuous-data system with cross-coupling shown in Figure IV-2. A signal-flow graph representation of this system is given in Figure IV-3. It is noted that the signal-flow graph representation contains three loops, one in each channel due to feedback, and the other, due to cross-coupling. The characteristic equation for this system may be obtained by the application of Mason's gain formula and is

$$(1 + D_1 G_{11})(1 + D_2 G_{22}) - D_1 D_2 G_{12} G_{21} = 0. \quad (\text{IV-20})$$

It is intended to develop a frequency-response design technique for the system of Figure IV-2 by opening each of the above-mentioned loops and obtaining an "open-loop" transfer function [9] for each loop.

Let the feedback loop of the Y_1 channel be opened after the E_1 node in the signal-flow graph of Figure IV-3, as shown in Figure IV-4. The transfer function, $-E'_1/E_1$, will now be obtained by application of Mason's gain formula to the signal-flow graph of Figure IV-4. This open-loop transfer function is

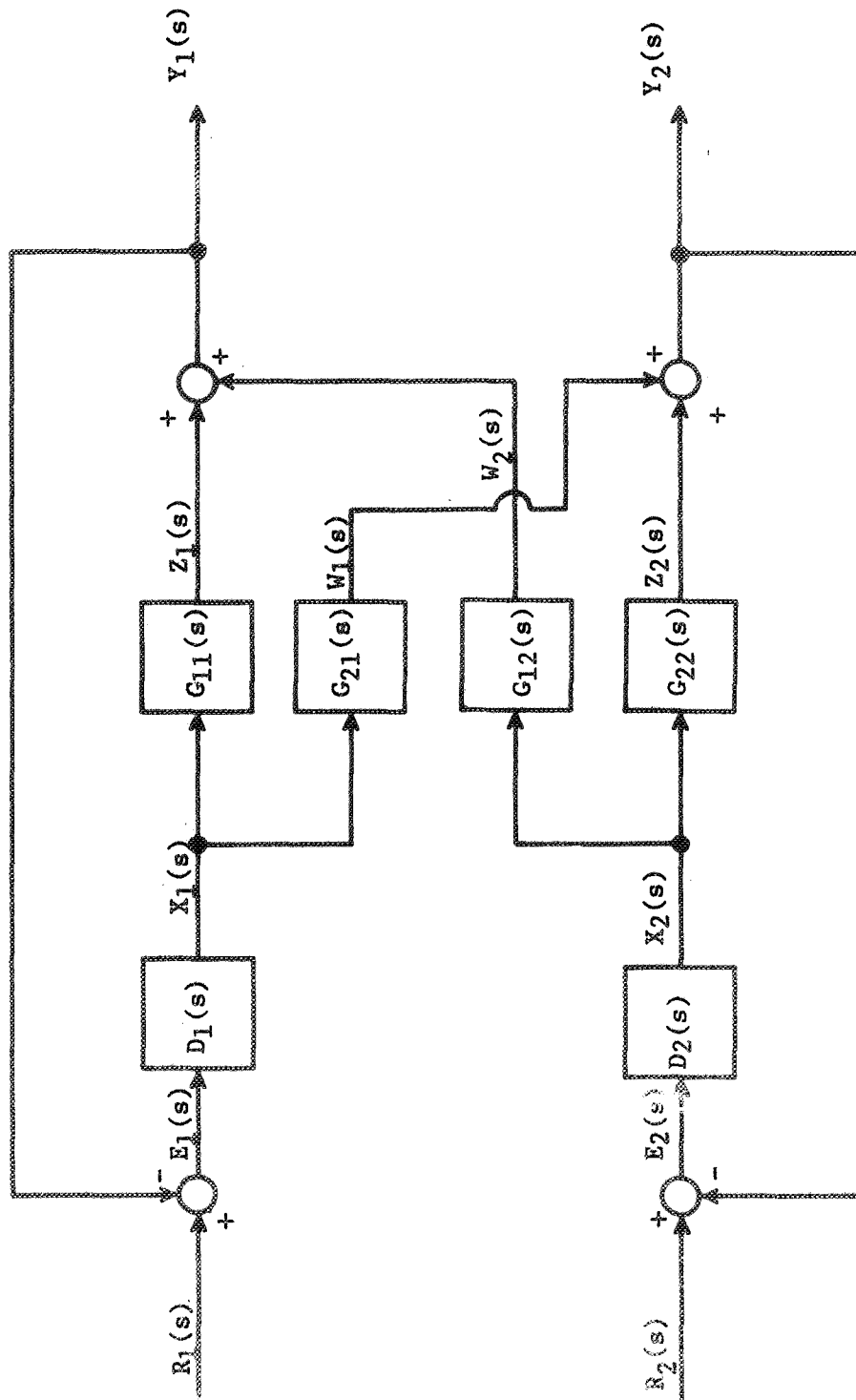


Figure IV-2. Two input-two output, continuous-data system.

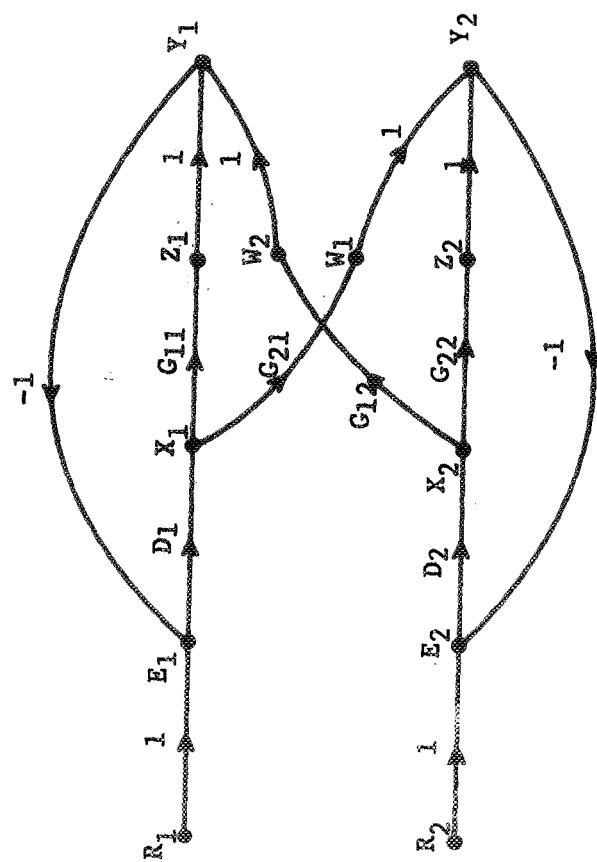


Figure IV-3. Signal-flow graph for Figure IV-2.

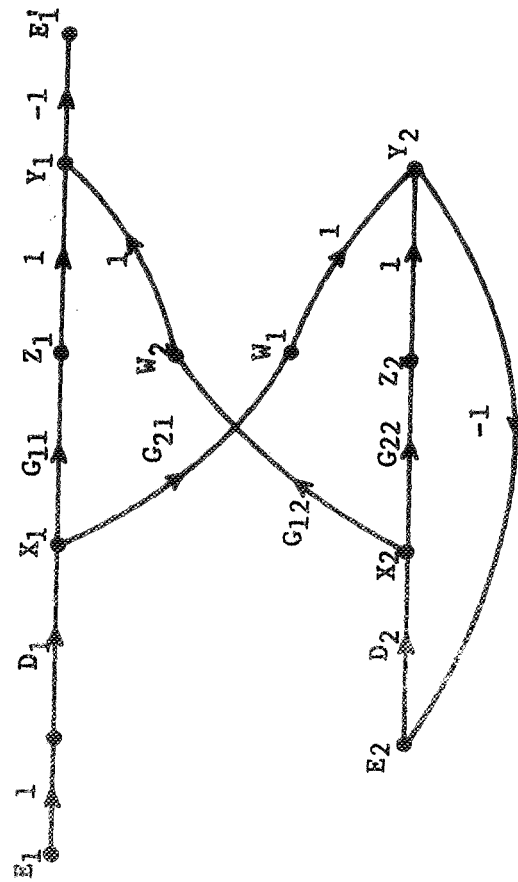


Figure IV-4. Figure IV-3 opened after E_1 node.

$$-\frac{E_1'}{E_1} = \frac{(1 + D_2 G_{22}) D_1 G_{11} - D_1 D_2 G_{12} G_{21}}{1 + D_2 G_{22}} \quad (IV-21)$$

The above may be written

$$-\frac{E_1'}{E_1} = D_1 \left\{ G_{11} - \frac{D_2 G_{12} G_{21}}{1 + D_2 G_{22}} \right\} \quad (IV-22)$$

It is desired to apply the Nyquist criterion to the uncompensated form of (IV-22). One would then plot

$$-\frac{E_1'}{E_1} = G_{11} - \frac{G_{12} G_{21}}{1 + G_{22}} \quad (IV-23)$$

as a function of frequency and determine the gain margin and phase margin for (IV-23). The design procedure would then be to specify the compensators D_1 and D_2 so as to obtain the desired gain and phase margins for (IV-22). The procedure is facilitated if, over the frequencies of interest, the term $G_{12} G_{21} / (1 + G_{22})$ is negligible with respect to G_{11} , i.e., if the system is approximately decoupled. Since it is generally desired to decouple the system, if the above is not the case, then it may be possible to specify the compensator D_2 so as to approximately decouple the system.

Now, consider the system of Figure IV-3 opened after the E_2 node, as shown in Figure IV-5. The open-loop transfer function is

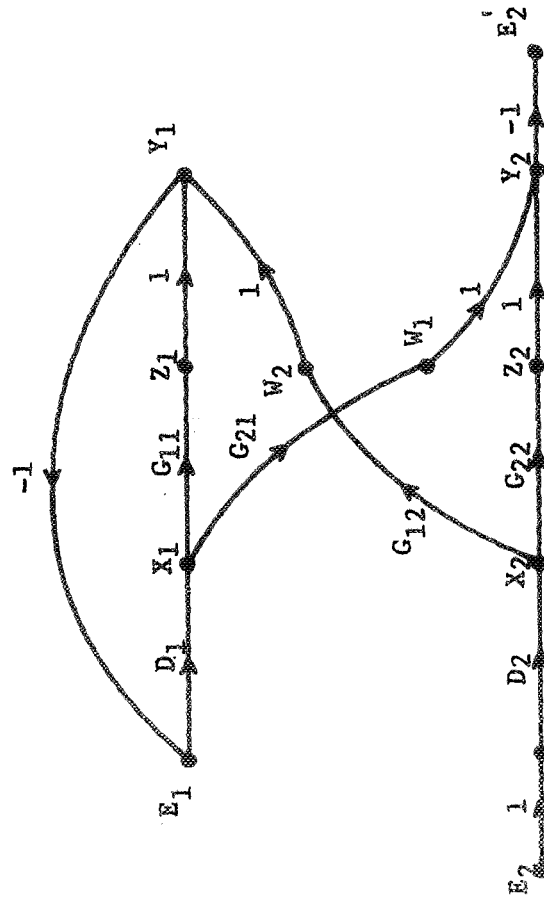


Figure IV-5. Figure IV-3 opened after E_2 node.

$$-\frac{E_2'}{E_2} = D_2 \left\{ G_{22} - \frac{D_1 G_{21} G_{12}}{1 + D_1 G_{11}} \right\} \quad (\text{IV-24})$$

It is observed that, if it is desired to decouple the system, the compensator D_1 should be specified so as to cause the term $D_1 G_{21} G_{12} / (1 + D_1 G_{11})$ to be negligible with respect to G_{22} . Then the compensators D_1 and D_2 must not only achieve the desired gain and phase margins in (IV-22) and (IV-24), but must also decouple the system in the stated manner. Hence, one may proceed to specify the compensators by first checking the degree of coupling of the uncompensated open-loop transfer functions, designating a preliminary compensation to decouple the system, refining the preliminary compensation to achieve gain and phase margin, then checking the compensated open-loop transfer functions to insure decoupling.

If the system has been decoupled by the design procedure, then it should follow that the open-loop transfer function for the remaining loop (due to cross-coupling) should have more than sufficient gain and phase margins. This is shown to be the case if the system of Figure IV-3 is opened after the X_1 node in the G_{21} branch, as shown in Figure IV-6.

The open-loop transfer function is

$$-\frac{X_1'}{X_1} = -\frac{D_1 G_{21}}{1 + D_1 G_{11}} \cdot \frac{D_2 G_{12}}{1 + D_2 G_{22}} \quad (\text{IV-25})$$

The same transfer function is obtained if the system is opened after the X_2 node in the G_{12} branch. We may also write (IV-25) in the form

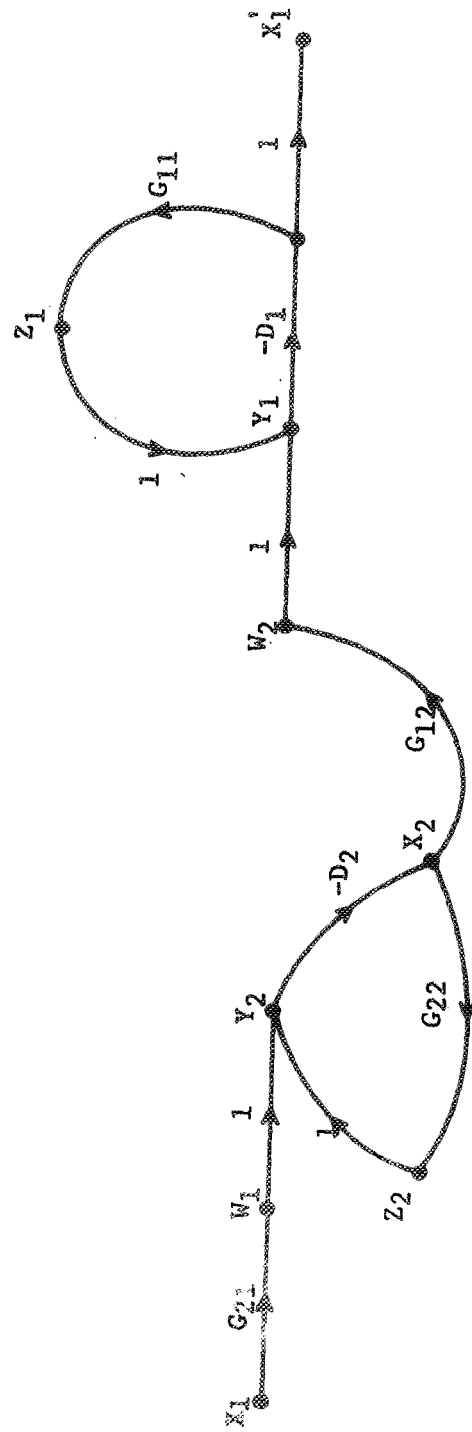


Figure IV-6. Figure IV-3 opened after X_1 node in G_{21} branch.

$$-\frac{X_1^i}{X_1} = -\frac{D_1 G_{21} G_{12}}{1 + D_1 G_{11}} - \frac{D_2 G_{12} G_{21}}{1 + D_2 G_{22}} - \frac{1}{G_{12} G_{21}} \quad (IV-26)$$

It is observed that the decoupling procedure should cause (IV-26) to be negligibly small. Further, the denominators, $(1 + D_1 G_{11})$ and $(1 + D_2 G_{22})$, have been designed so as to not contain zeroes which lie in the right-half s -plane. Hence, by the Nyquist criterion, (IV-25) represents a stable system characteristic equation.

To illustrate the design procedure, consider the system of Figure IV-2 with

$$G_{11} = G_{22} = \frac{4(s/8 + 1)(-s/8 + 1)}{(s/10)^2 + 2(.05)s/10 + 1} \quad (IV-27)$$

and

$$G_{21} = G_{12} = \frac{1}{s/10 + 1} \quad (IV-28)$$

Since the system is symmetrical, it is only necessary to consider the open-loop transfer function, $-E_1^i/E_1$. A computer program (Appendix B) was written to obtain the frequency response of (IV-23). Data was obtained for G_{11} , $G_{21}G_{12}/(1 + G_{22})$, and the total uncompensated open-loop transfer function. This data was plotted as a Nyquist diagram and appears in Figure IV-7. It is observed that the total uncompensated open-loop transfer function may be accurately approximated by the G_{11} term.

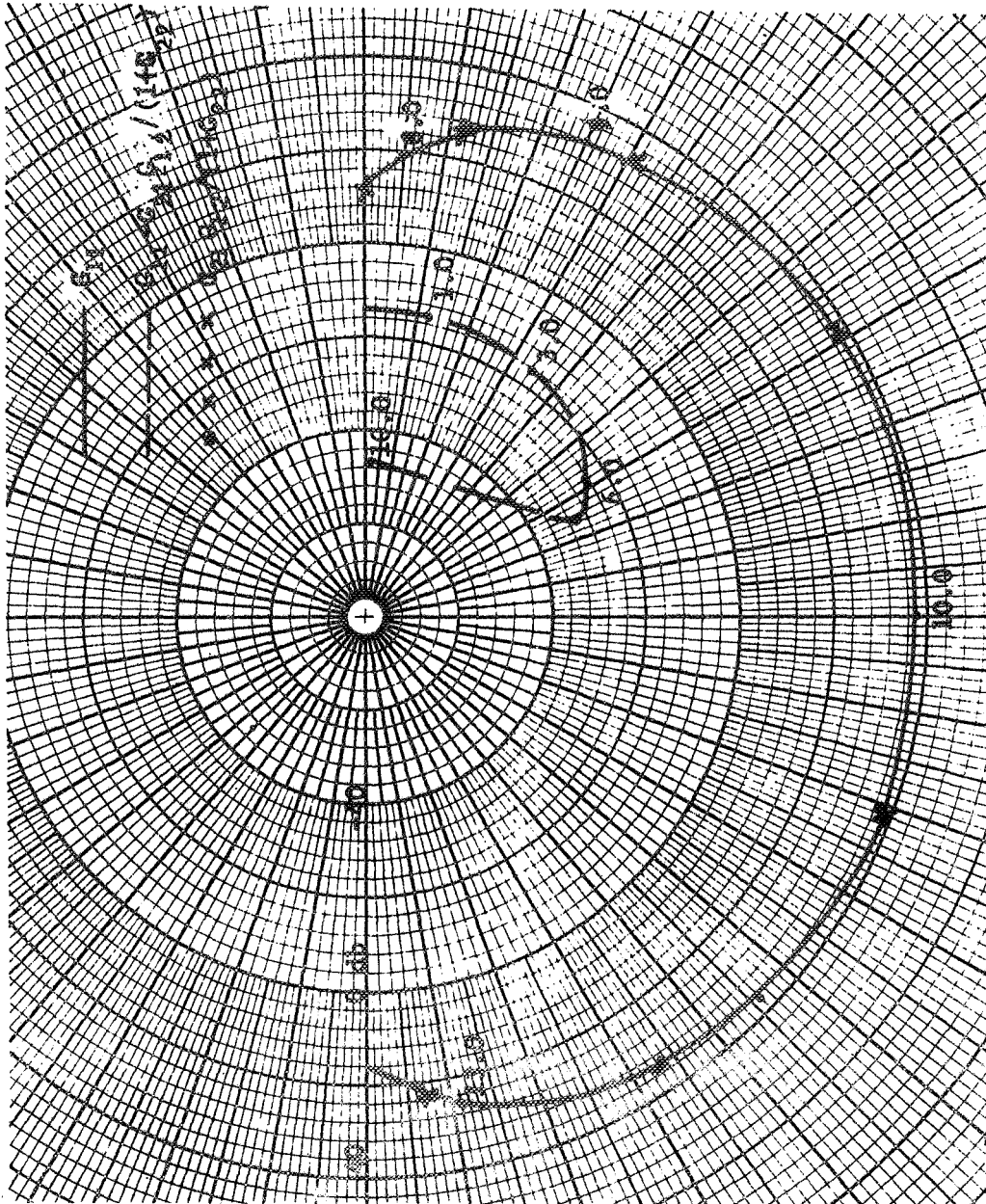


Figure IV-7. Uncompensated Nyquist diagram.

Hence, it will not be necessary to initially specify the compensation so as to decouple the system. However this example will illustrate all other points of the design procedure. Later in this chapter, an example is given for which it is necessary to specify the compensation so as to decouple the system.

It is also observed that the system is unstable, by the Nyquist criterion, since G_{11} encircles the 0 db pt. once in the clockwise direction. Then the compensation must stabilize the system and obtain the required gain and phase margins.

A Bode plot was made for G_{11} , from which it was determined that a compensation,

$$D_1 = \frac{1}{s(s/1.5 + 1)} \quad , \quad (IV-29)$$

would achieve a gain margin of approximately 6 db and a phase margin of approximately 30 degrees. Table IV-1 was then established to check the open-loop transfer function for decoupling. The value of each function listed in Table IV-1 is given in db magnitude and degrees phase shift at the various values of frequency. The term, $D_2 G_{22}/1 + D_2 G_{22}$ is obtained by means of the Nichols chart, as shown in Figure IV-8, where

$$D_2 G_{22} = D_1 G_{11} \quad . \quad (IV-30)$$

TABLE IV-1

Design Test for Decoupling

ω	G_{11}		$D_2 G_{22}$		D_2		$G_{12} \quad G_{21}$		$D_2 G_{12} G_{21}$	
			$1 + D_2 G_{22}$		$1 + D_2 G_{22}$				$1 + D_2 G_{22}$	
1.0	12.3	-.6	.6	-15	-11.7	-14.4	0.0	-12	-11.7	-26.4
1.5	12.5	-.9	1.4	-24	-11.1	-23.1	0.0	-18	-11.1	-41.1
2.0	12.9	-1.2	2.3	-35	-10.6	-33.8	0.0	-30	-10.6	-63.8
3.0	14.0	-1.9	3.4	-60	-10.6	-58.1	-.5	-46	-11.1	-104.1
4.0	15.5	-2.7	2.5	-104	-13.0	-101.3	-1.0	-54	-14.0	-155.3
5.0	17.4	-3.8	2.0	-120	-15.4	-116.2	-2.0	-60	-17.4	-176.2
6.0	19.8	-5.4	-1.0	-144	-20.8	-138.6	-3.0	-66	-23.8	-204.6
7.0	22.7	-7.8	-7.0	-162	-29.7	-154.2	-4.0	-72	-33.7	-226.2
7.6	24.9	-10.2	-4.0	-180	-28.9	-169.8	-4.0	-80	-32.9	-249.8

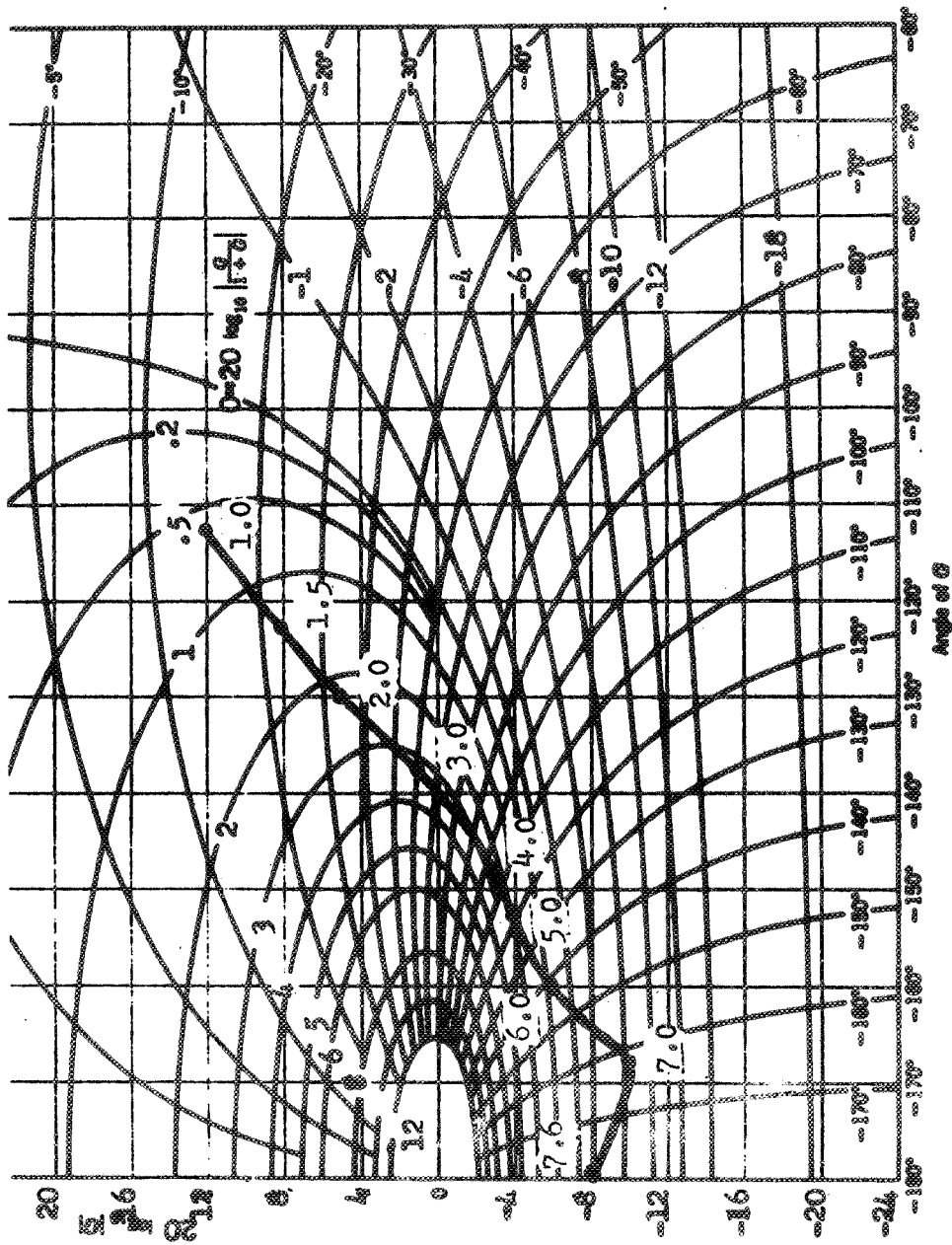


Figure IV-8. Nichols chart determination of $D_2 G_{22} / (1 + D_2 G_{22})$.

Then, from (IV-27), the term $D_2/(1 + D_2G_{22})$ is obtained. The term, $G_{12}G_{21}$, is then added to obtain the final entry in the table. Comparison of the values listed for the last term in the table with the values listed for G_{11} indicate that the system is reasonably decoupled for the range of frequencies shown, since

$$|G_{11}| > 10 \cdot |D_2G_{12}G_{21}/(1 + D_2G_{22})| \quad . \quad (\text{IV-31})$$

The range of frequencies listed was considered to be the critical range since it was attempted to establish the gain and phase margins for the open-loop transfer function over this frequency range.

A digital computer program (Appendix B) was then run to obtain the compensated system frequency response. The results are shown in Figure IV-9, indicating a gain margin of 6.5 db and a phase margin of 30°. The results of Table IV-1 are also verified.

A digital computer program was then written to simulate the compensated system utilizing the IBM S/360 Continuous System Modeling Program. This program is given in Appendix C. The results of the simulation are given in Figure IV-10, where the output $y_1(t)$ is given for a step input in the $y_1(t)$ channel and in input in the $y_2(t)$ channel. The output $y_2(t)$ is also given for the same conditions. It is noted that the peak value of $y_2(t)$ is reasonably small, settling out to a steady-state value of zero.

In this example and in the example which follows in section C of this chapter, no attempt is made to arrive at a "best" compensation. The examples are used only to illustrate the proposed design procedure.

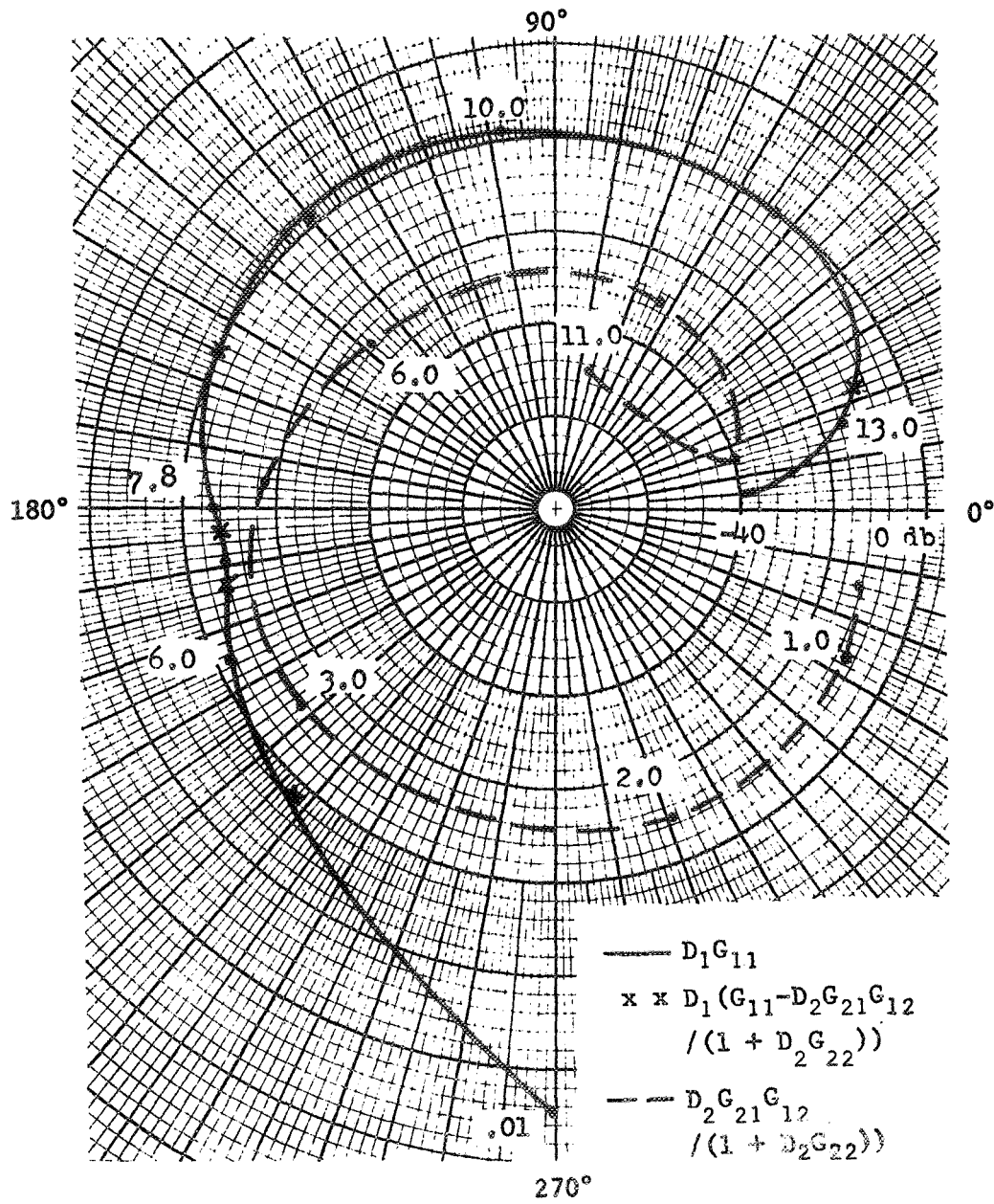


Figure IV-9. Compensated Nyquist diagram.



Figure IV-10. System time-response for $r_1(t) = u(t)$, $r_2(t) = 0$.

C. Extension of the Open-Loop Technique
to Two-Channel, Sampled-Data Systems.

The analysis of the continuous, two-channel, coupled system will now be extended to the sampled-data, two-channel coupled system of Figure IV-11. The system of Figure IV-11 will first be analyzed for the case that all sampling in the system is synchronous and at the same rate. The case for multirate sampling will then be considered and carried to the case that the fast-rate sampling is at a different rate in each channel.

Figure IV-12 is a signal-flow graph representation of the system of Figure IV-11, with single-rate sampling, opened at $E_1(z)$. The open-loop transfer function, $-E'_1(z)/E_1(z)$, is obtained by applying Mason's gain formula and is

$$-\frac{E'_1(z)}{E_1(z)} = D_1(z) \left\{ G_{11}(z) - \frac{D_2(z)G_{21}(z)G_{12}(z)}{1 + D_2(z)G_{22}(z)} \right\}, \quad (\text{IV-32})$$

where

$$G_{ij}(z) = Z \left\{ \frac{1 - \exp(-Ts)}{s} \cdot G_{ij}(s) \right\}. \quad (\text{IV-33})$$

Likewise, if the system is opened at the signal $E_2(z)$, the following open-loop transfer function is obtained:

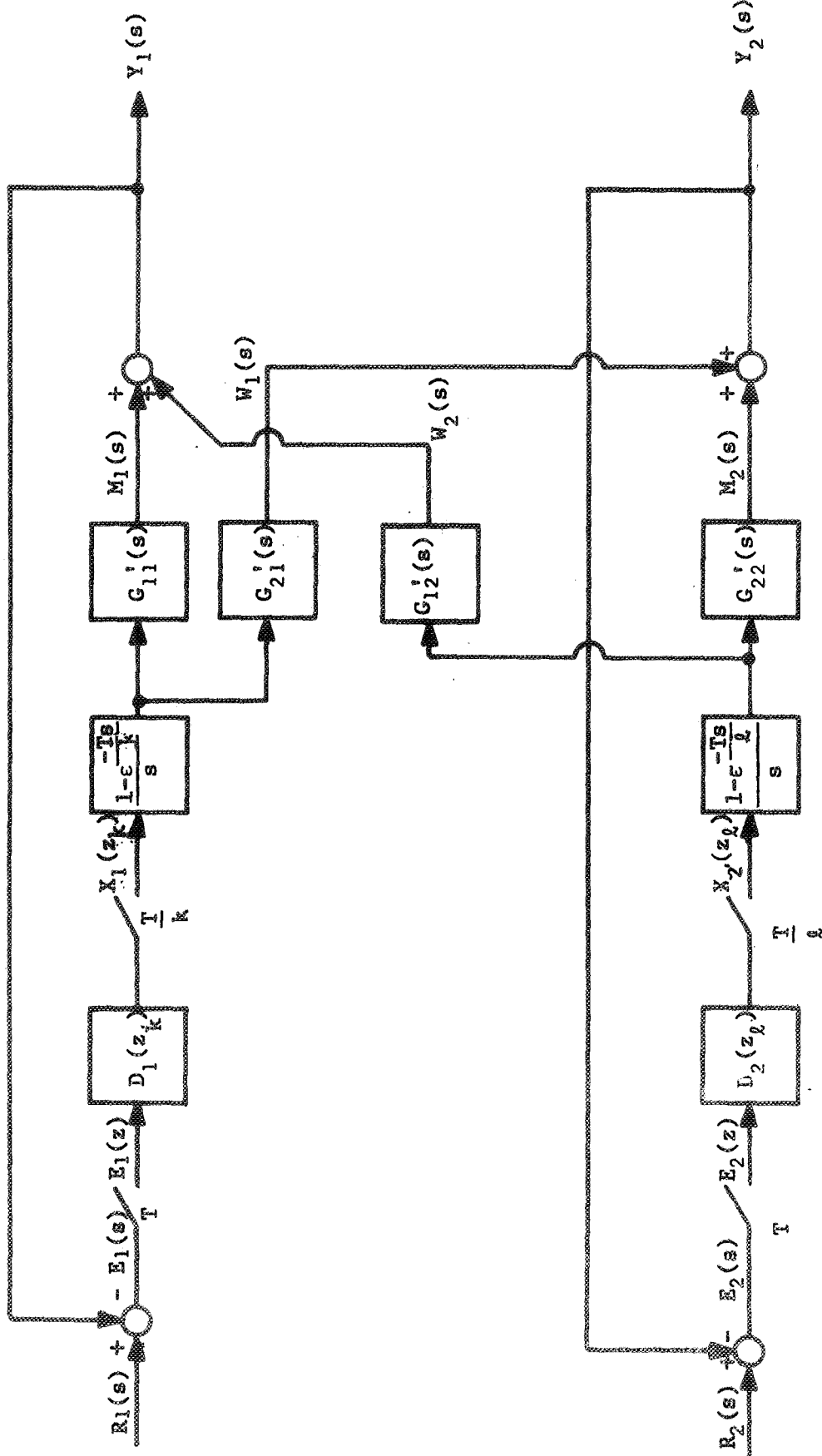


Figure IV-11. Two-channel, cross-coupled, sampled-data system.

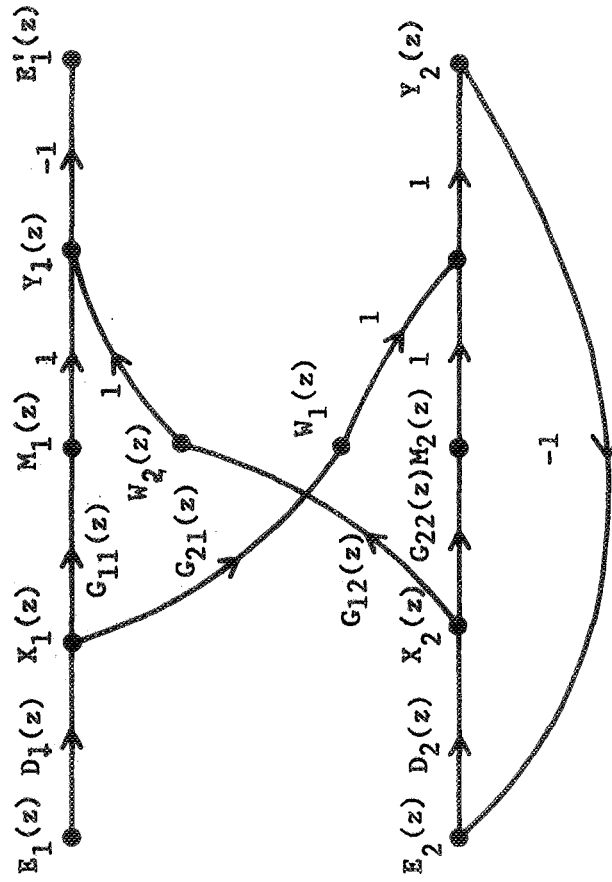


Figure IV-12. Single-rate system opened at $E_1(z)$.

$$-\frac{E_2^i(z)}{E_2(z)} = D_2(z) \left\{ G_{22}(z) - \frac{D_1(z)G_{21}(z)G_{12}(z)}{1 + D_1(z)G_{11}(z)} \right\}. \quad (\text{IV-34})$$

Hence, the same design technique as was applied to the continuous case may also be applied to the single-rate discrete case. However, in considering the loop due to cross-coupling, an important consideration arises. Whereas, for the continuous case, it does not matter whether this loop is opened in front of or after the cross-coupling transfer functions, for the sampled-data case, an approximation technique must be utilized in order to obtain an open-loop transfer function if this loop is opened in front of the cross-coupling transfer function [7]. However, an open-loop transfer function can be written if a data-hold is added in front of the cross-coupling transfer function. The addition of the data-hold in no way affects the operation of the system. An open-loop transfer function may also be written if the loop is opened after the cross-coupling transfer function. To obtain the open-loop transfer function for this condition, the system of Figure IV-11 will be opened after the $G_{21}^i(s)$ transfer function block, as shown in Figure IV-13. Note that Figure IV-13 is a z-transform signal-flow graph representation of the above condition. The open-loop transfer function, $-W_1^i(z)/W_1(z)$, is

$$-\frac{W_1^i(z)}{W_1(z)} = \frac{-D_1(z)G_{21}(z)}{1 + D_1(z)G_{11}(z)} \cdot \frac{D_2(z)G_{12}(z)}{1 + D_2(z)G_{22}(z)}. \quad (\text{IV-35})$$

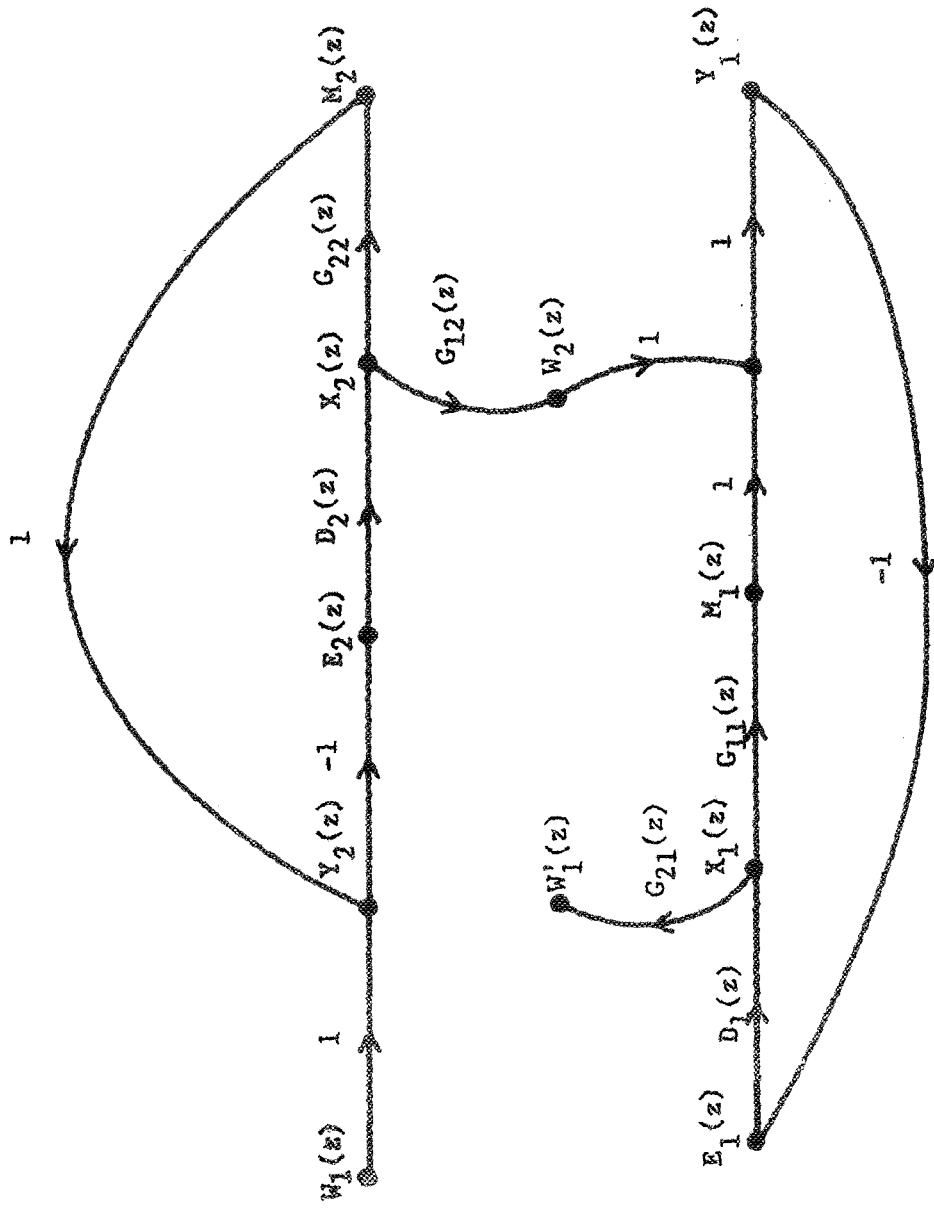


Figure IV-13. Single-rate system opened after cross-coupling transfer function block.

The w -plane design procedure [1] for sampled-data systems may now be extended to the multiple input-multiple output case. That is, the w -transform representation of (IV-32), (IV-34), and (IV-35) may be obtained. The compensated form of these equations would be

$$-\frac{E_1'(w)}{E_1(w)} = D_1(w) \left\{ G_{11}(w) - \frac{D_2(w)G_{21}(w)G_{12}(w)}{1 + D_2(w)G_{22}(w)} \right\}, \quad (\text{IV-36})$$

$$-\frac{E_2'(w)}{E_2(w)} = D_2(w) \left\{ G_{22}(w) - \frac{D_1(w)G_{21}(w)G_{12}(w)}{1 + D_1(w)G_{11}(w)} \right\}, \quad (\text{IV-37})$$

and

$$-\frac{W_1'(w)}{W_1(w)} = \frac{-D_1(w)G_{21}(w)}{1 + D_1(w)G_{11}(w)} + \frac{D_2(w)G_{12}(w)}{1 + D_2(w)G_{22}(w)}. \quad (\text{IV-38})$$

A Bode plot design procedure may be used, since the region of stability is the left-half w -plane. In order to decouple the system, we observe, as in the continuous case, that the second term on the right of equations (IV-36) and (IV-37) must be made negligible with respect to the first term. If this is done, then by application of the Nyquist criterion, equation (IV-38) represents a stable system. Essentially the same procedure for compensator design as was presented for the continuous case may also be followed here. At this point, the multirate sampled-data

case will be developed. An example which illustrates the design procedure for a sampled-data system will then be presented.

For the system of Figure IV-11, let k and l be integers greater than unity, k not necessarily equal to l , but the ratio of l to k is an integer, r . Opening the system at $E_1(z)$, we may write the following set of discrete equations:

$$Y_1(z) = M_1(z) + W_2(z) \quad , \quad (\text{IV-39})$$

$$M_1(z) = E_1(z) \frac{1}{k} \sum_{p=0}^{k-1} D_1(z\epsilon^{j\phi_p^i})_k G_{11}(z\epsilon^{j\phi_p^i})_k \quad , \quad (\text{IV-40})$$

$$W_2(z) = E_2(z) \frac{1}{l} \sum_{p=0}^{l-1} D_2(z\epsilon^{j\phi_p^i})_l G_{12}(z\epsilon^{j\phi_p^i})_l \quad , \quad (\text{IV-41})$$

$$E_1'(z) = -Y_1(z) \quad , \quad (\text{IV-42})$$

$$E_2(z) = -Y_2(z) \quad , \quad (\text{IV-43})$$

$$Y_2(z) = M_2(z) + W_1(z) \quad , \quad (\text{IV-44})$$

$$W_1(z) = E_1(z) \frac{1}{k} \sum_{p=0}^{k-1} D_1(z\epsilon^{j\phi_p^i})_k G_{21}(z\epsilon^{j\phi_p^i})_k \quad , \quad (\text{IV-45})$$

$$M_2(z) = E_2(z) \frac{1}{l} \sum_{p=0}^{l-1} D_2(z\epsilon^{j\phi_p^i})_l G_{22}(z\epsilon^{j\phi_p^i})_l \quad , \quad (\text{IV-46})$$

where

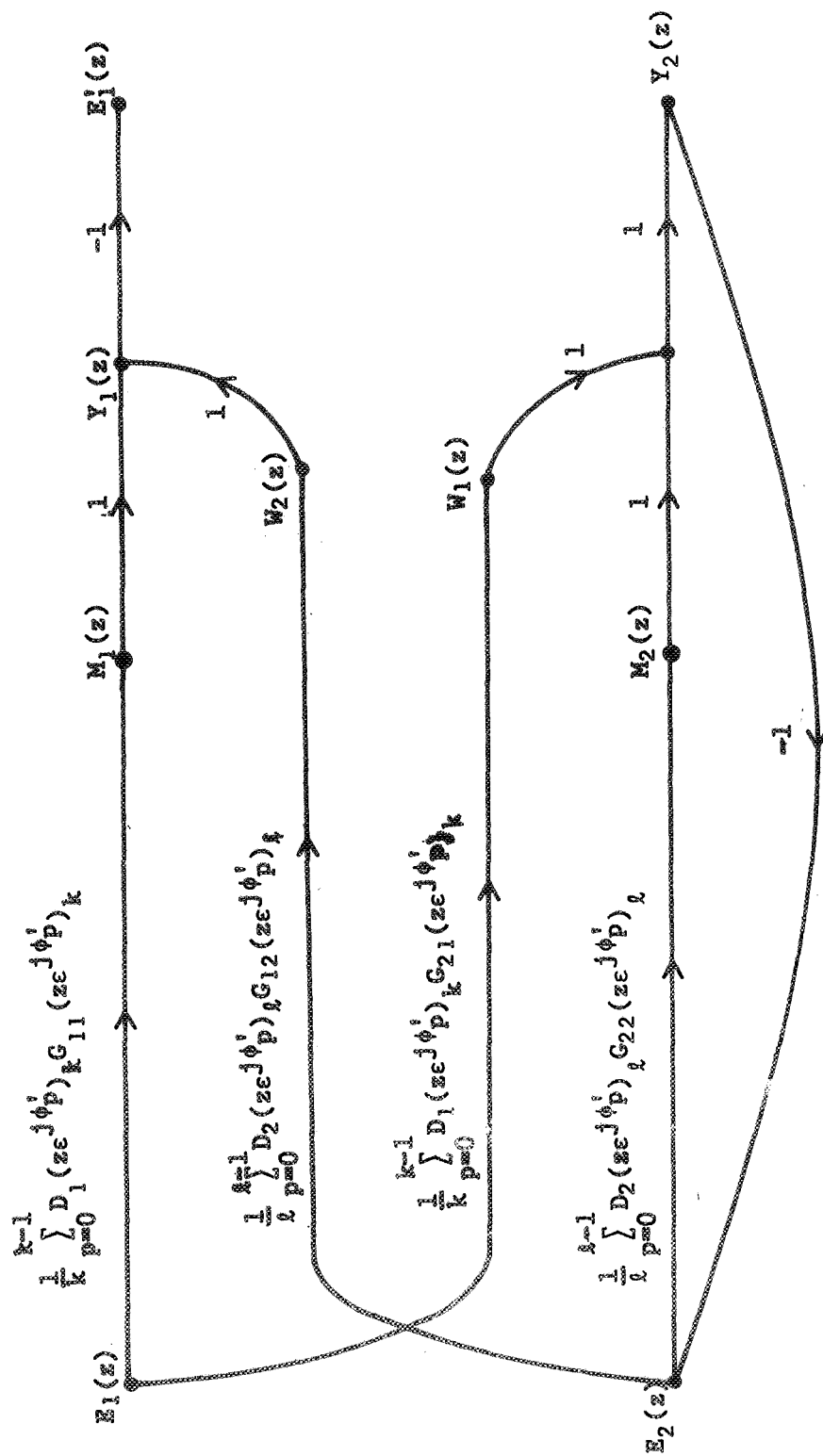
$$\phi_p^i = 2\pi p \quad . \quad (IV-47)$$

Figure IV-14 is a signal-flow graph representation of the above set of equations. The open-loop transfer function is

$$\begin{aligned} - \frac{E_1'(z)}{E_1(z)} &= \frac{1}{k} \sum_{p=0}^{k-1} D_1(z\epsilon^{j\phi_p^i})_k G_{11}(z\epsilon^{j\phi_p^i})_k \\ &= \frac{\frac{1}{k} \sum_{p=0}^{k-1} D_1(z\epsilon^{j\phi_p^i})_k G_{21}(z\epsilon^{j\phi_p^i})_k \cdot \frac{1}{\ell} \sum_{p=0}^{\ell-1} D_2(z\epsilon^{j\phi_p^i})_\ell G_{12}(z\epsilon^{j\phi_p^i})_\ell}{1 + \frac{1}{\ell} \sum_{p=0}^{\ell-1} D_2(z\epsilon^{j\phi_p^i})_\ell G_{22}(z\epsilon^{j\phi_p^i})_\ell} \quad . \end{aligned} \quad (IV-48)$$

In the same manner, if the system is opened at $E_2(z)$, the open-loop transfer function is

$$\begin{aligned} - \frac{E_2'(z)}{E_2(z)} &= \frac{1}{\ell} \sum_{p=0}^{\ell-1} D_2(z\epsilon^{j\phi_p^i})_\ell G_{22}(z\epsilon^{j\phi_p^i})_\ell \\ &= \frac{\frac{1}{\ell} \sum_{p=0}^{\ell-1} D_2(z\epsilon^{j\phi_p^i})_\ell G_{12}(z\epsilon^{j\phi_p^i})_\ell \cdot \frac{1}{k} \sum_{p=0}^{k-1} D_1(z\epsilon^{j\phi_p^i})_k G_{21}(z\epsilon^{j\phi_p^i})_k}{1 + \frac{1}{k} \sum_{p=0}^{k-1} D_1(z\epsilon^{j\phi_p^i})_k G_{11}(z\epsilon^{j\phi_p^i})_k} \quad . \end{aligned} \quad (IV-49)$$

Figure IV-14. Two input-two output, multirate system opened at $E_1(z)$.

If the remaining loop is opened after the $G_{21}'(s)$ block, the open-loop transfer function is

$$\begin{aligned}
 - \frac{W_1'(z)}{W_1(z)} = - \frac{\frac{1}{k} \sum_{p=0}^{k-1} D_1(z\epsilon^j \phi_p^i)_k G_{21}(z\epsilon^j \phi_p^i)_k}{1 + \frac{1}{k} \sum_{p=0}^{k-1} D_1(z\epsilon^j \phi_p^i)_k G_{11}(z\epsilon^j \phi_p^i)_k} \\
 \cdot \frac{\frac{1}{\ell} \sum_{p=0}^{\ell-1} D_2(z\epsilon^j \phi_p^i)_\ell G_{12}(z\epsilon^j \phi_p^i)_\ell}{1 + \frac{1}{\ell} \sum_{p=0}^{\ell-1} D_2(z\epsilon^j \phi_p^i)_\ell G_{22}(z\epsilon^j \phi_p^i)_\ell} \quad (IV-50)
 \end{aligned}$$

It is noted that if the system is decoupled by the design procedure, (IV-50) represents a stable system characteristic equation, as in the previous cases.

It is desired to extend the results of Chapter III for the single-loop, multirate case to the two input-two output case. This will be done by transforming (IV-48) to the z_k -plane and (IV-49) to the z_ℓ -plane, then taking the w_k and w_ℓ transforms, respectively, of the resulting relationships.

Proceeding with (IV-48), the substitution of $r \cdot k$ for ℓ and z_k for $z^{1/k}$ obtains

$$\begin{aligned}
-\frac{E_1(z_k)}{E_1(z_k)} &= \frac{1}{k} \sum_{p=0}^{k-1} D_1(z_k \epsilon^{j\phi_{pk}}) G_{11}(z_k \epsilon^{j\phi_{pk}}) \\
&\quad - \frac{\frac{1}{k} \sum_{p=0}^{k-1} D_1(z_k \epsilon^{j\phi_{pk}}) G_{21}(z_k \epsilon^{j\phi_{pk}}) \cdot \frac{1}{l} \sum_{p=0}^{l-1} D_2(z_k \epsilon^{j\phi_{pk}}) G_{12}(z_k \epsilon^{j\phi_{pk}})_{\frac{1}{r}}}{1 + \frac{1}{l} \sum_{p=0}^{l-1} D_2(z_k \epsilon^{j\phi_{pk}}) G_{22}(z_k \epsilon^{j\phi_{pk}})_{\frac{1}{r}}}
\end{aligned}
\tag{IV-51}$$

For (IV-49), the substitution of l/r for k and z_l for $z^{1/l}$ obtains

$$\begin{aligned}
-\frac{E_2(z_l)}{E_2(z_l)} &= \frac{1}{l} \sum_{p=0}^{l-1} D_2(z_l \epsilon^{j\phi_{pl}}) G_{22}(z_l \epsilon^{j\phi_{pl}}) \\
&\quad - \frac{\frac{1}{l} \sum_{p=0}^{l-1} D_2(z_l \epsilon^{j\phi_{pl}}) G_{12}(z_l \epsilon^{j\phi_{pl}}) \cdot \frac{1}{k} \sum_{p=0}^{k-1} D_1(z_l \epsilon^{j\phi_{pl}}) G_{21}(z_l \epsilon^{j\phi_{pl}})_{\frac{1}{r}}}{1 + \frac{1}{k} \sum_{p=0}^{k-1} D_1(z_l \epsilon^{j\phi_{pl}}) G_{11}(z_l \epsilon^{j\phi_{pl}})_{\frac{1}{r}}}
\end{aligned}
\tag{IV-52}$$

For (IV-51) and (IV-52),

$$\phi_{pk} = \frac{2\pi p}{k} \tag{IV-53}$$

and

$$\phi_{pl} = \frac{2\pi p}{l} \tag{IV-54}$$

As previously noted, in general, the compensators must be specified so as to attenuate the frequency sidebands inherently present in the sampled outputs of the compensators and distributed about multiples of $2\pi/T$ radians/seconds [6]. With regard to equations (IV-51) and (IV-52), this specification would require each of the summations in the two equations to be low-pass with respect to the slow-rate sampling frequency. That is, each of the summation terms would be accurately approximated by the first term in the summation. It will be assumed that the compensated system must satisfy the above condition. Then equations (IV-51) and (IV-52) may be written.

$$-\frac{E'_1(z_k)}{E_1(z_k)} = \frac{D_1(z_k)}{k} \left\{ G_{11}(z_k) - \frac{\frac{1}{l} D_2(z_k)_r G_{21}(z_k) G_{12}(z_k)_r}{1 + \frac{1}{l} D_2(z_k)_r G_{22}(z_k)_r} \right\}. \quad (\text{IV-55})$$

and

$$-\frac{E'_2(z_l)}{E_2(z_l)} = \frac{D_2(z_l)}{l} \left\{ G_{22}(z_l) - \frac{\frac{1}{k} D_1(z_l)_{\frac{1}{r}} G_{21}(z_l)_{\frac{1}{r}} G_{12}(z_l)}{1 + \frac{1}{k} D_1(z_l)_{\frac{1}{r}} G_{11}(z_l)_{\frac{1}{r}}} \right\}. \quad (\text{IV-56})$$

It is observed that each of the above equations is written in terms of the fast-rate variable corresponding to the fast-rate sampling frequency associated with the compensator transfer function which appears outside the parenthesis in each case. It will be assumed that it is

desired to decouple the system. The first step in the design procedure is to obtain the uncompensated frequency response for the equations (IV-55) and (IV-56). This is done by means of the procedure presented in Chapter III concerning the digital computation of the frequency response. This procedure provides for the computation of the frequency response at various values of ω in the s -domain. The degree of decoupling of the two uncompensated open-loop transfer functions may be checked by comparing the second term of each equation against the respective first term at various values of ω . If it is determined that the uncompensated open-loop transfer functions are not sufficiently decoupled, a preliminary compensation to decouple the system may be specified by making a Bode plot of $(1/l)G_{22}(w_l)$, plotting db magnitude and degree phase shift against $\log_{10}(w_l)$, where

$$w_l = \frac{z_l - 1}{z_l + 1} \quad (IV-57)$$

The compensator $D_2(w_l)$ may then be specified to decouple (IV-55) by adjusting $(1/l)D_2(w_l)G_{22}(w_l)$ such that $D_2(w_l)G_{12}(w_l)G_{21}(w_l)/l + D_2(w_l)G_{22}(w_l)$ is sufficiently minimized. This procedure may be facilitated by utilizing the Nichols chart, locating the term $(1/l)D_2(w_l)G_{22}(w_l)$ in a region of the Nichols chart so as to minimize $D_2(w_l)G_{22}(w_l)/l + D_2(w_l)G_{22}(w_l)$. The preliminary specification for $D_1(w_k)$ is obtained in the same manner. The specification of the compensation may then be refined by adjusting the

Bode plots of $(1/k)D_1(w_k)G_{11}(w_k)$ and $(1/l)D_2(w_l)G_{22}(w_l)$ to achieve the desired gain and phase margins. The compensated open-loop transfer functions should then be checked to insure that the desired degree of decoupling has not been lost.

The procedure outlined in the preceding paragraphs will now be illustrated by an example. For the system of Figure IV-11, let

$$G'_{11}(s) = \frac{10}{(s+1)(s/10+1)} \quad (\text{IV-58})$$

$$G'_{22}(s) = \frac{10}{(s+1)(s/15+1)} \quad , \quad (\text{IV-59})$$

and

$$G'_{12}(s) = G'_{21}(s) = \frac{1}{s/6+1} \quad . \quad (\text{IV-60})$$

Also, let T be .1 seconds, $k = 2$, and $l = 4$. The computer program of Appendix D was utilized to obtain the frequency-response for the open-loop transfer functions, $-E'_1(w_2)/E_1(w_2)$ and $-E'_2(w_4)/E_2(w_4)$. The results of the frequency-response program are plotted as a Nyquist diagram in Figures IV-15 and IV-16, where values of w_2 and w_4 are indicated respectively. It is noted from Figures IV-15 and IV-16 that a strong degree of coupling exists between the channels of the system.

In order to apply the Nyquist Criterion to determine the stability of the system, it is necessary to determine the number of poles of the

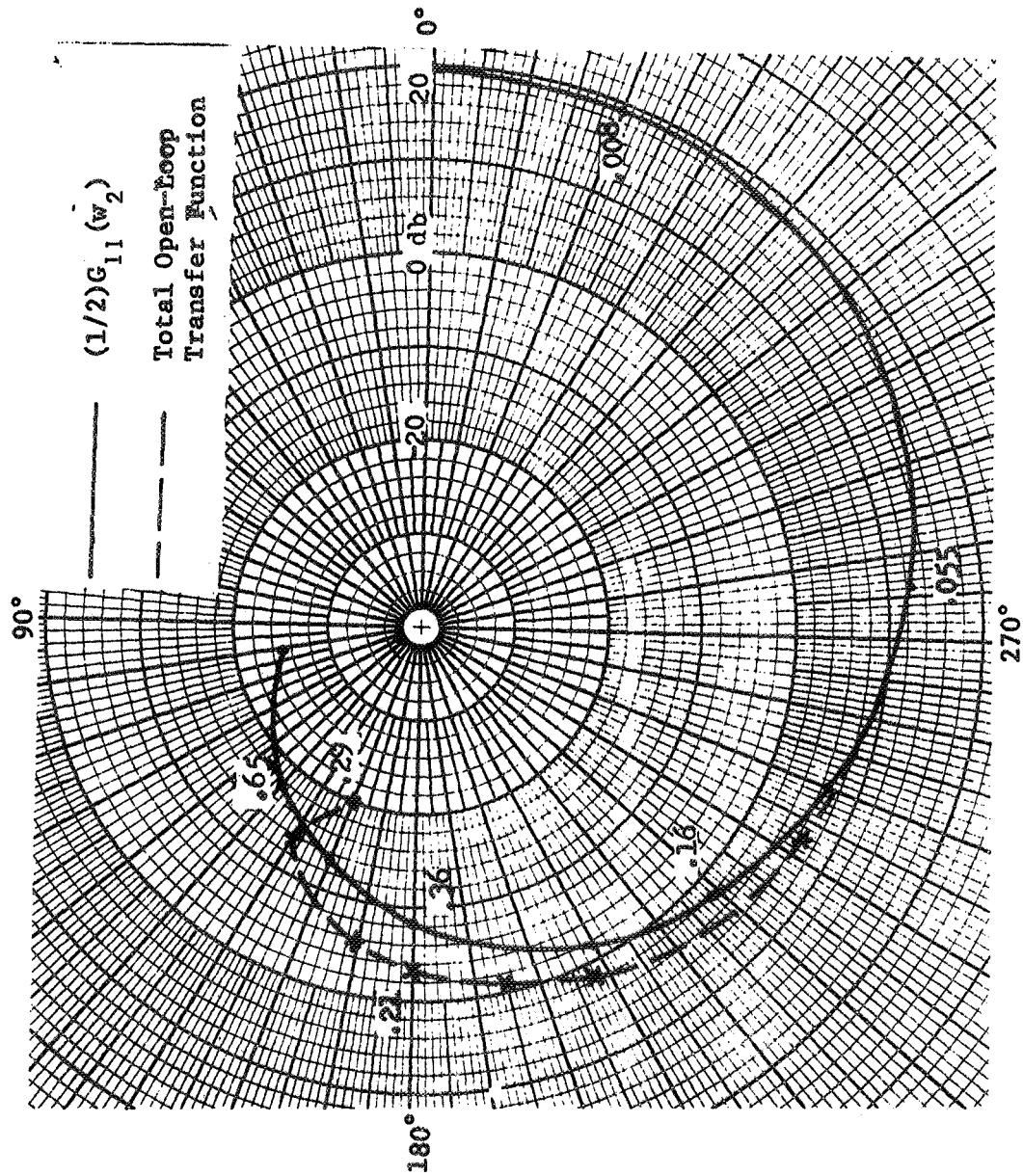


Figure IV-15. Uncompensated Nyquist diagram for $-E_1^*(w_2)/E_1(w_2)$.

uncompensated forms of equations (IV-55) and (IV-56) which lie in the right-half w_2 and w_4 -planes, respectively. Consider the uncompensated form of (IV-55). The poles of this equation are the poles of $G_{11}(w_2)$, $G_{21}(w_2)$, $G_{12}(w_2)_r$ and the zeroes of $1 + (1/4)G_{22}(w_2)_r$. The poles of $G_{11}(w_2)$, $G_{21}(w_2)$, $G_{12}(w_2)_r$, and $G_{22}(w_2)_r$ may be determined by means of the results of Chapter III (see equation III-18). Application of this procedure indicates that the aforementioned transfer functions contain no poles which lie in the right-half w_2 -plane. Observation of the diagram for $(1/4)G_{22}(w_4)$ in Figure IV-16 and application of the Nyquist Criterion shown that $1 + (1/4)G_{22}(w_2)_r$ has no zeroes in the right-half w_2 -plane. Then the open-loop transfer function, $-E'_1(w_2)/E_1(w_2)$, has no poles which lie in the right-half w_2 -plane. Application of the Nyquist Criterion to the Nyquist diagram of Figure IV-15 for the total uncompensated open-loop transfer function indicates that this open-loop transfer function is stable, with a gain margin of 3 db and a phase margin of 20 degrees. Application of the same procedure to the uncompensated open-loop transfer function, $-E_2(w_4)/E_2(w_4)$, indicates that this transfer function is also stable, with a gain margin of 9 db and a phase margin of 20 degrees.

The computer program of Appendix E was utilized to obtain a simulation of the uncompensated system. The results of the simulation are given in Figure IV-17, where the outputs $y_1(t)$ and $y_2(t)$ are plotted for a step input at $x_1(t)$ and no input at $x_2(t)$. These results also indicate a strong degree of coupling between channels. Further, there is considerable overshoot and oscillation present in both outputs.

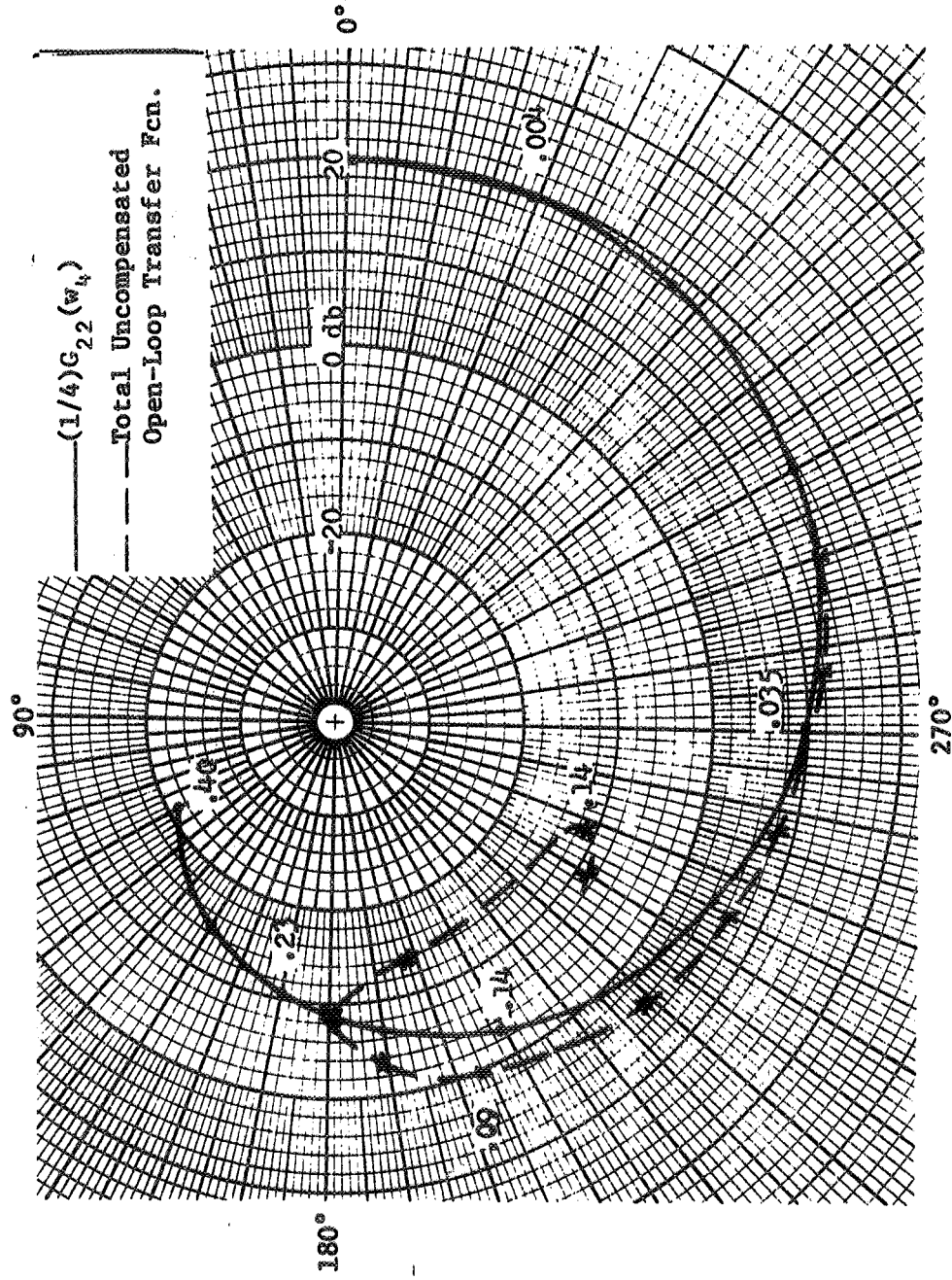


Figure IV-16. Uncompensated Nyquist diagram for $-E_2'(w_4)/E_2(w_4)$.

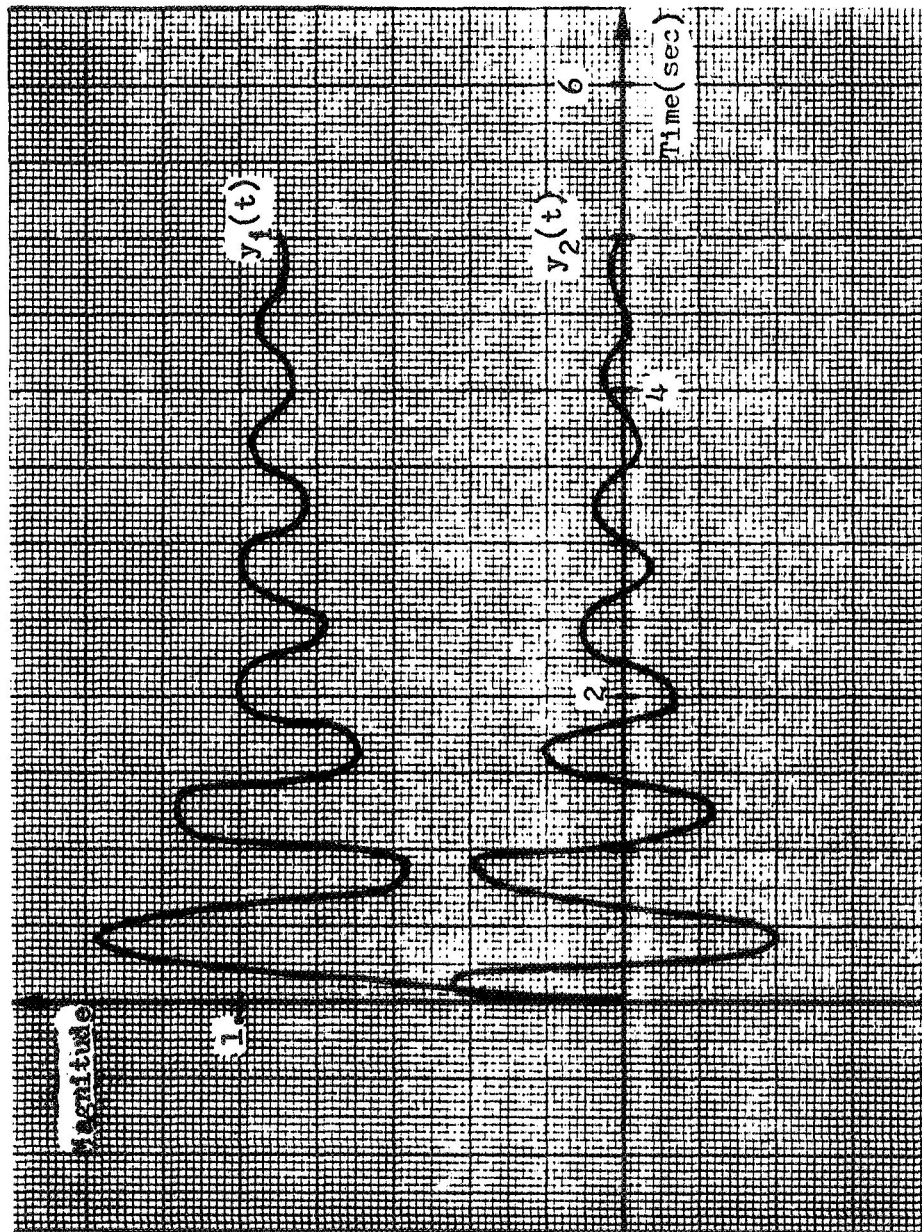


Figure IV-17. Uncompensated system time-response, $r_1(t) = u(t)$, $r_2(t) = 0$.

It will be attempted to compensate this system such that the degree of coupling is significantly reduced, such that the gain margin is at least 6 db and the phase margin is at least 30 degrees in each channel, and such that an s-domain closed-loop frequency bandwidth of 3 rad/sec is maintained. The specification for the compensator $D_1(w_2)$ will first be considered. The first step in the design procedure is to make a Bode plot for $G_{11}(w_2)$, $G_{21}(w_2)$, and $G_{22}(w_2)_r$. These Bode plots are shown in Figures IV-18 and IV-19. The bandwidth requirement of 3 rad/sec in the s-domain corresponds to an approximate value in the w_2 -plane of 7.9×10^{-2} . Hence, $(1/2)D_1(w_2)G_{11}(w_2)$ should be greater than 0 db for all values of w_2 less than 7.9×10^{-2} . A compensation

$$D_1(w_2) = \frac{.5}{\frac{w_2}{.079} + 1} \quad (\text{IV-61})$$

will cause the magnitude of $(1/2)D_1(w_2)G_{11}(w_2)$ to be 0 db at w_2 equal to 7.9×10^{-2} . The phase angle of $D_1(w_2)G_{11}(w_2)$ is -145° at this value of w_2 . From the Nichols chart of Figure IV-20, the magnitude of $D_1(w_2)G_{11}(w_2)/2 + D_1(w_2)G_{21}(w_2)$ is determined to be 4.5 db. The magnitudes of $(1/2)G_{11}(w_2)$ and $(1/2)G_{21}(w_2)$ are 9 db and -1 db respectively. Hence, the magnitude of $D_1(w_2)G_{21}(w_2)G_{12}(w_2)_2/8 + (4)D_1(w_2)G_{11}(w_2)$ is approximately -6.5 db at w_2 equal to 7.9×10^{-2} . Compared to the magnitude of $(1/4)G_{22}(w_2)_2$ at this value of w_2 , the above result is observed to provide a reasonable degree of decoupling for (IV-56).

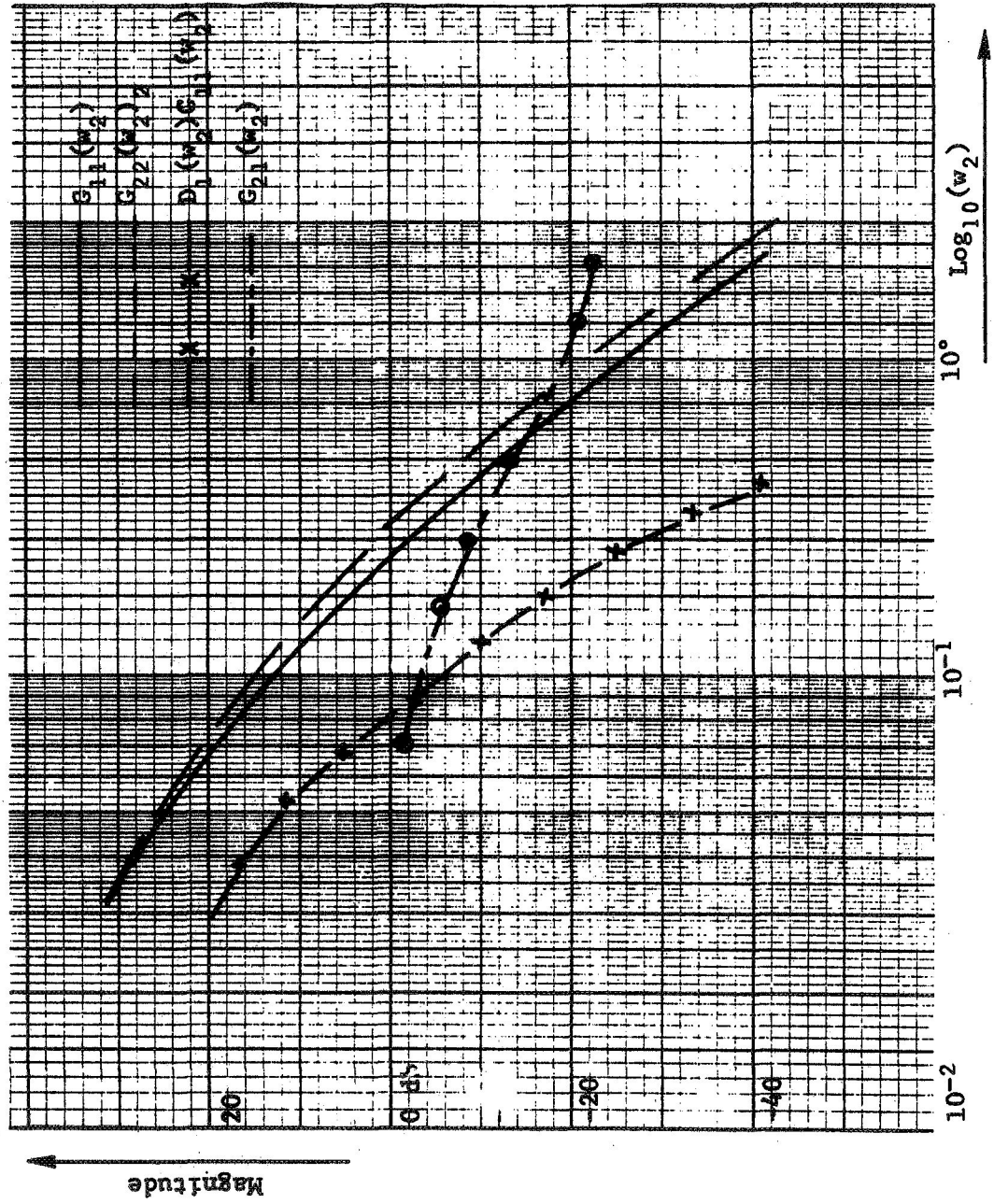


Figure IV-18. Db magnitude vs. $\text{Log}_{10}(w_2)$.

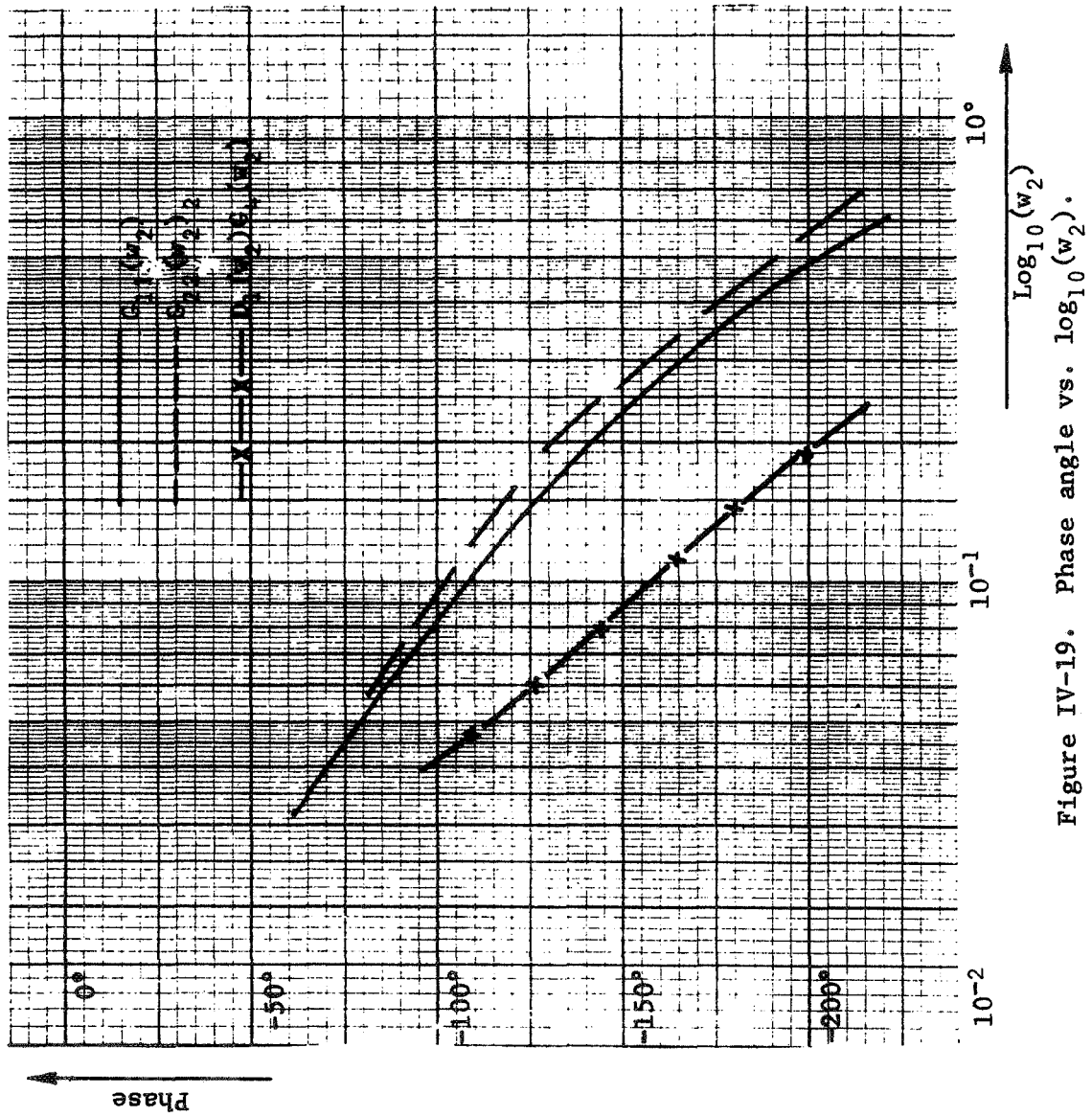


Figure IV-19. Phase angle vs. $\log_{10}(w_2)$.

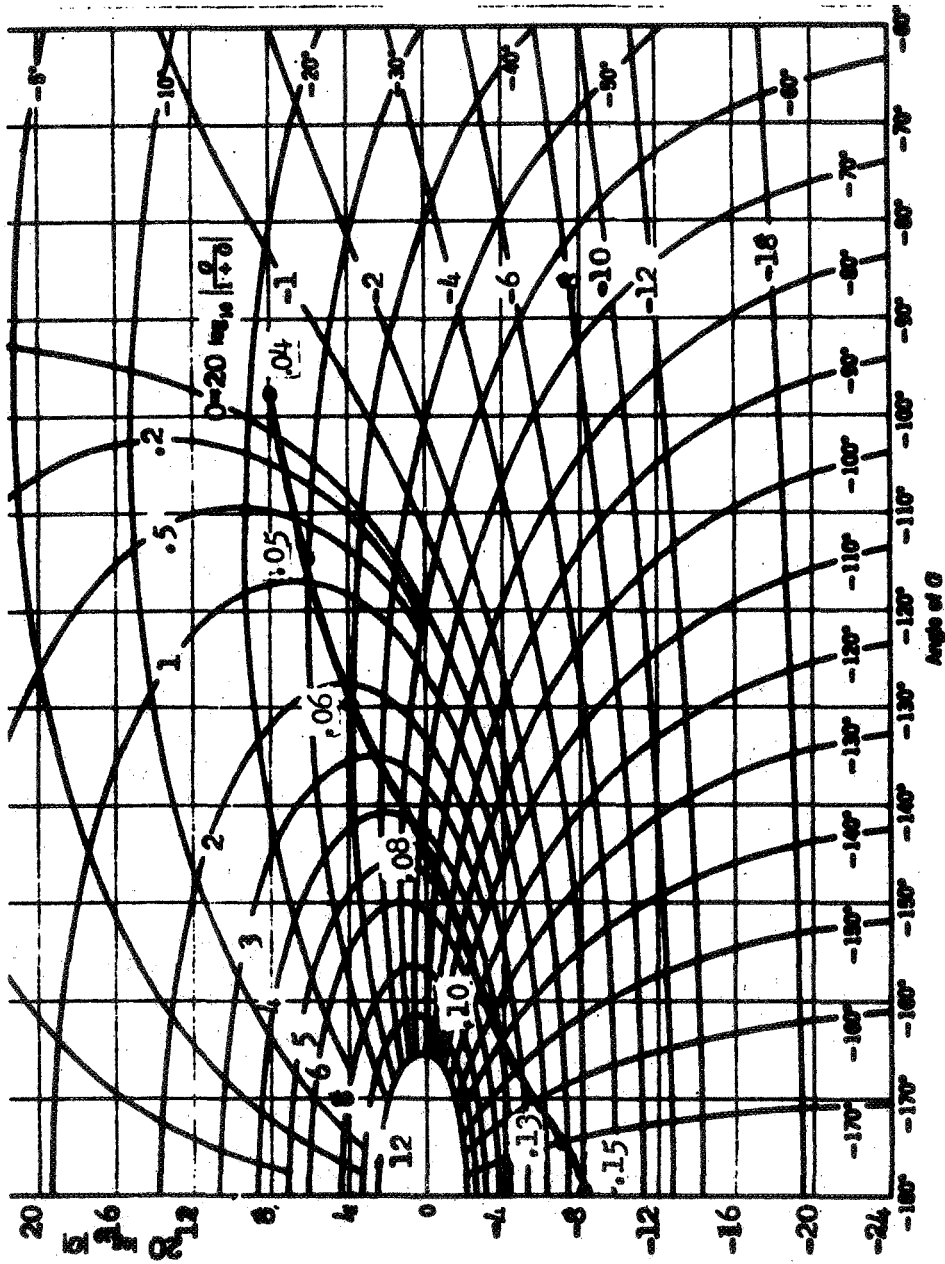


Figure IV-20. Nichols chart determination of $D_1(w_2)G_{11}(w_2)/2 + D_1(w_2)G_{11}(w_2)$.

Thus far, the compensator $D_1(w_2)$ has been specified so as to provide approximately the desired closed-loop bandwidth, achieve a reasonable degree of decoupling, and attain the required phase margin. It is now necessary to determine if the desired gain margin has been attained. The Bode plots of Figures IV-18 and IV-19 indicate that $(1/2)D_1(w_2)G_{11}(w_2)$ attains a phase shift of -180 degrees at w_2 equal to 1.4×10^{-1} , with a gain margin of 8 db. The Nichols chart of Figure IV-20 indicates the magnitude of $D_1(w_2)G_{11}(w_2)/2 + D_1(w_2)G_{11}(w_2)$ is -4 db. At this value of w_2 , $(1/2)G_{11}(w_2)$ is 3.5 db, $(1/4)G_{22}(w_2)_2$ is 4.5 db, and $(1/2)G_{21}(w_2)$ is -2.5 db. $(1/4)G_{12}(w_2)_2$ is approximately equal to $(1/2)G_{21}(w_2)$. Hence, $D_1(w_2)G_{21}(w_2)G_{12}(w_2)_2/8 + (4)D_1(w_2)G_{11}(w_2)$ has an approximate magnitude of -12.5 db at w_2 equal to 1.4×10^{-1} . A reasonable degree of decoupling is again seen to exist for (IV-56). Since Figures IV-18 and IV-19 indicate that $(1/4)G_{22}(w_2)_2$ has substantially the same gain and phase characteristics as $(1/2)G_{11}(w_2)$, it is expected that if $D_2(w_4)$ is made the same as the specification of $D_1(w_2)$, the design specifications will also be met in the second channel. The w_2 -plane frequency of 7.9×10^{-2} corresponds to a w_4 -plane frequency of 3.9×10^{-2} . Hence, the specification of $D_2(w_4)$ should be

$$D_2(w_4) = \frac{.5}{\frac{w_4}{.039} + 1} \quad (\text{IV-62})$$

With the aid of the Nichols chart of Figure IV-20, a test of the compensation may be made to check the degree of coupling. This test

may be of the form of Table IV-2. The values listed in Table IV-2 indicate db magnitude corresponding to w_2 frequency values. The values listed in the final column, when compared to the values listed for $(1/2)G_{11}(w_2)$, indicate that a reasonable degree of decoupling does exist.

The frequency-response for the compensated system was then computed, the results of which are given in Figures IV-21 and IV-22. These Figures indicate that the total open-loop transfer functions are accurately approximated by the $(1/2)D_1(w_2)G_{11}(w_2)$ and $(1/4)D_2(w_4)G_{22}(w_4)$ terms, respectively. Also, Figure IV-21 indicates a phase margin of 35 degrees and a gain margin of 10 db. Figure IV-22 indicates a phase margin of 40 degrees and a gain margin of 10.5 db.

A digital computer simulation of the compensated system was performed by means of the program of Appendix E, which utilizes the IBM System 360 Continuous System Modeling Program. The results of the simulation are given in Figures IV-23 and IV-24. Both of these figures indicate that the system is reasonably decoupled. Also, the response in each channel corresponding to a step input in the respective channel is seen to be relatively fast with a reasonably small settling time.

It is to be noted that the above results were achieved with simple first-order compensators. It should be expected that even better results would be achieved with second- or third-order compensators. It is also to be noted that the case treated by the example is the multi-rate sampled-data system with unequal fast-rate sampling in each channel. It would be very difficult to treat this particular case by means of the current state-space decoupling techniques [12]-[15], since it would

be necessary to obtain a discrete state variable description of the system.

Table IV-2. Design Test for Decoupling

w_2	G_{11}	$\frac{D_{22}G_{22}}{1+D_{22}G_{22}}$	$\frac{D_{22}}{1+D_{22}G_{22}}$	$G_{12}G_{21}$	$\frac{D_{22}G_{12}G_{21}}{1+D_{22}G_{22}}$
.04	14.5	-.2	-14.7	0.	-14.7
.05	13.0	.75	-12.25	-.50	-12.75
.06	11.0	2.3	-8.7	-1.0	-9.7
.08	8.5	4.5	-4.0	-2.0	-6.0
.10	6.9	5.0	-1.9	-3.0	-4.9
.13	4.1	-1.5	-5.6	-5.0	-10.6
.14	3.5	-4.0	-7.5	-5.5	-13.0

Figure IV-21. Compensated Nyquist diagram for $-E_1'(w_2)/E_1(w_2)$.

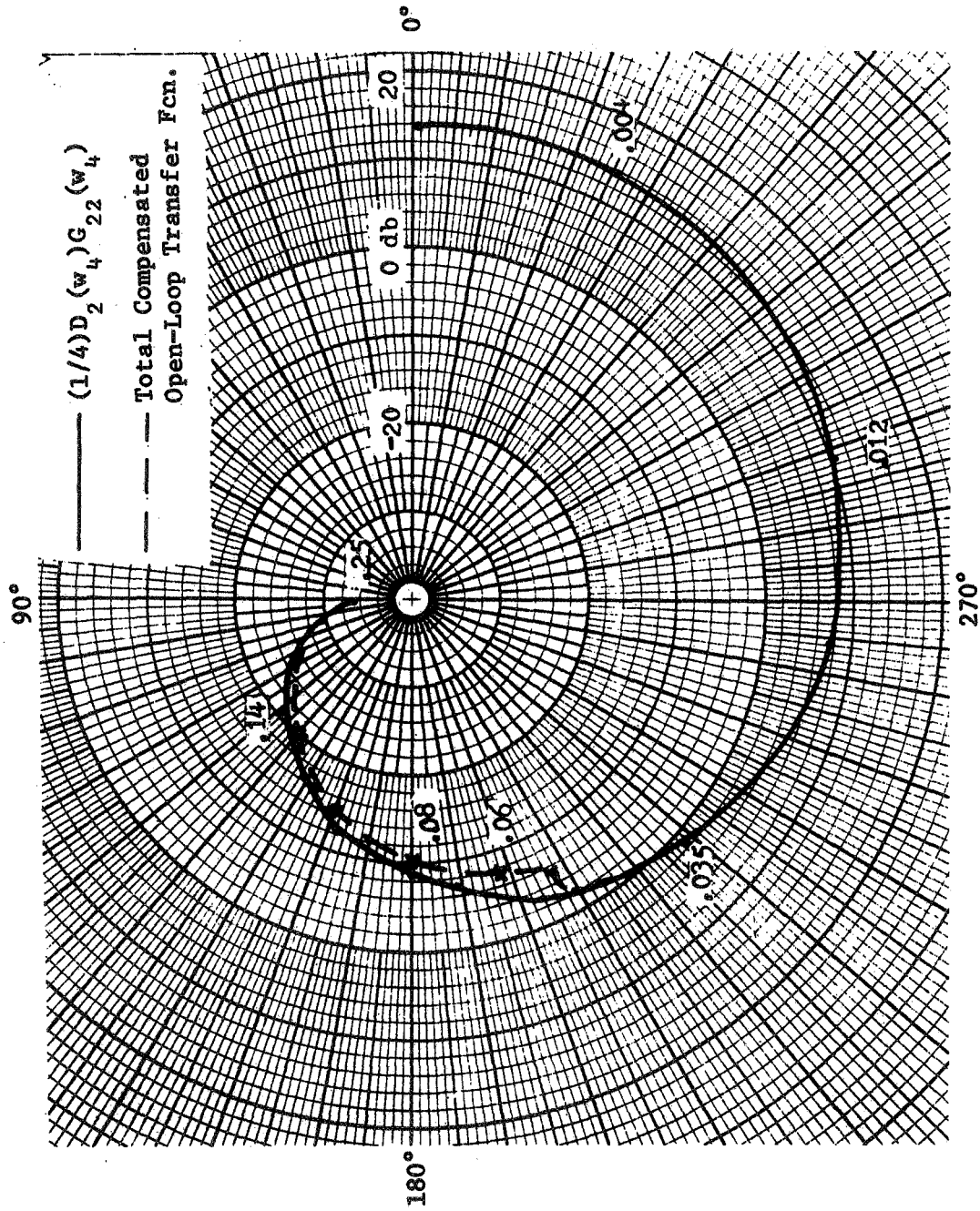


Figure IV-22. Compensated Nyquist diagram for $-E'_2(w_4)/E_2(w_4)$.

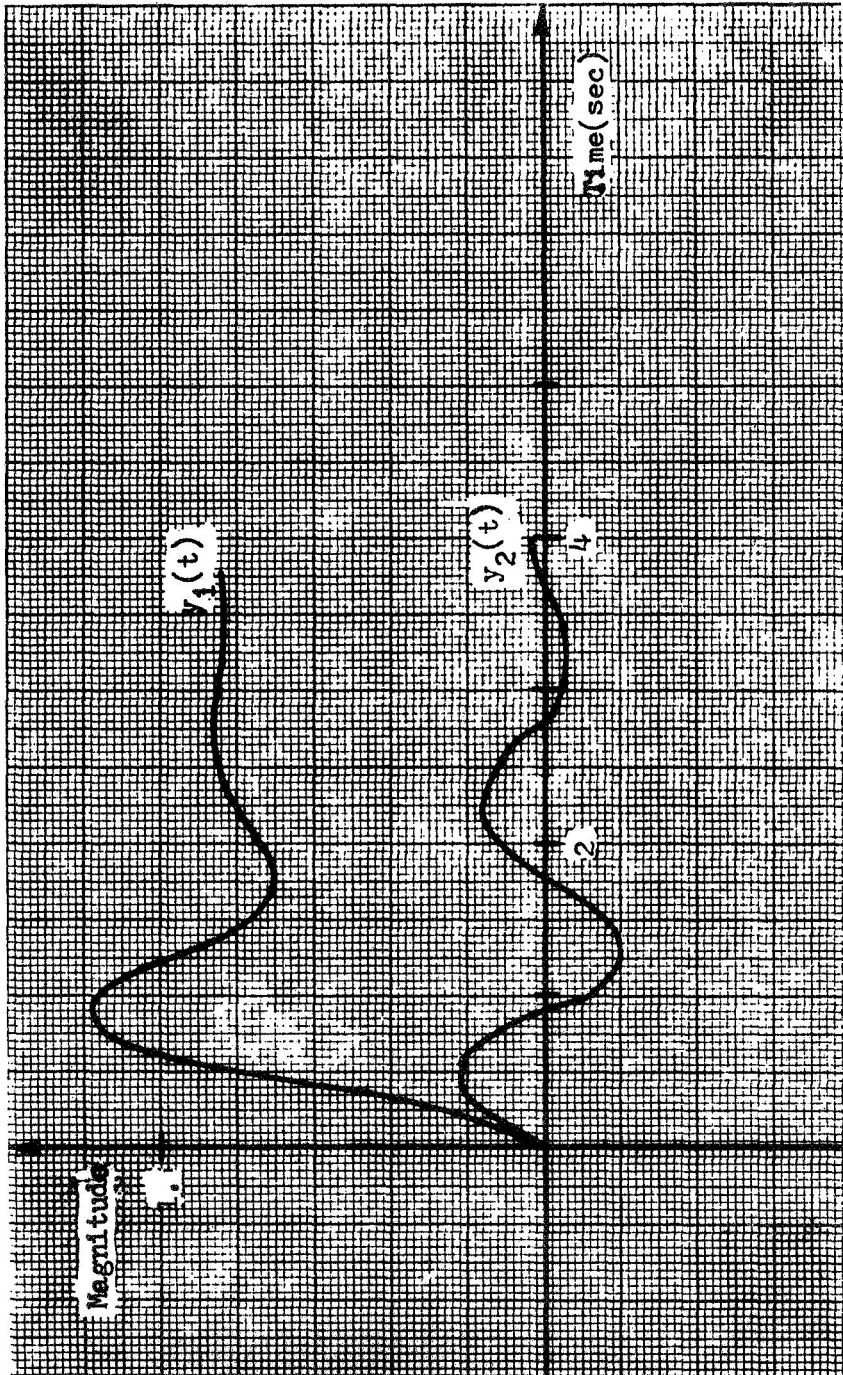


Figure IV-23. Compensated system response, $r_1(t) = u(t)$, $r_2(t) = 0$.

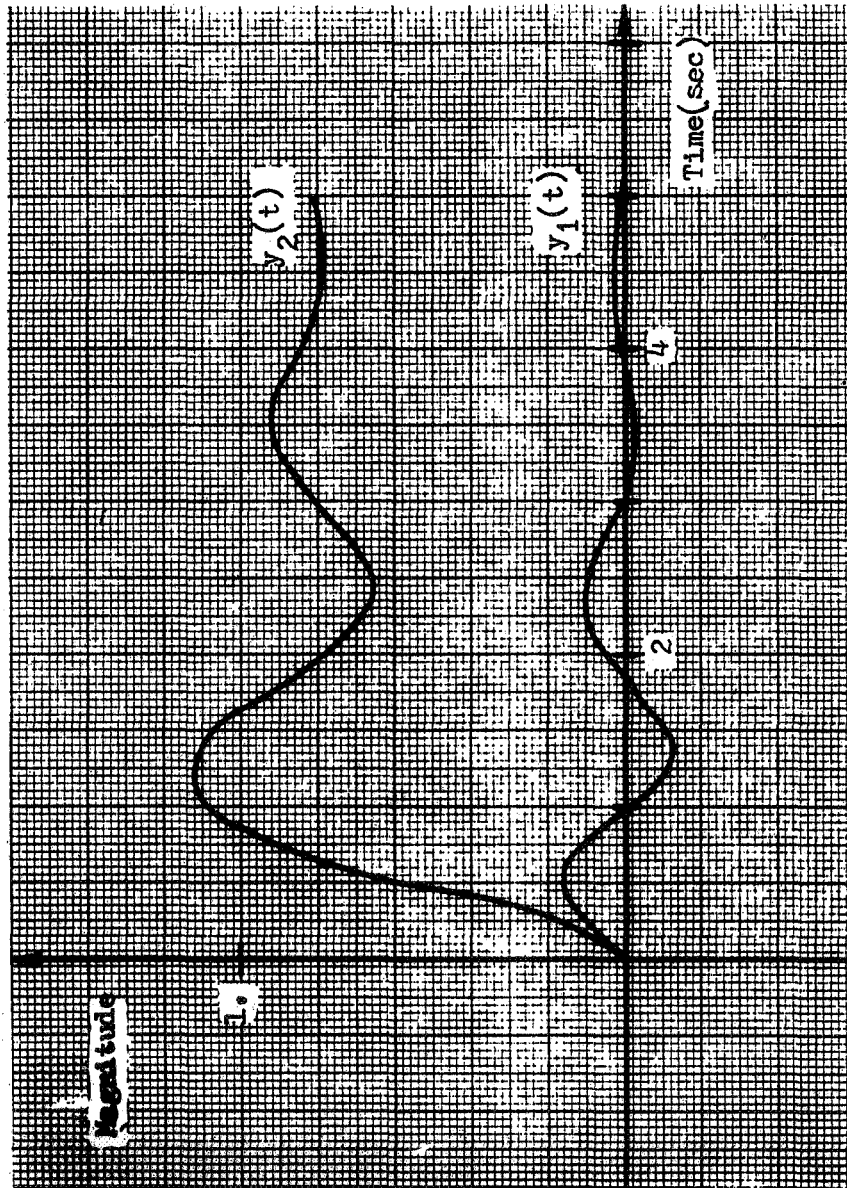


Figure IV-24. Compensated system response, $r_2(t) = u(t)$, $r_1(t) = 0$.

V. THE OPEN-LOOP DESIGN TECHNIQUE FOR SYSTEMS WITH MORE THAN TWO INPUTS AND OUTPUTS

As presented in the previous chapter, the open-loop technique for two input-two output systems consists of three primary steps. First of all, an open-loop transfer function must be written for each of the channels opened at the error sampler. Secondly, in order to apply the Nyquist criterion to the open-loop transfer function, the number of open-loop right half plane poles must be determined and an open-loop frequency response must be obtained. Finally, a compensation must be specified in each channel so as to approximately decouple the system and to meet the various other design specifications.

In order to extend the open-loop technique to systems having more than two inputs and outputs, it is desirable to develop straightforward methods to facilitate the aforementioned procedures. The paragraphs which follow will present the open-loop technique in terms of the general n input- n output system. The technique will then be illustrated by application to a three input-three output system.

A. Procedure for Obtaining Open-Loop Transfer Functions.

It was shown in the previous chapter that it is only necessary to consider the open-loop transfer functions corresponding to each of the

channels opened at the error sampler. Hence, the procedure which is presented here is developed for this specific purpose.

Consider the system of Figure V-1. Suppose that it is desired to determine the open-loop transfer function for the system opened at the error sampler in the first channel. A signal flow graph may be drawn for the system under this condition, similar to the signal flow graph of Figure IV-4. The input node of the signal flow graph corresponds to the output of the error sampler at which the system is opened. The output node of the signal flow graph corresponds to the input to the error sampler. Mason's gain formula would then be applied to the signal flow graph to determine the open-loop transfer function. The application of Mason's gain formula requires determining the various feed-forward paths for the open-loop system, the various loops, and the cofactors for each of the paths [16]. The structure of the system of Figure V-1 allows for setting forth certain rules for determining the various paths, loops, and cofactors with a minimum of effort.

The various feed-forward path transfer functions for the system opened at the error sampler in any given channel are determined by proceeding from the input node of the signal flow graph of the open-loop system to the output node in the direction of the arrows and in every possible manner without touching any of the nodes of the signal flow graph more than once. For the system of Figure V-1, it is observed that, given a channel opened at the error sampler, there will be several possible paths from the output of the error sampler to the output of the

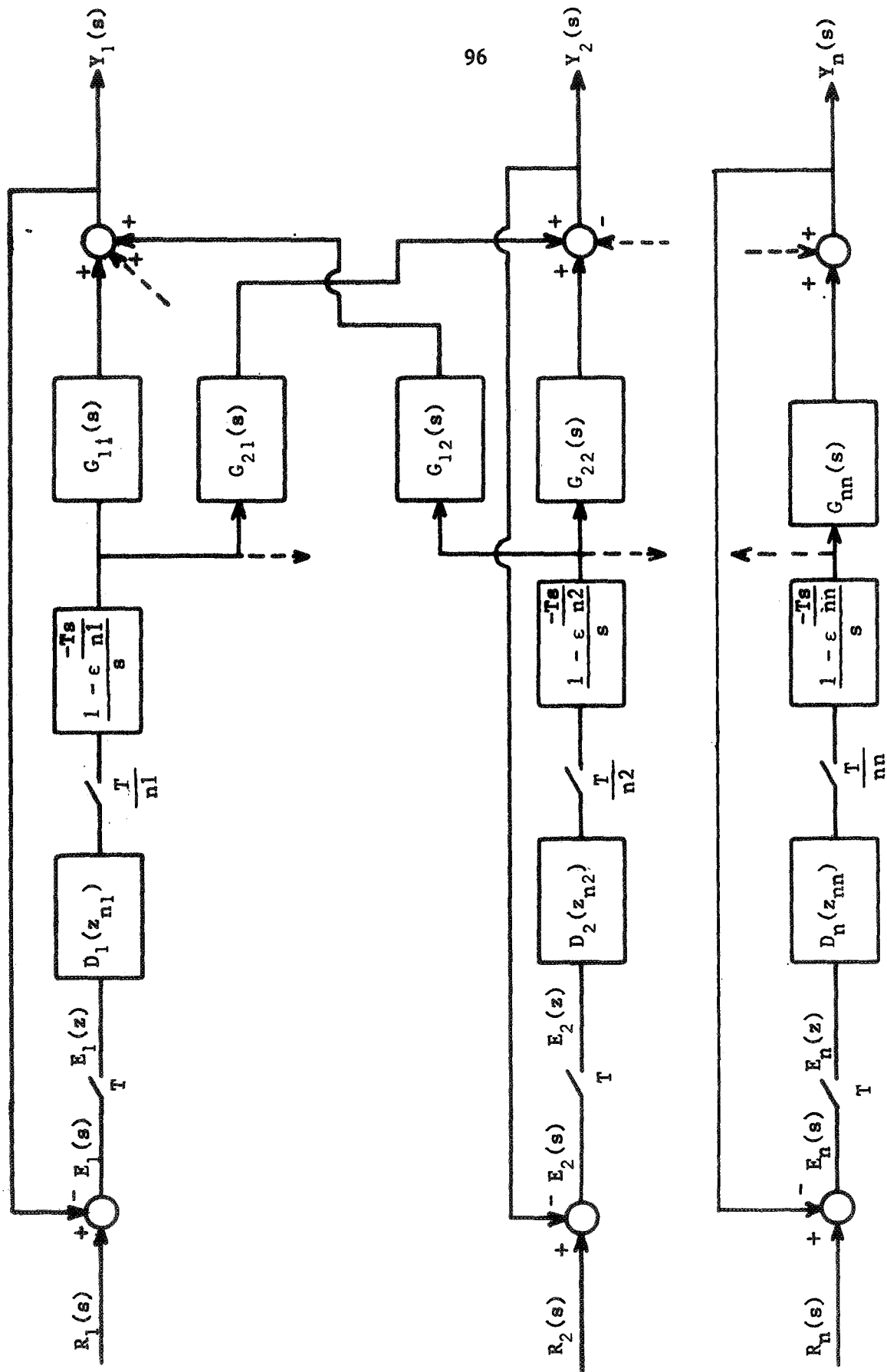


Figure V-1. Multirate sampled-data system with n -inputs and n -outputs.

open channel, due to the coupling between channels. There is the obvious path through the open channel controller and plant transfer function combination. Then, considering any one of the remaining channels, one may proceed from the output of the error sampler through the open channel controller and cross-coupling transfer function combination to the output of the other channel, around the feedback loop, then through the other channel controller and cross-coupling transfer function combination to the output of the open channel. Also, there are similar paths obtained by considering any two of the remaining channels at a time, any three, etc. The following procedure will obtain all the feed-forward path transfer functions for the system opened at the error sampler in any channel:

1. For P_1 , write the negative of the controller-plant transfer function combination for the open channel.
2. For P_2, P_3, \dots, P_n , write the products of the controller - cross-coupling transfer function pairs from the open channel to each of the remaining channels.
3. For the remaining paths, write all possible different combinations of controller - cross-coupling transfer functions three at a time, four at a time, \dots , n at a time which begin at the open channel and terminate on the open channel without touching any other channel more than once. Take the negative of all odd combinations.

$$\cdot (1/n_3) \sum_{p=0}^{n_3-1} D_3(z\epsilon^{j\phi p})_{n_3} G_{13}(z\epsilon^{j\phi p})_{n_3} \quad (V-4)$$

and

$$\begin{aligned} P_5 = & - (1/n_1) \sum_{p=0}^{n_1-1} D_1(z\epsilon^{j\phi p})_{n_1} G_{31}(z\epsilon^{j\phi p})_{n_1} \\ & \cdot (1/n_3) \sum_{p=0}^{n_3-1} D_3(z\epsilon^{j\phi p})_{n_3} G_{23}(z\epsilon^{j\phi p})_{n_3} \\ & \cdot (1/n_2) \sum_{p=0}^{n_2-1} D_2(z\epsilon^{j\phi p})_{n_2} G_{12}(z\epsilon^{j\phi p})_{n_2} \quad (V-5) \end{aligned}$$

The above results were checked by constructing the signal flow graph for the three input-three output system opened at the error sampler in the first channel and applying Mason's gain formula to determine the open-loop transfer function, as shown in Appendix F. It is observed that the results of the prescribed method agree with the results of Appendix F.

Loop transfer functions are obtained by starting from any given signal flow graph node and proceeding in the direction of the arrows to any other node or series of nodes and then back to the initial node, without touching any other node more than once. For the system of Figure V-1 opened in any channel, all such loop transfer functions may be written by writing the transfer functions around all the closed feedback loops, then writing all possible different combinations of cross-coupling

transfer functions which begin in any channel except the open channel and end in the same channel. To illustrate this procedure, consider the three input-three output system of the type of Figure V-1 again with the system opened at the error-sampler in the first channel. Then

$$L_1 = - (1/n_2) \sum_{p=0}^{n_2-1} D_2(z\epsilon^{j\phi p})_{n_2} G_{22}(z\epsilon^{j\phi p})_{n_2} \quad (V-6)$$

and

$$L_2 = - (1/n_3) \sum_{p=0}^{n_3-1} D_3(z\epsilon^{j\phi p})_{n_3} G_{33}(z\epsilon^{j\phi p})_{n_3} \quad (V-7)$$

Omitting the first channel, the remaining cross-coupling transfer functions are $(1/n_2) \sum_{p=0}^{n_2-1} D_2(z\epsilon^{j\phi p})_{n_2} G_{32}(z\epsilon^{j\phi p})_{n_2}$ and $(1/n_3) \sum_{p=0}^{n_3-1} D_3(z\epsilon^{j\phi p})_{n_3} G_{23}(z\epsilon^{j\phi p})_{n_3}$. Then

$$L_3 = (1/n_2) \sum_{p=0}^{n_2-1} D_2(z\epsilon^{j\phi p})_{n_2} G_{32}(z\epsilon^{j\phi p})_{n_2} \\ + (1/n_3) \sum_{p=0}^{n_3-1} D_3(z\epsilon^{j\phi p})_{n_3} G_{23}(z\epsilon^{j\phi p})_{n_3} \quad (V-8)$$

The above results also agree with the results of Appendix F.

From Mason's gain formula, the determinant of the open-loop transfer function is formed according to [16]

$$\Delta = 1 - (\text{sum of all loops}) + (\text{sum of the products of all non-touching loops taken two at a time}) - (\text{sum of the products of all non-touching loops taken three at a time}) + \dots$$

(V-9)

The cofactors, Δ_i , for the various paths are also formed according to (V-9), where only those loops which do not touch on the path are utilized. Applying the above to the three input-three output system, the open-loop transfer function for the system opened at the error sampler in the first channel is

$$-\frac{E'_1(z)}{E_1(z)} = -\frac{P_1\Delta_1 + P_2\Delta_2 + P_3\Delta_3 + P_4\Delta_4 + P_5\Delta_5}{1 - (L_1 + L_2 + L_3) + (L_1L_2)}, \quad (\text{V-10})$$

where

$$\Delta_1 = 1 - (L_1 + L_2 + L_3) + (L_1L_2), \quad (\text{V-11})$$

$$\Delta_2 = 1 + L_2, \quad (\text{V-12})$$

$$\Delta_3 = 1 + L_1, \quad (\text{V-13})$$

and

$$\Delta_4 = \Delta_5 = 1. \quad (\text{V-14})$$

If it is assumed that the system is low-pass with respect to the sampling frequency, V-10 may be written

$$\begin{aligned}
 - \frac{E_1'(z)}{E_1(z)} = & (1/n1)D_1(z)_{n1}G_{11}(z)_{n1} \\
 & - \left\{ (1/n1)D_1(z)_{n1}G_{21}(z)_{n1} \cdot (1/n2)D_2(z)_{n2}G_{12}(z)_{n2} \right. \\
 & \cdot (1 + (1/n3)D_3(z)_{n3}G_{33}(z)_{n3}) + (1/n1)D_1(z)_{n1}G_{31}(z)_{n1} \\
 & \cdot (1/n3)D_3(z)_{n3}G_{13}(z)_{n3} \cdot (1 + (1/n2)D_2(z)_{n2}G_{22}(z)_{n2}) \\
 & - (1/n1)D_1(z)_{n1}G_{21}(z)_{n1} \cdot (1/n2)D_2(z)_{n2}G_{32}(z)_{n2} \\
 & \cdot (1/n3)D_3(z)_{n3}G_{13}(z)_{n3} - (1/n1)D_1(z)_{n1}G_{31}(z)_{n1} \\
 & \left. \cdot (1/n3)D_3(z)_{n3}G_{23}(z)_{n3} \cdot (1/n2)D_2(z)_{n2}G_{12}(z)_{n2} \right\} \\
 & \hline
 & \Delta
 \end{aligned}
 \tag{V-15}$$

where

$$\begin{aligned}
 \Delta = & (1 + (1/n2)D_2(z)_{n2}G_{22}(z)_{n2}) \cdot (1 + (1/n3)D_3(z)_{n3}G_{33}(z)_{n3}) \\
 & - (1/n2)D_2(z)_{n2}G_{32}(z)_{n2} \cdot (1/n3)D_3(z)_{n3}G_{23}(z)_{n3} \cdot \tag{V-16}
 \end{aligned}$$

The above open-loop transfer function agrees with the open-loop transfer function of Appendix F.

B. Procedure for Determining Open-Loop Poles

From the previous section it is observed that the cofactor, Δ_1 , of the P_1 path will always be equal to the denominator, Δ , of the open-loop transfer function for the system opened at the error sampler in any channel. This is true because there are no closed loops touching on the open channel. Hence, the open-loop transfer function may always be written in the form

$$-\frac{E_1'(z)}{E_1(z)} = P_1' - \frac{F}{\Delta} \quad , \quad (V-17)$$

where P_1' is $-P_1$ and F consists of the sums of the remaining path and cofactor products.

The poles of (V-17) are the poles of P_1' , the poles of F , and the zeroes of Δ . For the uncompensated system, the P_1' path transfer function will be entirely due to the plant transfer function which lies in the open channel feed-forward path. Hence, the poles of the uncompensated P_1' path which lie outside the unit circle in the multirate z -plane may be determined according to (III-18).

For the second term on the right of the uncompensated form of (V-17), it is observed that the numerator, F , is a function of all the plant transfer functions, except the open channel plant transfer function, and all of the cross-coupling transfer functions. Also, the denominator, Δ , is a function of all the plant transfer functions, except

the open channel plant transfer function, and all the cross-coupling transfer functions not associated with the open channel. Then the numerator and denominator have common poles, a situation which may be described by

$$G = \frac{A_1 + A_2 + \dots + A_q}{1 + B_1 + B_2 + \dots + B_k} , \quad (V-18)$$

where the common denominators of the two sums $A_1 + A_2 + \dots + A_k$ and $B_1 + B_2 + \dots + B_k$ are the same. Multiplying top and bottom of (V-18) by this common denominator factor cancels out the poles of G due to the A_1, A_2, \dots, A_k terms [17]. Hence, the poles of G which are due to the numerator of (V-18) are the poles due to the $A_{k+1}, A_{k+2}, \dots, A_q$ terms only. Likewise, the poles of (V-17) which are due to F are the poles of F which are not in common with the poles of Δ . These poles will be the poles of the cross-coupling transfer function pairs between the open-channel and each of the other channels. Again, the number of these poles which lie outside the unit circle in the multirate z -plane may be determined by (III-18).

The zeroes of the denominator, Δ , of (V-17) which lie outside the unit circle in the multirate z -plane may be easily determined also, with the aid of frequency response information. This is due to the fact that all the feedback loops are non-touching and hence, the portion of Δ involving these loops may be written

$$\prod_{\substack{i=1 \\ i \neq k}}^n (1 + (1/n_i) \sum_{p=0}^{n_i-1} D_i(z \epsilon^{j\phi_p})_{n_i} G_{ii}(z \epsilon^{j\phi_p})_{n_i}) \quad , \quad (V-19)$$

where k corresponds to the open channel. In order to determine the zeroes of Δ , one would set it equal to zero. Then, dividing through by (V-19), one obtains

$$1 + \frac{H}{\prod_{\substack{i=1 \\ i \neq k}}^n (1 + (1/n_i) \sum_{p=0}^{n_i-1} D_i(z \epsilon^{j\phi_p})_{n_i} G_{ii}(z \epsilon^{j\phi_p})_{n_i})} = 0 \quad , \quad (V-20)$$

where H consists of all the terms of Δ which remain after forming the term of (V-19).

The Nyquist criterion may be easily applied to (V-20) to determine the zeroes which lie outside the unit circle in the multirate z -plane. For the uncompensated form of (V-20), the poles of each of the $(1/n_i) \sum_{p=0}^{n_i-1} G_{ii}(z \epsilon^{j\phi_p})_{n_i}$ terms which lie outside the unit circle may be determined by (III-18). Given the frequency response for each of the above terms, the zeroes of each of the terms $1 + (1/n_i) \sum_{p=0}^{n_i-1} G_{ii}(z \epsilon^{j\phi_p})_{n_i}$ which lie outside the unit circle may be determined by application of the Nyquist criterion in each case. Equation (III-18) may be applied to H to determine the number of poles it contains which lie outside the unit circle. The sum of the number of zeroes and poles thus determined obtains the number of poles of (V-20) which lie outside the unit circle.

If the frequency-response for H/I is then obtained, where I is the denominator of (V-20), the Nyquist criterion may be applied to determine the zeroes of (V-20) which lie outside the unit circle. For the compensated system, the procedure is considerably simplified, since it is assumed that the compensation will be such that the denominator of (V-20) will have no zeroes which lie outside the unit circle.

The methods presented in the preceding paragraphs will now be illustrated by again considering a three input-three output system of the type shown in Figure V-1, with

$$G'_{11}(s) = \frac{10}{(s+1)(s/10+1)} \quad , \quad (V-21)$$

$$G'_{22}(s) = \frac{10}{(s+1)(s/15+1)} \quad , \quad (V-22)$$

$$G'_{33}(s) = \frac{10}{(s+1)(s/12+1)} \quad , \quad (V-23)$$

$$G'_{21}(s) = G'_{31}(s) = \frac{1}{(s/4+1)} \quad , \quad (V-24)$$

$$G'_{12}(s) = G'_{32}(s) = \frac{1}{(s/4+1)} \quad , \quad (V-25)$$

and

$$G'_{13}(s) = G'_{23}(s) = \frac{1}{(s/6 + 1)} \quad (V-26)$$

Also, let $T = .1$, $n_1 = 2$, $n_2 = 4$, and $n_3 = 8$. Let the system be opened at the error sampler in the first channel. Then the uncompensated open-loop transfer function is of the form of (V-17), where

$$P'_1 = (1/2) \sum_{p=0}^1 G'_{11}(ze^{j\phi_p})_2 \quad (V-27)$$

Since $G'_{11}(s)$ has no poles which lie in the right half s -plane, application of (III-18) to (V-27) shows that P'_1 has no poles which lie outside the unit circle in the z_2 -plane.

Only the poles of F of (V-17) which are due to the cross-coupling transfer function pairs between the first and second channels and the first and third channels need be considered in determining the poles of the above uncompensated open-loop transfer function which lie outside the unit circle. Since none of these have poles which lie in the right half s -plane, application of (III-18) shows that F contributes no poles which lie outside the unit circle.

It is now necessary to determine if the denominator, Δ , contributes any zeroes which lie outside the unit circle to the uncompensated open-loop transfer function. From the preceding paragraphs, one would then form

$$1 + \frac{(1/4) \sum_{p=0}^3 G_{32}(z\epsilon^{j\phi p})_4 \cdot (1/8) \sum_{p=0}^7 G_{23}(z\epsilon^{j\phi p})_8}{\prod_{i=2}^3 (1 + (1/n_i) \sum_{p=0}^{n_i-1} G_{ii}(z\epsilon^{j\phi p})_{n_i})} = 0 \quad (V-28)$$

The frequency response was obtained for each of the terms $(1/4) \sum_{p=0}^3 G_{22}(z\epsilon^{j\phi p})_4$, $(1/8) \sum_{p=0}^7 G_{33}(z\epsilon^{j\phi p})_8$, and the total second term on the left of (V-28). This information is shown in the form of a Nyquist diagram for each of the terms, in Figure V-2. Since the terms $G'_{22}(s)$ and $G'_{33}(s)$ have no poles in the right half s -plane, application of (III-18) to $(1/4) \sum_{p=0}^3 G_{22}(z\epsilon^{j\phi p})_4$ and $(1/8) \sum_{p=0}^7 G_{33}(z\epsilon^{j\phi p})_8$ shows that neither of these has poles which lie outside the unit circle. Then, application of the Nyquist criterion to Figure V-2 shows that the denominator of the second term on the left of (V-28) has no zeroes which lie outside the unit circle. The numerator contributes no such poles, since $G'_{32}(s)$ and $G'_{23}(s)$ have no poles which lie in the right half s -plane. Then, (V-28) has no zeroes which lie outside the unit circle. It is therefore concluded for this example that the uncompensated open-loop transfer function has no poles which lie outside the unit circle.

C. The Design Procedure.

The objective of the design procedure is to approximately decouple the system as well as to meet design specifications such as gain margin, phase margin, and bandwidth. For the two input-two output case, it was possible to write the open-loop transfer function for the system opened

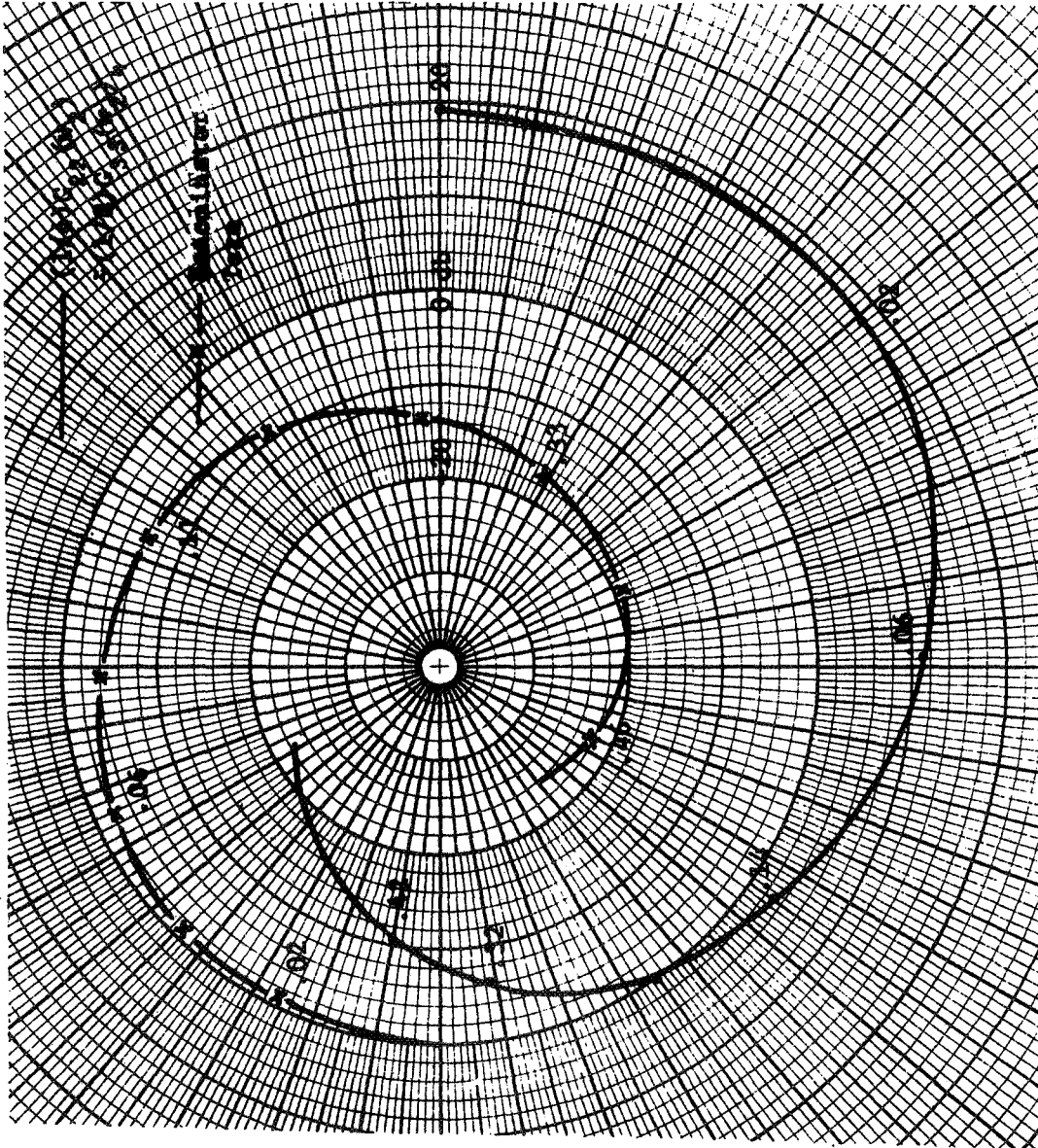


Figure V-2. Nyquist diagrams to determine right half plane zeroes.

at the error-sampler in either channel in the form of the feed-forward transfer function for that channel, minus a term which was a function of the cross-coupling between channels. In Part A of this chapter, it has been shown that for the general n input- n output system, the open-loop transfer function may be written in the form of the feed-forward transfer function for the open channel, minus a term which is a function of the cross-coupling between all channels. For the two input-two output case, a frequency response design technique which utilized the Nichols chart was developed. This technique can be extended to the n input- n output case with little difficulty.

For the n input- n output case, the design procedure will consider each of the n controllers individually. The requirements on each controller are to achieve gain margin, phase margin, bandwidth, and steady-state error, generally, and to effect an approximately decoupled system. The last requirement can be thought of as a restricting factor in selecting the compensation in each channel to achieve the usual design requirements. That is, in considering each of the controllers, the system is opened at the error sampler in the channel corresponding to the controller under consideration. It is then determined what the requirements are on the decoupled open-loop transfer function in order to achieve gain margin, phase margin, etc. The form of the compensation is determined in light of the requirements that must be met in order to approximately decouple the system. The requirements for decoupling can be determined by considering the coupling between the open channel and each

of the remaining channels, one at a time. The techniques developed for the two input-two output case can then be applied to each of these coupled pairs, where the requirements for decoupling for each of these pairs are determined. The worst case is then taken to be the requirement for decoupling on the digital controller under consideration.

The example of the previous section will be utilized to illustrate the design procedure. For the system described by equations (V-21) - (V-26) and Figure V-1, it has been shown by the procedure of section B of this chapter that the uncompensated open-loop transfer function for the system opened at the error sampler in the first channel has no poles which lie outside the unit circle in the z_2 -plane. It can be shown by application of the same procedure to the uncompensated open-loop transfer functions for the system opened at the error samplers in the second and third channels that these open-loop transfer functions have no poles which lie outside the unit circle in the z_4 and z_8 -planes respectively. The computer program of Appendix D was utilized to compute the frequency response for each of the open-loop transfer functions. These frequency responses are plotted as Nyquist diagrams in Figures V-3, V-4, and V-5. In each case, the approximation to the open-loop transfer function and the total open-loop transfer function have been plotted. Application of the Nyquist criterion to each of the diagrams shows that the uncompensated open-loop transfer functions are stable. However, it is observed that a strong degree of coupling exists between channels.

The computer program of Appendix E was utilized to obtain a simulation of the system for a unit step forcing function at $r_1(t)$. The

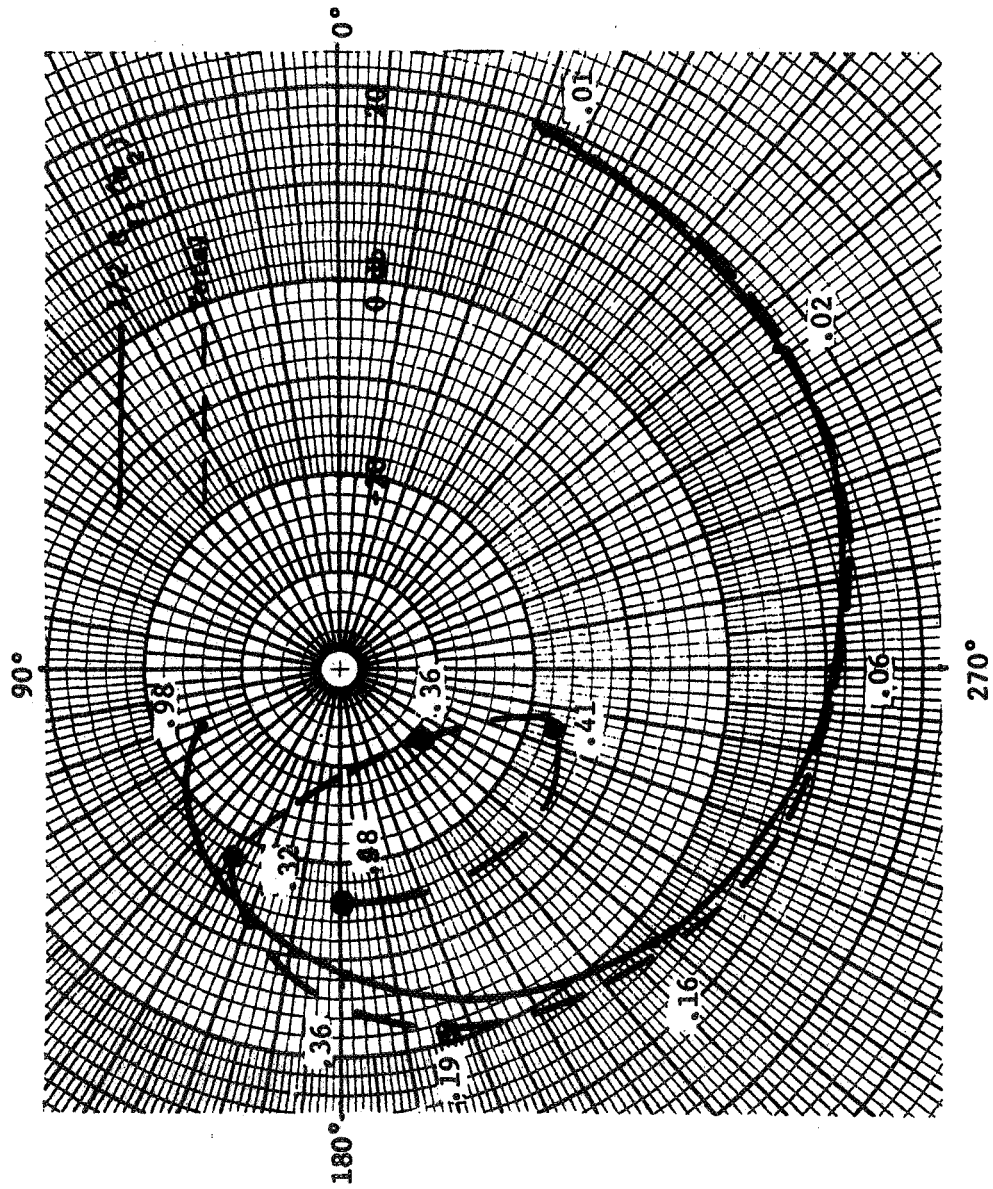


Figure V-3. Uncompensated Nyquist diagram for $-E_1'(w_2)/E_1(w_2)$.

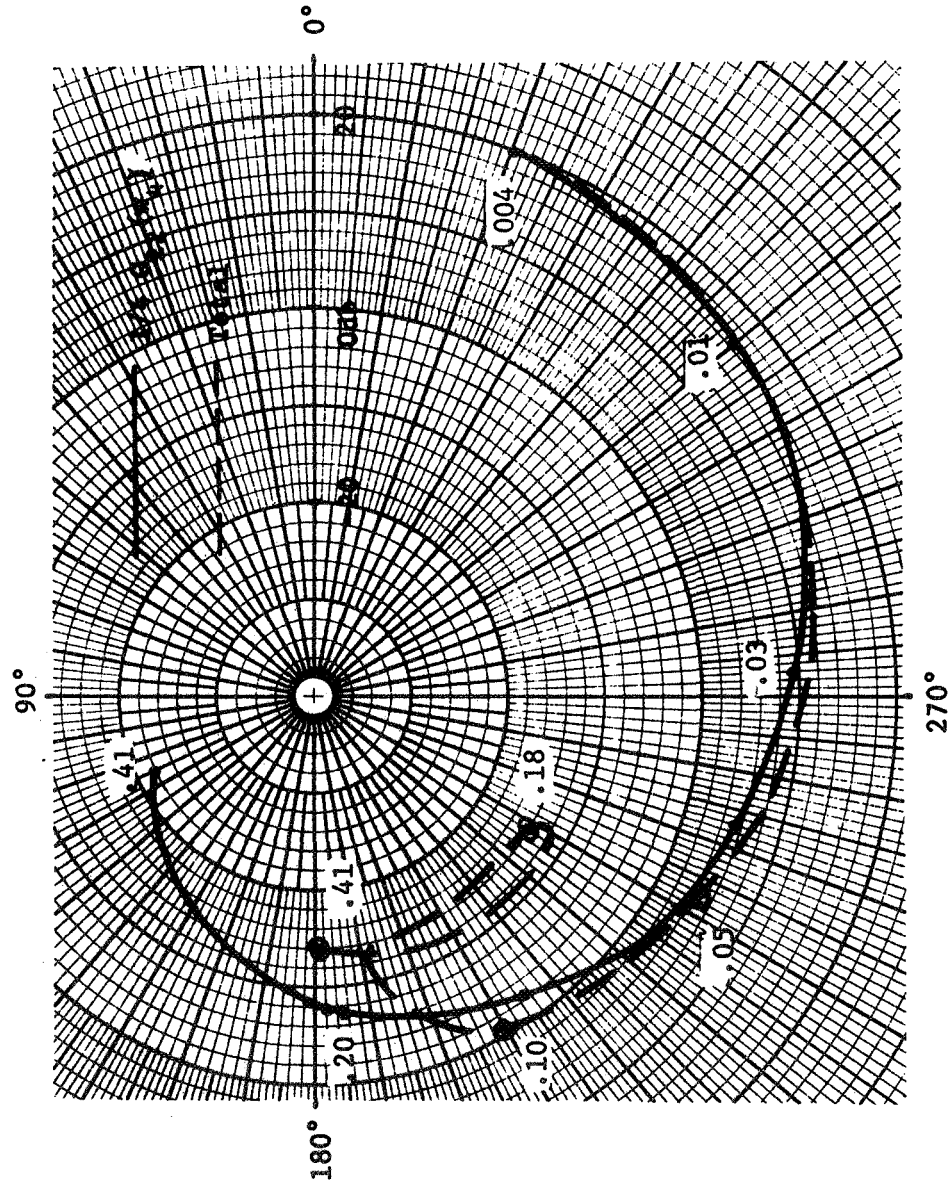


Figure V-4. Uncompensated Nyquist diagram for $-E_2^i(w_t)/E_2(w_t)$.

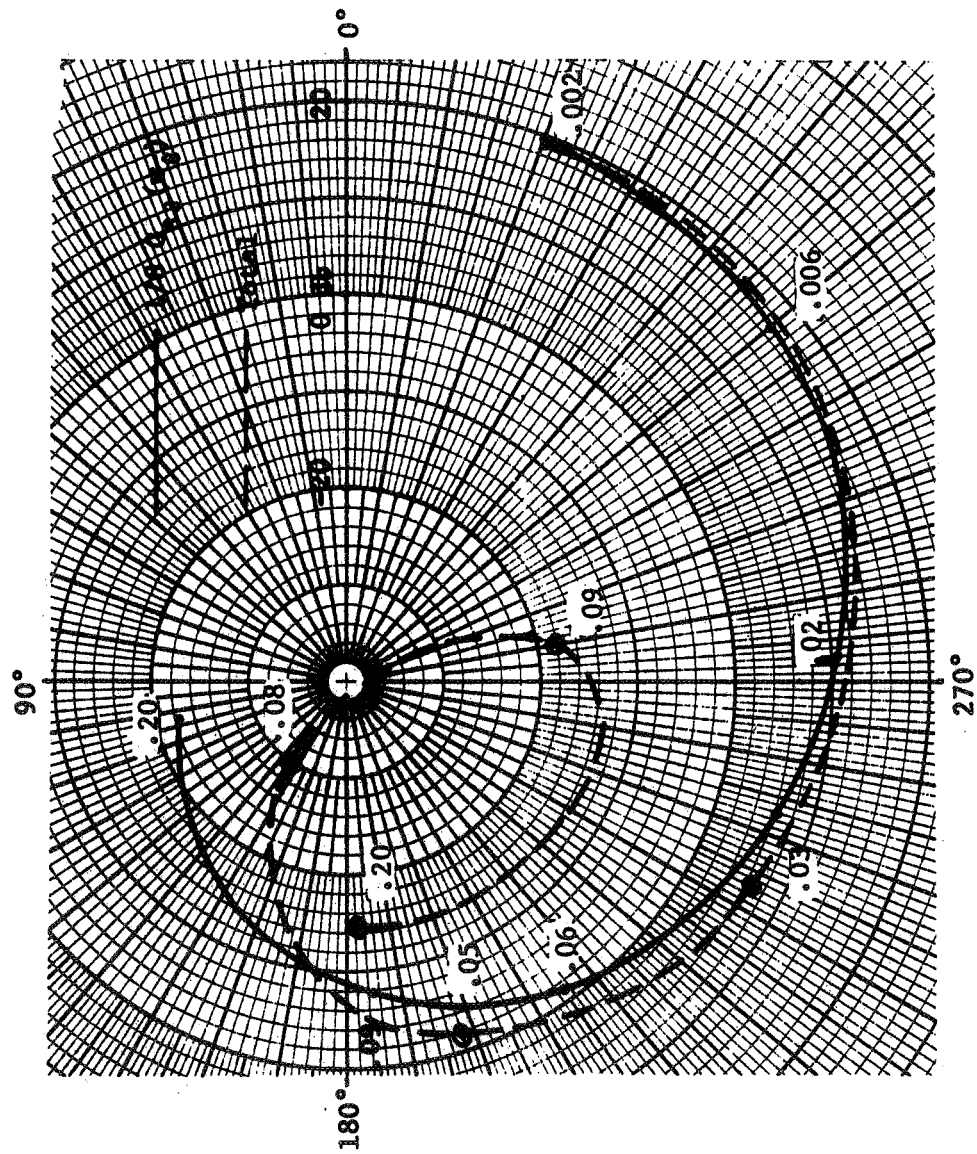


Figure V-5. Uncompensated Nyquist diagram for $-E_3^i(w_8)/E_3(w_8)$.

results of this simulation are plotted in Figure V-6. It is observed that the output $y_1(t)$ is somewhat oscillatory, with a steady-state error of approximately 10 per cent. The remaining two outputs are observed to have a maximum value of .32, verifying the strong coupling observed in the frequency response of Figure V-3.

It will be attempted to design a compensation for each channel so as to obtain at least a 6 db gain margin and a 30 degree phase margin in each open-loop transfer function, to obtain a zero steady-state error for a step input in any channel, and to significantly reduce the coupling between channels. The specification for the compensator $D_1(w_2)$ will be considered first. The initial step in the design procedure is to obtain a Bode plot for each of the plant transfer functions and each of the cross-coupling transfer functions. These Bode plots are shown in Figures V-7 through V-10. The open-loop transfer function for the system opened at the error sampler in the first channel is given by (V-15), where it is assumed that the system is low-pass with respect to the slow-rate sampling frequency. Imposing this requirement on the specification of the compensators, it is noted that if the system is approximately decoupled, the open-loop transfer function of (V-15) is approximated by the first term. The requirements for gain margin, phase margin, and steady-state error must then be satisfied by this term. To satisfy the requirement for zero steady-state error for a step input, $D_1(w_2)$ must contain a pole at the origin in the w_2 -plane. Adding this pole to the Bode plot for $(1/2)G_{11}(w_2)$, one must then determine the additional poles

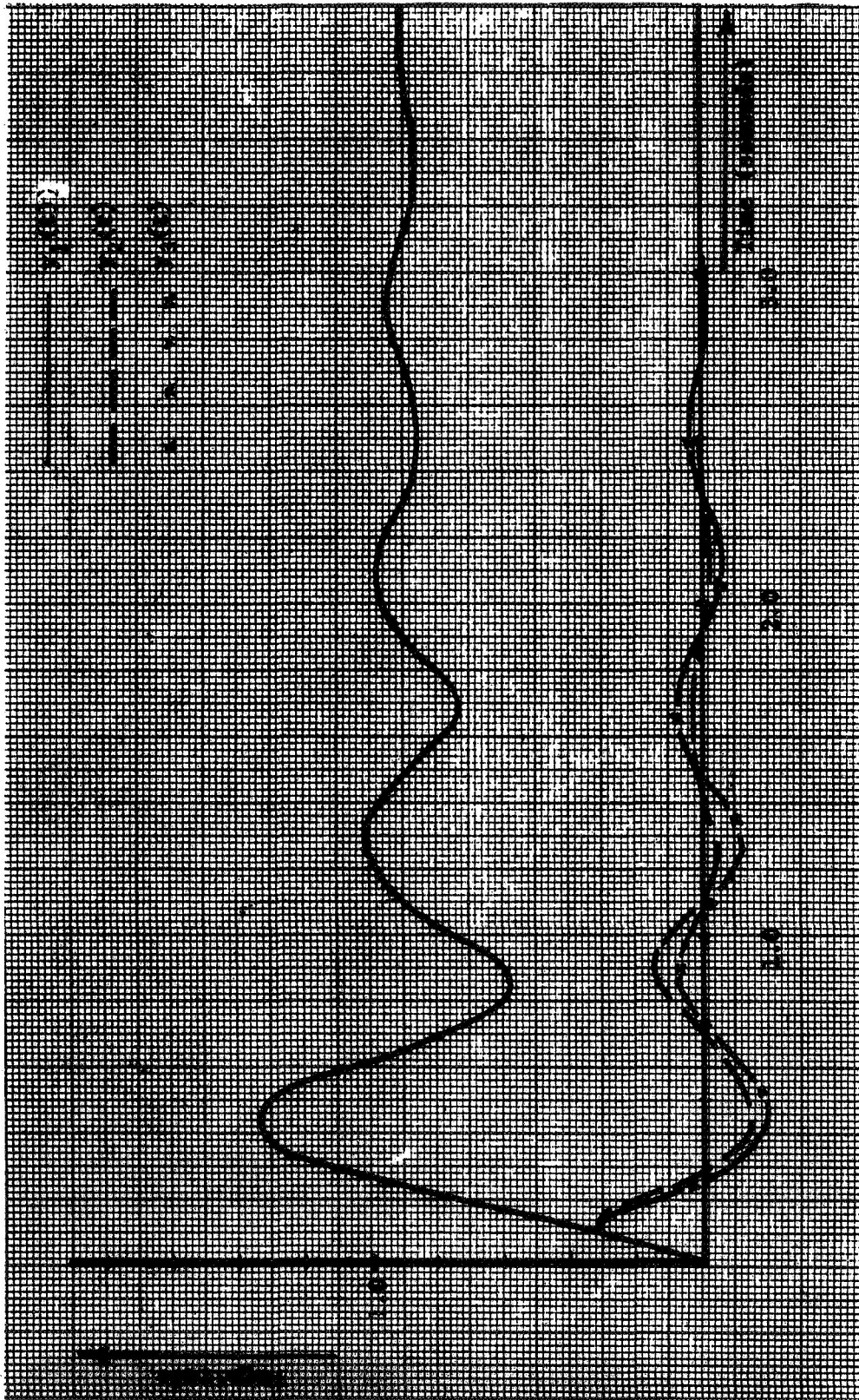


Figure V-6. Uncompensated system outputs for step input a $r_1(t)$.

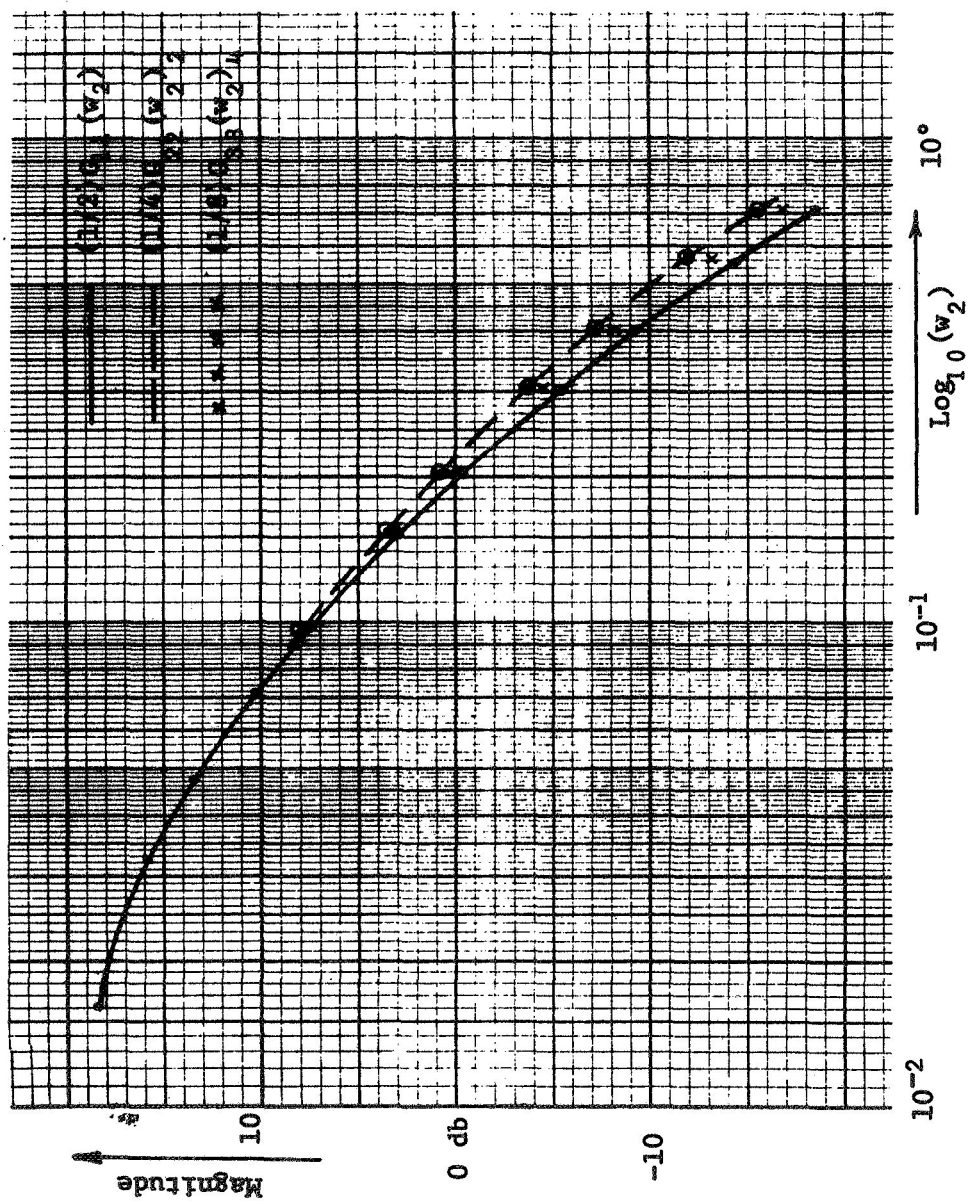


Figure V-7. Magnitude characteristics.

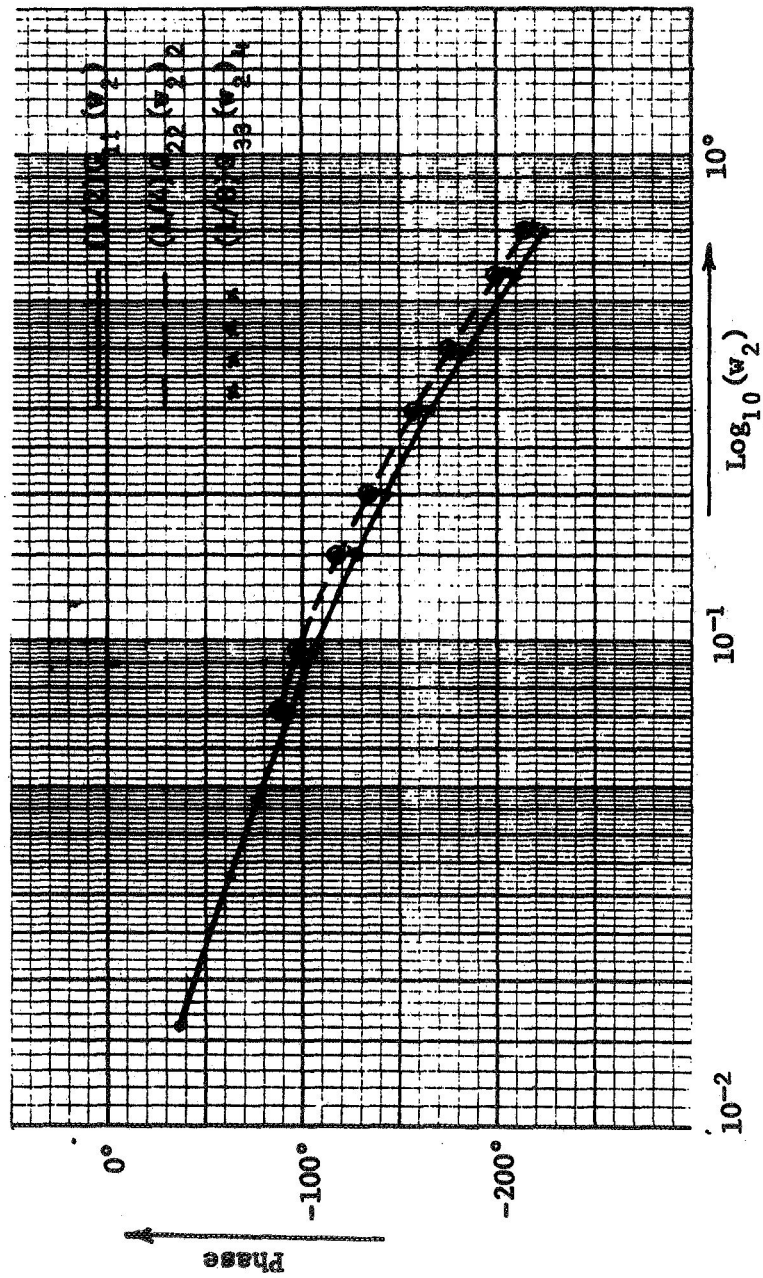


Figure V-8. Phase angle characteristics.

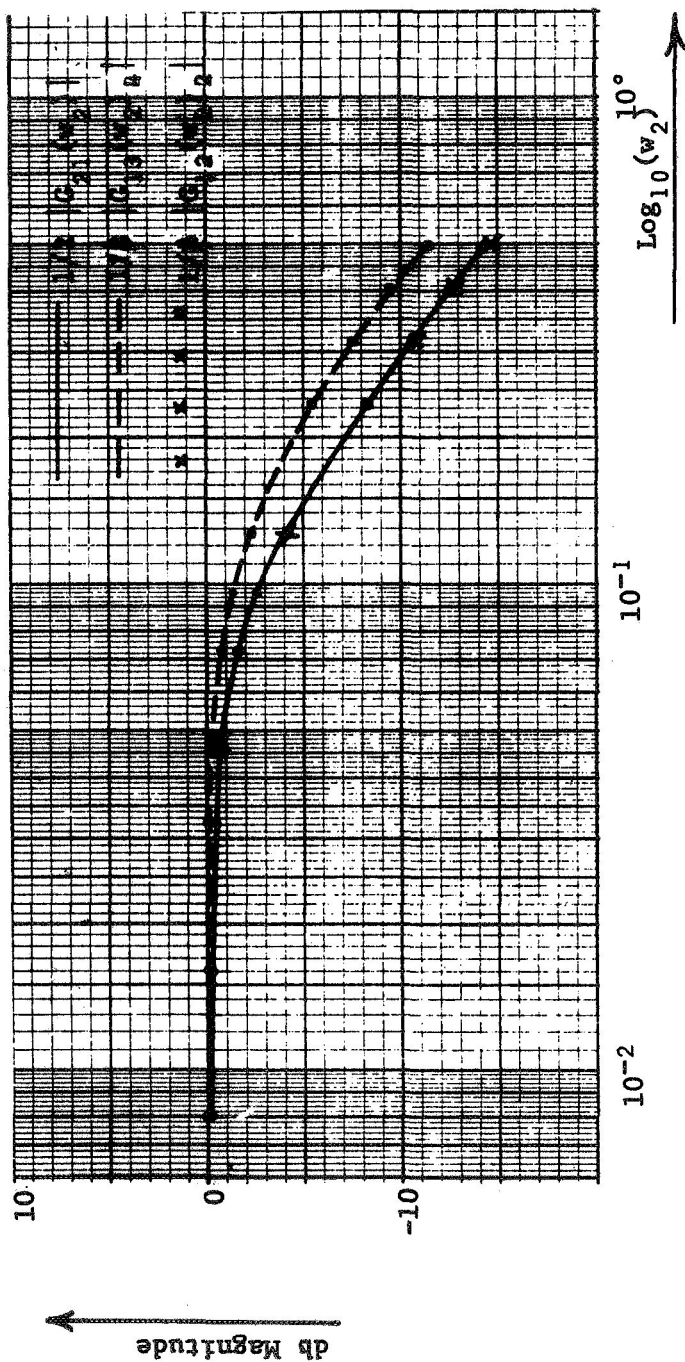


Figure V-9. Cross-coupling transfer function db magnitudes vs. $\log_{10}(w_2)$.

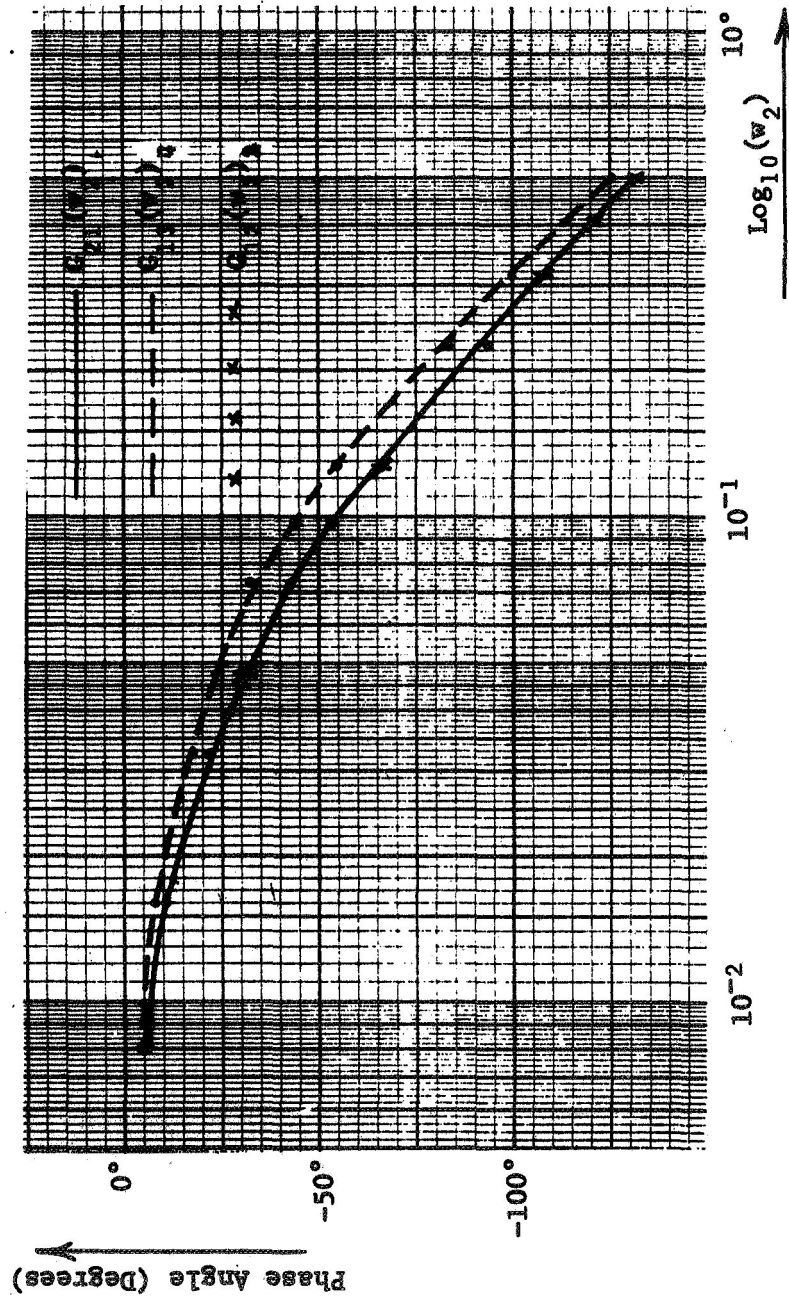


Figure V-10. Cross-coupling transfer function phase angles vs. $\log_{10}(w_2)$.

and zeroes necessary to satisfy the gain and phase margin requirements. These poles and zeroes must be chosen in light of the need to significantly reduce the coupling between channels. The degree of coupling present in the system will be ascertained by considering the coupling present between the first and second channels and then, between the first and third channels. The worst case is then chosen to be the requirement on decoupling for the controller $D_1(w_2)$ and the specification of the controller is made according to (IV-55) and (IV-56). That is, the procedure is reduced to the two input-two output case of Chapter IV.

A desired phase margin of at least 30 degrees requires that, when $(1/2)D_1(w_2)G_{11}(w_2)$ is 0 db, the corresponding phase angle must be no less than -150 degrees. Figure V-9 shows that the magnitude characteristic for $(1/8)G_{13}(w_2)_4$ is above the magnitude characteristic for $(1/4)G_{12}(w_2)_2$. Hence, the coupling between the first and third channels will be taken to be stronger than the coupling between the first and second channels. Now, if a zero with a break frequency in the w_2 -plane of 7.9×10^{-2} is added to the specification of $D_1(w_2)$, as well as a gain factor of $.997 \times 10^{-2}$, the approximate compensated open-loop transfer function will have a phase margin of approximately 40 degrees at a w_2 -plane frequency of 5×10^{-2} . From the Nichols chart of Figure V-11, the corresponding magnitude of $(1/2)D_1(w_2)G_{11}(w_2)/(1 + (1/2)D_1(w_2)G_{11}(w_2))$ is approximately 3.5 db. At the same frequency, $(1/2)G_{11}(w_2)$ has a magnitude of 13 db, $(1/2)G_{21}(w_2)$ has a magnitude of 0 db, and $(1/8)G_{13}(w_2)_4$ has a magnitude of -1 db. Then, the magnitude of

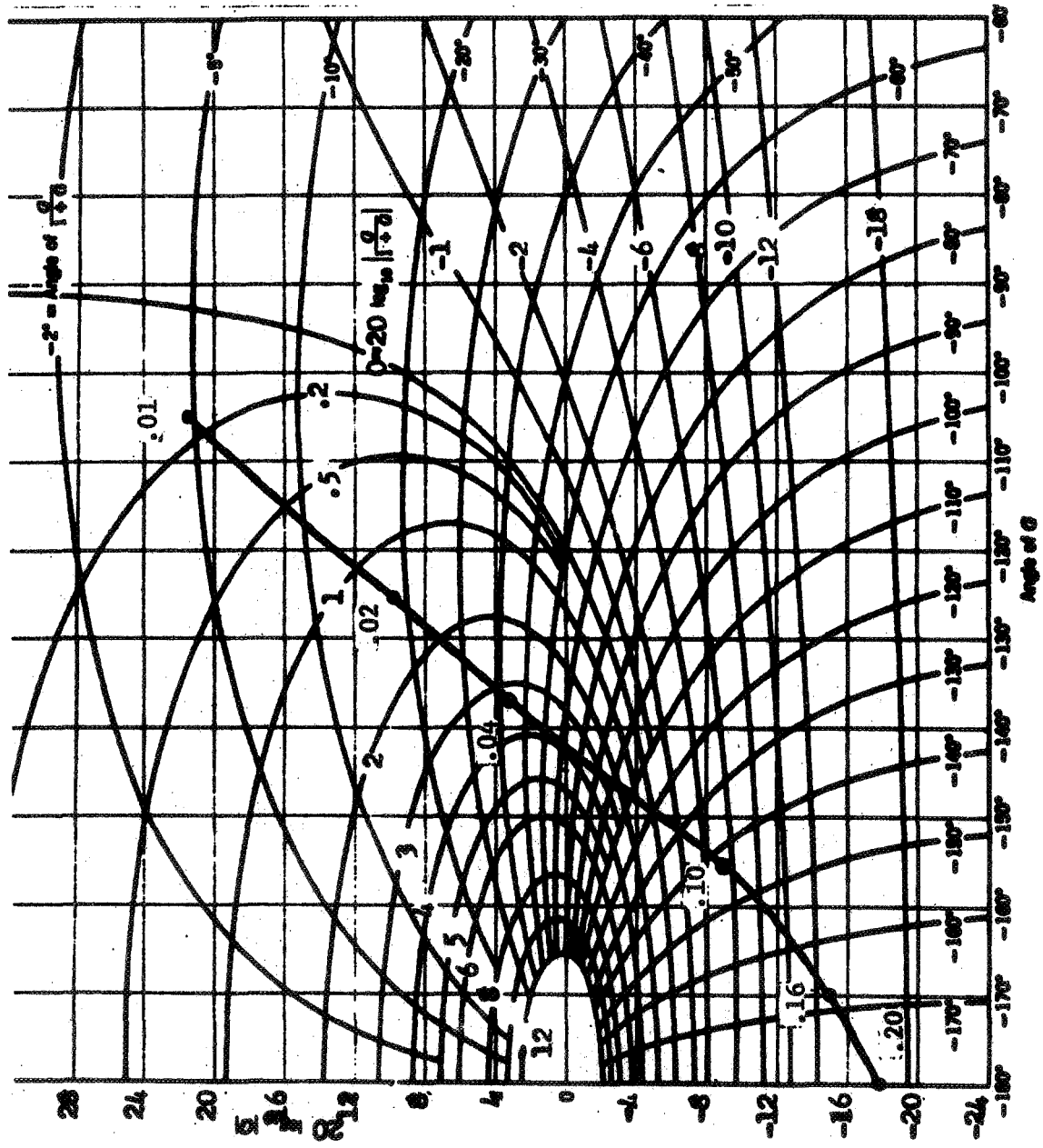


Figure V-11. Nichols chart determination of $(1/2)D_1(w_2)G_{11}(w_2)/(1 + (1/2)D_1(w_2)G_{11}(w_2))$.

$(1/16)D_1(w_2)G_{31}(w_2)G_{13}(w_2)_4 / (1 + (1/2)D_1(w_2)G_{11}(w_2))$ is -10.5 db. Since the magnitude of $(1/8)G_{33}(w_2)_4$ at a w_2 value of .05 is approximately 13 db, (IV-56) is reasonably decoupled at this w_2 -plane frequency.

If a pole with a w_2 -plane break frequency of 7.9×10^{-1} is now added to the specification of $D_1(w_2)$, the approximate open-loop transfer function will achieve a phase shift of -180 degrees at the w_2 -plane frequency of .20, with a magnitude of approximately -18 db. From Figure V-11, the magnitude of $(1/2)D_1(w_2)G_{11}(w_2) / (1 + (1/2)D_1(w_2)G_{11}(w_2))$ is approximately -16 db. For the same w_2 -plane frequency, $(1/2)G_{11}(w_2)$ has a magnitude of 0 db, $(1/2)G_{21}(w_2)$ has a magnitude of -7 db, and $(1/8)G_{13}(w_2)_4$ has a magnitude of -4.5 db. Hence, the magnitude of $(1/16)D_1(w_2)G_{31}(w_2)G_{13}(w_2)_4 / (1 + (1/2)D_1(w_2)G_{11}(w_2))$ is -27.5 db. Compared with the magnitude of approximately .5 db for $(1/8)G_{33}(w_2)_4$ at w_2 equal to .20, (IV-56) is again found to be reasonably decoupled.

The complete specification of $D_1(w_2)$ is then

$$D_1(w_2) = \frac{(.997 \times 10^{-2})(\frac{w_2}{.079} + 1)}{w_2(\frac{w_2}{.79} + 1)} \quad (V-29)$$

This compensation has been tentatively determined to meet the given requirements for gain margin, phase margin, steady-state error, and decoupling for the open-loop transfer function for the first channel. Since the Bode plots of Figures V-7 through V-10 indicate that all the

plant transfer function gain and phase characteristics are relatively close together and the cross-coupling transfer function characteristics are also closely the same, it is expected that the specification of the remaining compensators may be made the same as the specification for $D_1(w_2)$. This is done by specifying a pole at the origin in the w_4 and w_8 -planes for the respective compensators $D_2(w_4)$ and $D_3(w_8)$. The break frequencies for the remaining pole and zero of $D_1(w_2)$ are then transformed to the w_4 -plane for $D_2(w_4)$ and to the w_8 -plane for $D_3(w_8)$. In specifying the compensator $D_1(w_2)$, a phase margin of 40 degrees was achieved at a w_2 -plane frequency of 5×10^{-2} . This w_2 -plane frequency transforms to a w_4 -plane frequency of approximately 2.6×10^{-2} and a w_8 -plane frequency of approximately 1.3×10^{-2} . From Figure V-7, it is observed that a pole at the origin in the w_4 -plane will contribute an additional 5.5 db to the approximate open-loop transfer function above the db gain computed for the w_2 -plane compensation. A pole at the origin in the w_8 -plane contributes an additional 11.5 db. Adjusting the gain factors for each compensator accordingly, the specifications for $D_2(w_4)$ and $D_3(w_8)$ are

$$D_2(w_4) = \frac{(.529 \times 10^{-2}) \left(\frac{w_4}{.039} + 1 \right)}{w_4 \left(\frac{w_4}{.39} + 1 \right)} \quad (V-30)$$

and

$$D_3(w_8) = \frac{(.25 \times 10^{-2}) \left(\frac{w_8}{.02} + 1 \right)}{w_8 \left(\frac{w_8}{.2} + 1 \right)} \quad (V-31)$$

To check the compensation, a frequency response for the compensated system was computed. The results for the first channel are given as a Nyquist diagram in Figure V-12. It is observed that the total compensated open-loop transfer function may be approximated by the $(1/2)D_1(w_2)G_{11}(w_2)$ term. Also, the gain margin is approximately 19 db and the phase margin is approximately 35 degrees.

A digital computer simulation of the system was also run for a unit step forcing function at $r_1(t)$. The results of this simulation are given in Figure V-13. It is observed that $y_1(t)$ is much less oscillatory, with a zero steady-state error. Further, the peak magnitudes of $y_2(t)$ and $y_3(t)$ are .15 and .17, respectively. This is approximately half the uncompensated magnitudes.

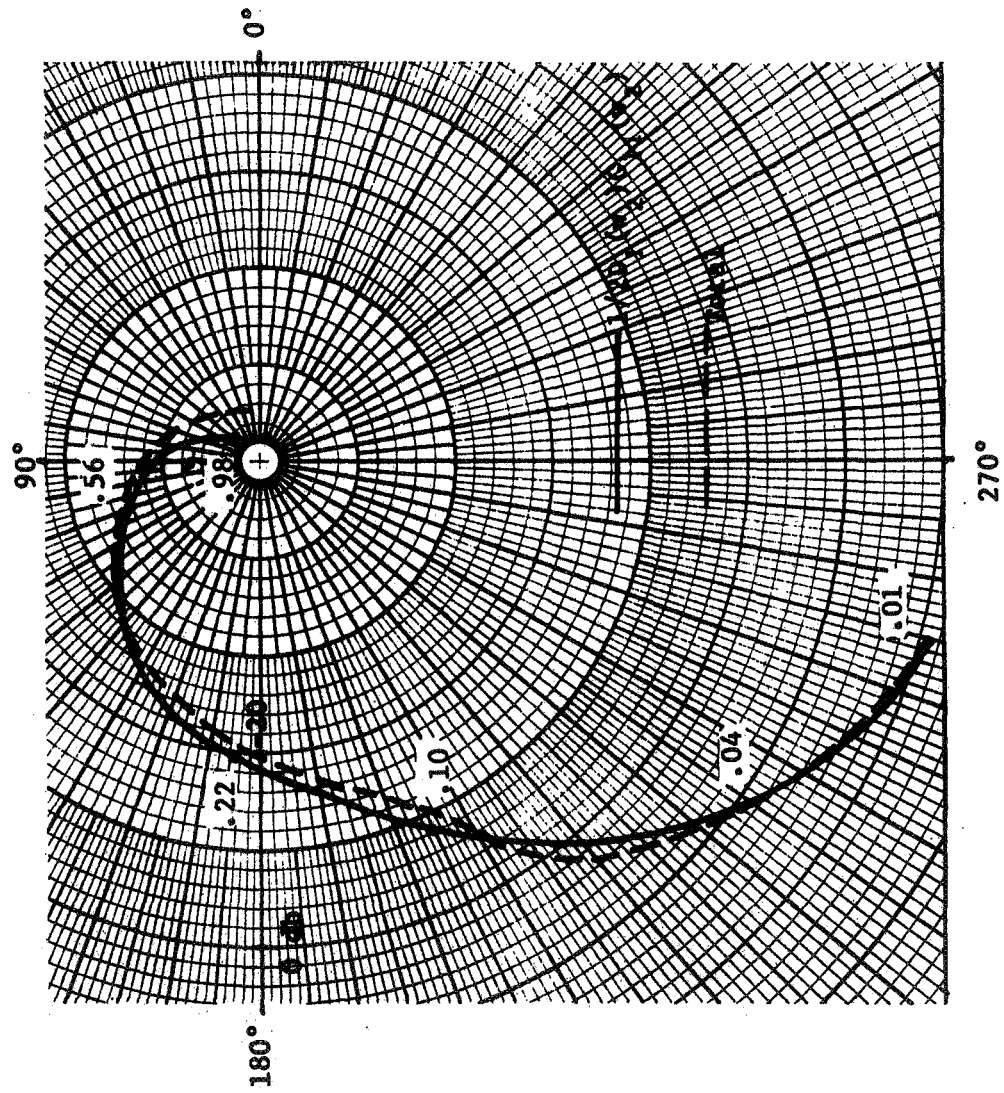


Figure V-12. Compensated Nyquist diagram for $-E_1'(w_2)/E_1(w_2)$.

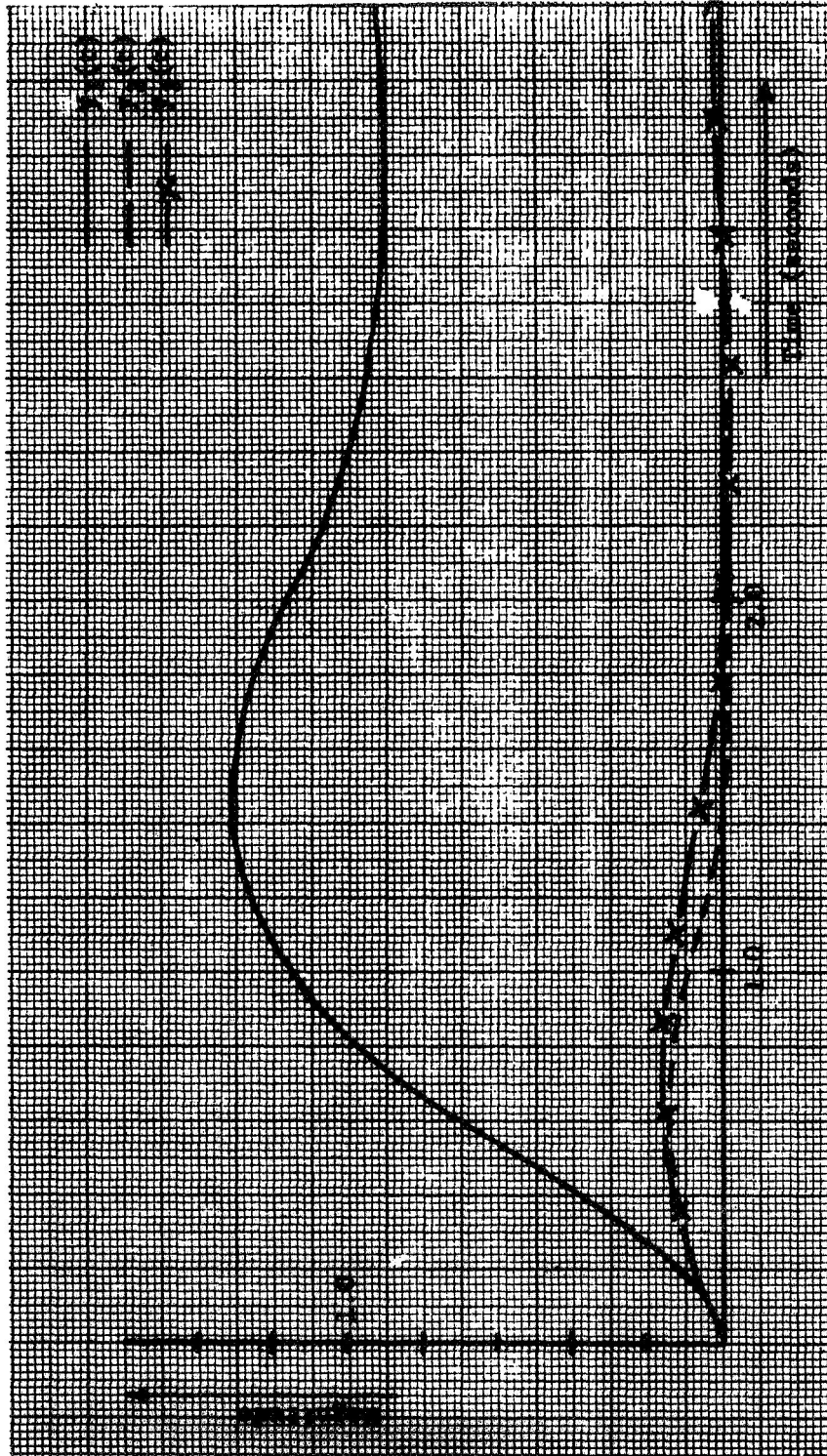


Figure V-13. Compensated system outputs for step input at $r_1(t)$.

VI. CONCLUSIONS

A Bode plot design technique for single loop, linear, multirate sampled-data systems was presented in Chapter III. The basis of this technique is the transformation from the z_n -plane to the w_n -plane. A relationship for writing the w_n -form uncompensated open-loop multirate system transfer function directly was developed. Since application of the Nyquist criterion to this open-loop transfer function requires that one determine the number of poles of the open-loop transfer function which lie in the right half w_n -plane, a procedure was developed by which the number of such poles may be determined directly from the s -domain plant transfer function.

It was then shown that the Bode plot for each term of the n -term summation representing the w_n -form uncompensated open-loop transfer function may be observed directly from the Bode plot for the first term of the summation. This observation led to the development of an upper bound for the choice of the multirate n . This upper bound is based on the effect of the magnitudes of the terms beyond the first term of the uncompensated open-loop transfer function on the magnitude of the total sum. Whereas it was pointed out that the actual effect of these terms depends on the phase angle of each term at any particular value of frequency in the s -plane, it was assumed for the purposes of developing the upper bound that all the terms added directly. Hence, the upper bound

developed may be somewhat conservative in actual practice. The assumption made in applying the upper bound is that the compensated open-loop transfer function will be required to be low-pass with respect to the slow-rate sampling frequency.

It was also shown that the Bode plot for the uncompensated open-loop multirate system transfer function could be obtained directly from the single-rate open-loop transfer function. This is done by merely transforming the w -plane frequencies to the corresponding w_n -plane frequencies. This procedure is facilitated by means of a $\log_{10} \tan(\theta)$ vs. θ template. Combining this procedure with the upper bound criterion, one may begin the analysis of the multirate system by considering the equivalent slow single rate system. The multirate n may be chosen according to the upper bound criterion. The Bode plot for the multirate open-loop transfer function may then be drawn from the Bode plot for the single rate case.

The computation of the multirate system frequency response on the digital computer is then considered. An infinite series s -domain form of the multirate system open-loop transfer function is developed for this purpose. The advantage of the use of this infinite series form is that certain numerical inaccuracies, which may occur when the frequency response is calculated in the z_n -plane, are avoided.

Finally, a multirate system identity is presented which obtains the z_n -form of the z -transform of the product of a multirate signal with a continuous plant s -domain transfer function. This identity is used to

determine the multirate system output for a quantization disturbance at the digital controller output accumulator.

An extension of the method of Povejsil and Fuchs to multirate sampled-data systems was made in Chapter IV. This extension was made first for the three input-three output case for which the fast-rate sampling is the same in each channel. The method was then extended to the case for which the fast-rate sampling may not necessarily be the same in each channel. The various inadequacies of this method as regards multirate sampled-data systems were pointed out.

The open-loop frequency response design technique for multiple input-multiple output systems was then presented. This technique is initially developed for the two input-two output, continuous, linear system. The objective of the technique is to achieve a compensation in the feed forward path of each channel of the system which approximately decouples the system as much as necessary and also, achieves the normal design requirements. It was found that only the open-loop transfer functions for the system opened at the error signal in each channel need be considered. After developing the open-loop technique for the continuous case, an example is presented to illustrate the procedure. It was not the purpose of the example to achieve a best compensation in the practical design sense, but rather, to illustrate the design technique. For this purpose, the results of the example are more than satisfactory.

The open-loop frequency response technique was then extended to the sampled-data multiple input-multiple output system. Initially, the

single rate, two input-two output case was considered. The technique was extended then to the multirate case for which the fast-rate sampling in each channel is unequal, but related by an integer. An example was presented to illustrate the procedure for the multirate case. Again, it was not attempted to achieve a best design. The results of this example again demonstrated the effectiveness of the technique.

The case for systems having more than two inputs and two outputs was developed in Chapter V. In order that the open-loop technique be effective for the general case, it was necessary to develop procedures for obtaining open-loop transfer functions as simply as possible, for determining the open-loop poles which lie outside the unit circle in the multirate z -plane, and for determining the desired compensation. A three input-three output, multirate system for which the fast-rate sampling is unequal in each channel was utilized to illustrate these procedures.

It is felt that the open-loop technique is a very effective design technique for the multiple input-multiple output, multirate sampled-data system, particularly if it is not necessary to exactly decouple the system. Although the technique may be applied to systems having any number of inputs and outputs, it is most effective for the cases of two and three inputs and outputs.

REFERENCES

- [1]. B. C. Kuo, Analysis and Synthesis of Sampled-Data Control Systems, Prentice-Hall, Inc., Englewood Cliffs, N. J., 1963.
- [2]. G. M. Kranc, "Compensation of an Error-Sampled System by a Multirate Controller," Trans. A. I. E. E., Part 2, July, 1957, pp. 149-159.
- [3]. G. M. Kranc, "Input-Output Analysis of Multirate Feedback Systems," Trans. I. R. E., Vol. AC-3, November, 1957, pp. 21-28.
- [4]. R. E. Kalman and J. E. Bertram, "A Unified Approach to the Theory of Sampling Systems," Journal of the Franklin Institute, Vol. 267, No. 5, May, 1959, pp. 403-436.
- [5]. C. L. Phillips and J. C. Johnson, "Design of Multirate Digital Controllers," Proc. Houston Conf. on Circuits, Systems, and Computers, (Houston, Texas), May, 1969.
- [6]. J. B. Knowles and R. Edwards, "A Critical Comparison of Multirate and Single-Rate Digital Control System Performance," Proc. 1969 JACC, pp. 366-375.
- [7]. C. L. Phillips, "A Note on the Frequency-Response Design Technique for Multirate Digital Controllers," Transactions on Automatic Control, Vol. AC-15, April, 1970, pp. 263-264.
- [8]. C. L. Phillips, et. al., Digital Compensation of the Thrust Vector Control System, Sixth Technical Report, NAS8-11274, Engineering Experiment Station, Auburn, Alabama, September, 1966.
- [9]. C. L. Phillips, et. al., Digital Compensation of the Thrust Vector Control System, Seventh Technical Report, NAS8-11274, Engineering Experiment Station, Auburn, Alabama, January, 1967.
- [10]. D. B. Newman, "The Analysis of Cross-Coupling Effects on the Stability of Two-Dimensional, Orthogonal, Feedback Control Systems," Transactions on Automatic Control, Vol. AC-5, September, 1960, pp. 314-320.
- [11]. D. J. Povejsil and A. M. Fuchs, "A Method for the Preliminary Synthesis of Complex Multiloop Control Systems," Trans. A. I. E. E., Part 2, Vol. 74, July, 1955, pp. 129-134.

- [12]. K. Chen, R. A. Mathias, and D. M. Sauter, "Design of Noninteracting Control Systems Using Bode Diagrams," Trans. A. I. E. E., Applications and Industry, Vol. 80, No. 58, January, 1962, pp. 336-346.
- [13]. P. L. Falb and W. A. Wolovich, "Decoupling in the Design and Synthesis of Multivariable Control Systems," Transactions on Automatic Control, Vol. AC-12, December, 1967, pp. 651-659.
- [14]. E. G. Gilbert, "The Decoupling of Multivariable Systems by State Feedback," SIAM J. Contr., Vol. 7, February, 1969, pp. 50-63.
- [15]. W. M. Wonham and A. S. Morse, "Decoupling and Pole Assignment in Linear Multivariable Systems: A Geometric Approach," SIAM J. Contr., Vol. 8, February, 1970, pp. 1-18.
- [16]. R. C. Dorf, Modern Control Systems, Addison-Wesley Publishing Company, Reading, Massachusetts, 1967.
- [17]. C. L. Phillips, et. al., Digital-Compensation of the Thrust Vector Control System, Fourth Technical Report, NAS8-11274, Engineering Experiment Station, Auburn, Alabama.

APPENDIX A
MULTIRATE SYSTEM FREQUENCY RESPONSE

```

C
C      MULTIRATE SYSTEM FREQUENCY-RESPONSE BY INFINITE SUM
C
      READ(5,30)Q1,Q2,Q3,Q4,Q6,Q7,Q8,Q9,Q10
30  FORMAT(9F6.0)
      PRINT 5,Q1,Q2,Q3,Q4,Q6,Q7,Q8,Q9,Q10
      5  FORMAT(9F6.0)
66  FORMAT(1H1,4X,30HFREQUENCY RESPONSE OUTPUT DATA///7X,
1   4HOMEG,9X,6HABSVAL,12X,2HDB,11X,5HPHASE,14X,1HW,/)
      PRINT 66
      COMPLEX TF,S,ANUM,DEN,HOL,TOTAL,G2,S1,Z,GCOMP,AN,
1   AD,XG,G(4),ZN,S2
      PI=3.1415927
      AK1=10.
      TS=.1
      N=3
      XN=N
      OMEG=.005
99  OMBGS=2.0*3.1415927/TS
4   NTILT=2
      NX=2*NTILT+1
C
C      DO-LOOP TO SUM ON P
C
      DO 60 I=1,N
      TF=CMPLX(0.0,0.0)
      P=I-1
      XP=P
C
C      DO-LOOP TO SUM ON J
C
      DO 24 J=1,NX
      XJ=-NTILT+J-1
      OMEG1=OMEG*(XN*XJ+XP)*OMEGS
      S=CMPLX(0.0,OMEG1)
      ANUM=(Q1*S+1.)*(Q2*S**2+Q3*S+Q4)
      DEN=(Q6*S+1.)*(Q7*S+1.)*(Q8*S**2+Q9*S+Q10)
      HOL=(1.-CEXP(-TS*S/XN))/S
      TOTAL=XN/TS*HOL*ANUM/DEN
24  TF=TF+TOTAL
60  G(I)=TF/XN
      L=N+1
      G(L)=CMPLX(0.0,0.0)
C
C      DO-LOOP TO COMPUTE TOTAL TRANSFER FUNCTION
C
      DO 70 K=1,N
70  G(L)=G(L)*G(K)
      K=1
65  XG=G(K)
      ABSV=CABS(XG)
      DB=20.*ALOG10(ABSV)

```

```
PHASE=57.29578*ATAN2(AIMAG(XG),REAL(XG))
THETA=TS*OMEG
WN=SIN(THETA/N)/(1.+COS(THETA/N))
PRINT25,OMEG,ABSV,DB,PHASE,WN
25 FORMAT(5X,F9.5,2X,E13.8,6X,F9.3,6X,F9.3,6X,F10.6)
IF(K.EQ.L)GO TO 81
K=L
GO TO 65
81 CONTINUE
EXIT=N*OMEGS/2.
DEL=EXIT/100.
OMEG=OMEG+DEL
IF(OMEG-EXIT)4,4,7
7 STOP
END
```

APPENDIX B
TWO INPUT-TWO OUTPUT, CONTINUOUS
SYSTEM FREQUENCY RESPONSE

```

C
C      TWO INPUT-TWO OUTPUT, CONTINUOUS SYSTEM FREQUENCY RESPONSE
C
      PRINT 66
66  FORMAT(1H1,4X,8HG11 GAIN,5X,9HG11 PHASE,6X,7HG2 GAIN,6X,
      18HG2 PHASE,6X,6HG GAIN, 7X,7HG PHASE,6X,7HG3 GAIN,
      1 5X,8HG3 PHASE,5X,5HOMEGA)
      COMPLEX G,S,CMLPX,G11,G22,G12,G21,E11,E22,G2,G,G3
      OMEG=0.0
      DO 300 I=1,301

C
C      COMPUTE FEED-FORWARD AND CROSS-COUPLING ELEMENTS
C
      S=CMLPX(0.0,OMEG)
      G11=4.*(S/8.+1.)*(1.-S/8.)/(1.(S/10.)*2+0.1*S/10.+1.)
      G22=G11
      G12=1./(S/10.+1.)
      G21=G12
      E11=1./(S*(S/1.5+1.))
      E22=E11

C
C      COMPUTE 2ND TERM FOR EACH OPEN-LOOP TRANSFER FUNCTION
C
      G2=E22*G12*G21/(1.+E22*G22)

C
C      COMPUTE TOTAL OPEN-LOOP FREQUENCY RESPONSE
C
      G=E11*(G11-G2)
      G3=G11*E11
      DB1=20.*ALOG10(CABS(G11))
      PHASE1=180./3.141590*ATAN2(AIMAG(G11),REAL(G11))
      DB2=20.*ALOG10(CABS(G2))
      PHASE2=180./3.141590*ATAN2(AIMAG(G2),REAL(G2))
      DB3=20.*ALOG10(CABS(G))
      PHASE3=180./3.141590*ATAN2(AIMAG(G),REAL(G))
      DB4=20.*ALOG10(CABS(G3))
      PHASE4=180./3.141590*ATAN2(AIMAG(G3),REAL(G3))
      PRINT 5,DB1,PHASE1,DB2,PHASE2,DB3,PHASE3,DB4,PHASE4,OMEG
5  FORMAT(2X,E12.5,2X,F11.5,2X,E12.5,2X,F11.5,2X,E12.5,
      1 2X,F11.5,2X,E12.5,2X,F11.5,2X,F6.2)
300 OMEG=OMEG+0.100
      STOP
      END

```

APPENDIX C
TWO INPUT-TWO OUTPUT CONTINUOUS
SYSTEM SIMULATION


```

C
C      SIMULATION OF TWO INPUT-TWO OUTPUT SYSTEM WITH CONTINUOUS
C      COMPENSATORS
C
C      DEFINE MACRO FOR PLANT TRANSFER FUNCTION
C
MACRO  Z1=PLANT(K2,C,D,X1)
      S2X=D*(X1-X)-SX
      SX=INTGRL(0.0,S2X)
      X=INTGRL(0.0,SX)
      Z1=K2*(-1./C*S2X+X)
ENDMAC
C
C      DEFINE MACRO FOR CROSS-COUPLING TRANSFER FUNCTION
C
MACRO  W1=CROSS(B,X1)
      SW1=B*(X1-W1)
      W1=INTGRL(0.0,SW1)
ENDMAC
C
C      DEFINE MACRO FOR CONTINUOUS COMPENSATION
C
MACRO  X1=GCOMP(K1,A,E1)
      S2X1=K1*E1-A*SX1
      SX1=INTGRL(0.0,S2X1)
      X1=INTGRL(0.0,SX1)
ENDMAC
PARAMETER A=1.5,B=10.,C=64.,D=100.,K1=1.5,K2=4.,K=2.
C
C      DEFINE CHANNEL ONE
C
      R1=STEP(0.)
      E1=K*(R1-Y1)
      X1=GCOMP(K1,A,E1)
      Z1=PLANT(K2,C,D,X1)
      W1=CROSS(B,X1)
C
C      DEFINE CHANNEL TWO
C
      R2=0.
      E2=R2-Y2
      X2=GCOMP(K1,A,E2)
      Z2=PLANT(K2,C,D,X2)
      W2=CROSS(B,X2)
      Y1=Z1+W2

```

141

```
      Y2=72+W1  
TIMER FINTIM=15.,OUTDEL=.1  
PRTPLT Y1(Y2)  
      PRTPLT Y2(Y1)  
END  
      R1=0.0  
      R2=STEP(0. )  
END  
STOP  
ENDJOB
```

APPENDIX D
THREE INPUT-THREE OUTPUT MULTIRATE
SYSTEM FREQUENCY-RESPONSE

C
C
C

THREE INPUT-THREE OUTPUT MULTIRATE SYSTEM FREQ RESPONSE

COMPLEX G5,G6,G7,G8,G9,G10,GA,GB,GC,GD,GE,GF,

1 G1,G2,G3

PI = 3.1415927

TS = .1

OMEG=.005

N1=2

N2=4

N3=8

NA=N1+1

NB=N2+1

NC=N3+1

OMEGS=(PI/TS)*2.

Q1=10.

Q2=4.

Q3=15.

Q4=12.

Q5=6.

XA=.8535

XK=.06009

XB=.117

YA=.9249

YK=.03950

YB=.4388

ZA=.96078

ZK=.02124

ZB=.66667

4 NTILT=1

C
C
C
CCOMPUTE FREQ RES FOR FEED FWD AND CROSS-COUPPLING
ELEMENTS FOR CHANNEL ONE

CALL FRES(N1,Q1,Q2,NTILT,OMEG,OMEGS,TS,PI,NA,XA,XK,XB,

1 DB1,PHASE1,DB2,PHASE2,DB3,PHASE3,DB4,PHASE4,WN1,

1 GA,GB)

PRINT25,OMEG,DB1,PHASE1,DB2,PHASE2,DB3,PHASE3,DB4,

1 PHASE4,WN1

25 FORMAT(1H0,2X,5HOMEG=,F7.3,4X,4HGI1=,E9.3,4X,F8.3,

1 4X,E9.3,4X,F8.3,2X,4HGI2=,E9.3,4X,F8.3,4X,E9.3,2X,

1 F8.3,2X,F7.3)

C
C
C
CCOMPUTE FREQ RES FOR FEED FWD AND CROSS-COUPPLING
ELEMENTS FOR CHANNEL TWO

CALL FRES(N2,Q3,Q2,NTILT,OMEG,OMEGS,TS,PI,NB,YA,YK,YB,

1 DB5,PHASE5,DB6,PHASE6,DB7,PHASE7,DB8,PHASE8,WN2,GC,GD)

PRINT35,OMEG,DB5,PHASE5,DB6,PHASE6,DB7,PHASE7,DB8,

1 PHASE8,WN2

35 FORMAT(3X,5HOMEG=,F7.3,4X,4HGI22=,E9.3,4X,F8.3,4X,E9.3,

1 4X,F8.3,2X,4HGI12=,E9.3,4X,F8.3,4X,E9.3,2X,F8.3,2X,F7.3)

C
C
C
C

CCMPUTE FREQ RES FOR FEED FWD AND CROSS-COUPPLING
ELEMENTS FOR CHANNEL THREE

CALL FBRES(N3,Q4,Q5,NTILT,CMEG,CMEGS,TS,PI,NC,ZA,ZK,ZB,
1 DB9,PHASE9,DB10,PHAS10,DB11,PHAS11,DB12,PHAS12,WN3,
1 GE,GF)
PRINT 65,OMEG,DB9,PHASE9,DB10,PHAS10,DB11,PHAS11,DB12,
1 PHAS12,WN3
65 FORMAT(3X,4+OMEG,F7.3,4X,4HG33=,E9.3,4X,F8.3,4X,E9.3,
14X,F8.3,2X,4HG13=,E9.3,4X,F8.3,4X,E9.3,2X,F8.3,2X,F7.3)

C
C
C
C

CCMPUTE 2ND TERM FOR EACH OPEN-LOOP TRANSFER FUNCTION

G5=(GB*GC*(1+GE)-2.*(GB*GC*GF+GB*GF*(1+GC)))/((1+GC)*
1 (1+GE)-GD*GF)
G6=(GD*GB*(1+GE)-2.*GD*GB*GF+GC*GF*(1+GA))/((1+GA)*
1 (1+GE)-GB*GF)
G7=(GF*GC*(1+GA)-2.*GF*GD*GB+GF*GB*(1+GC))/((1+GA)*
1 (1+GC)-GB*GC)

C
C
C

COMPUTE TOTAL OPEN-LOOP TRANSFER FUNCTIONS

G8=GA-G5
G9=GC-G6
G10=GE-G7

C
C
C

CCMPUTE DENOMINATOR FREQUENCY-RESPONSE

G1=-GC*GF/(1+GC)*(1+GE)
G2=-GB*GF/(1+GA)*(1+GE)
G3=-GB*GC/(1+GA)*(1+GC)
CBA=20.*ALOG10(CABS(G1))
PHASEA=57.29578*ATAN2(AIMAG(G1),REAL(G1))
CBB=20.*ALOG10(CABS(G2))
PHASEB=57.29578*ATAN2(AIMAG(G2),REAL(G2))
CBC=20.*ALOG10(CABS(G3))
PHASEC=57.29578*ATAN2(AIMAG(G3),REAL(G3))
CDB=20.*ALOG10(CABS(G8))
PHASED=57.29578*ATAN2(AIMAG(G8),REAL(G8))
CDE=20.*ALOG10(CABS(G9))
PHASEE=57.29578*ATAN2(AIMAG(G9),REAL(G9))
CDB=20.*ALOG10(CABS(G10))
PHASEF=57.29578*ATAN2(AIMAG(G10),REAL(G10))
PRINT 45,OMEG,CBA,PHASEA,CBB,PHASEB,CBC,PHASEC,
1 CBN,CBN2,WN3
45 FORMAT(3X,5+OMEG=,F7.3,2X,3HG1=,E9.3,2X,F8.3,2X,
1 3HG2=,E9.3,2X,F8.3,2X,3+G3=,E9.3,2X,F8.3,2X,
1 4+WN1=,E7.3,2X,4+WN2=,F7.3,2X,4+WN3=,F7.3)
PRINT 55,OMEG,CDB,PHASED,CDE,PHASEE,CDBF,PHASEF,WN1,
1 WN2,WN3
55 FORMAT(3X,5+OMEG=,F7.3,2X,3+G8=,E9.3,2X,F8.3,2X,

```

1 3HG9=,E9.3,2X,F8.3,2X,4F610=,E9.3,2X,F8.3,2X,4HWN1=,
1 F7.3,2X,4HWN2=,F7.3,2X,4HWN3=,F7.3)
EXIT=OMEGS/2.
CEL=EXIT/100.
CMEG=CMEG+DEL
IF(OMEG-EXIT)4,4,7
7 STOP
END
SUBROUTINE FRES(N1,C1,C2,NTILT,OMEG,OMEGS,TS,PI,N,XA,
1 XM,XB,CB1,PHASE1,CB2,PHASE2,CB3,PHASE3,CB4,PHASE4,
1 WN1,GA,GB)
COMPLEX G11,G21,S,G11P,G21P,HOL,T1,T2,S1,S2,ZN1,AN,
1 AD,C1,F1,G1(9),G2(9),A,B,GA,GB
NX = 2*NTILT+1
XN=NI
DO 60 I = 1,N1
G11 = CMPLX(0.,0.)
G21 = CMPLX(0.,0.)
P = I-1
XP=P
DO 24 J = 1,NX
XJ = -NTILT+J-1
CMEG1=CMEG+(XN*XJ+XP)*OMEGS
S = CMPLX(0.,OMEG1)
G11P=1C./(&S+1.)*(S/C1+1.)
G21P=1./(&S/C2+1.)
A=-TS*S/XN
B=CEXP(A)
FOR=(1.-B)/S
T1 = N1/TS+HCL*G11P
T2 = N1/TS+HCL*G21P
G11 = G11+T1
24 G21 = G21+T2
S1 = CMPLX(0.,OMEG)
PSI=2I*XP*PI/XN
S2 = CMPLX(0.,PSI)
ZN1=CEXP(S1+TS/XN+S2)
AN=XK*(ZN1+1.)*(ZN1-XA)
AD=4ZN1-1.)*(ZN1-XB)
C1 = AN/AD
F1 = CMPLX(0.,0.)
DO 40 P = 1,N1
40 F1 = H1+ZN1**(-M+1)
G11 = G11+D1*H1
G21=G21+C1*F1
G1(9)=G11/XN
60 G2(9)=G21/XN
L = NI+1
G1(L) = CMPLX(0.,0.)
G2(L) = CMPLX(0.,0.)
DO 70 K = 1,N1
G1(L) = G1(L)+G1(K)

```

```
70 G2(L) = G2(L)+G2(K)
   GA=G1(L)
   GB=G2(L)
   DB1 = 20.*ALOG10(CABS(G1(1)))
   PHASE1 = 57.29578*ATAN2(AIMAG(G1(1)),REAL(G1(1)))
   DB2 = 20.*ALOG10(CABS(G1(L)))
   PHASE2 = 57.29578*ATAN2(AIMAG(G1(L)),REAL(G1(L)))
   DB3 = 20.*ALOG10(CABS(G2(1)))
   PHASE3 = 57.29578*ATAN2(AIMAG(G2(1)),REAL(G2(1)))
   DB4 = 20.*ALOG10(CABS(G2(L)))
   PHASE4 = 57.29578*ATAN2(AIMAG(G2(L)),REAL(G2(L)))
   THETA = TS*OMEG
   WN1 = SIN(THETA/N1)/(1.+COS(THETA/N1))
   RETURN
   END
```

APPENDIX E
THREE INPUT-THREE OUTPUT MULTIRATE
SYSTEM SIMULATION


```

C
C   SIMULATION FOR THREE INPUT-THREE OUTPUT SYSTEM WITH DIGITAL
C   COMPENSATORS
C
C   DEFINE MACRO FOR PLANT TRANSFER FUNCTION
C
MACRO Z1=PLANT(K2,C,D,C1)
      Z2DOT=-C*ZDOT-D*Z+K2*D*C1
      ZDOT=INTGRL(0.,Z2DOT)
      Z=INTGRL(0.,ZDOT)
      Z1=Z
ENDMAC
C
C   DEFINE MACRO FOR CROSS-COUPLING TRANSFER FUNCTION
C
MACRO W1=CROSS(B,X1)
      SW1=B*(X1-W1)
      W1=INTGRL(0.0,SW1)
ENDMAC
C
C   DEFINE MACRO FOR Z-FORM DIGITAL COMPENSATION
C
MACRO B1,S1,X1=DCOMP(F1,G1,G2,A,B,S1,X1,X,YK,XK,TA)
      U1=X+F1*S1
      V1=YK*(G1*U1+G2*S1)
      S1=DELAY(1,TA,U1)
      T1=V1+B*X1
      B1=XK*(T1+A*X1)
      X1=DELAY(1,TA,T1)
ENDMAC
PARAMETER C=11.,D=10.,E=4.,F=16.,G=15.,P=13.,Q=12.,R=6.,...
          X1=0.,T=.1,N1=2,N2=4,K1=10.,K2=10.,K3=10.,K4=1.,X2=0.,...
          S1=0.,S2=0.,XK=.06009,A=1.,B=1.,YK=1.,F1=.117,G1=1.,...
          G2=-.8535,H=1.,HK=.039507,S3=0.,N3=8,X3=0.,S=1.,...
          SK=.021247,F2=.4388,F3=.66667,G3=-.9249,G4=-.96078
C
C   DEFINE CHANNEL ONE
C
      R1=STEP(0.)
      E1=R1-Y1
      E1Z=IMPULS(0.,T)
      A1=ZHOLD(E1Z,E1)
      X=A1
      TA=T/N1
NOSORT
      B1,S1,X1=DCOMP(F1,G1,G2,A,B,S1,X1,X,YK,XK,TA)
SORT
      R1Z=IMPULS(0.,T/N1)
      C1=ZHOLD(R1Z,R1)
      Z1=PLANT(K1,C,D,C1)
      W1=CROSS(E,C1)

```

```

C
C   DEFINE CHANNEL TWO
C
      R2=0.
      E2=R2-Y2
      E2Z=IMPULS(0.,T)
      A2=ZHOLD(E2Z,E2)
      Y=A2
      TB=T/N2
NOSORT      B2,S2,X2=DCOMP(F1,G1,G3,A,H,S2,X2,Y,YK,HK,TB)
SORT
      B2Z=IMPULS(0.,T/N2)
      C2=ZHOLD(B2Z,B2)
      Z2=PLANT(K3,P,Q,C2)
      W2=CROSS(E,C2)
C
C   DEFINE CHANNEL THREE
C
      R3=0.
      E3=R3-Y3
      E3Z=IMPULS(0.,T)
      A3=ZHOLD(E3Z,E3)
      Z=A3
      TC=T/N3
NOSORT      B3,S3,X3 =DCOMP(F1,G1,G4,A,S,S3,X3,Z,YK,SK,TC)
SORT
      B3Z=IMPULS(0.,T/N3)
      C3=ZHOLD(B3Z,B3)
      Z3=PLANT(K3,P,Q,C3)
      W3=CROSS(R,C3)
      Y1=Z1+W2+W3
      Y2=Z2+W1+W3
      Y3=Z3+W1+W2
TIMER DELT=.0125,FINTIM=7.,OUTDEL=.0125
METHOD RKSFX
PRTPLT Y1(X,X1,B1),Y2(Y,X2,B2),Y3(7,X3,B3)
END
STOP
ENDJOB

```

APPENDIX F
THREE INPUT-THREE OUTPUT OPEN-
LOOP TRANSFER FUNCTION

Appendix F

In this appendix, the open-loop transfer function which was developed in Chapter V for the three input-three output system will also be developed by direct application of Mason's gain formula to the discrete signal flow graph for the system opened at the error sampler in the first channel. This signal flow graph is given in Figure F-1.

The following set of feed-forward paths may be written from the signal flow graph:

$$P_1 = E_1 - Z_1 - Y_1 - E_1' \quad , \quad (F-1)$$

$$P_2 = E_1 - W_3 - Y_2 - E_2 - W_1 - Y_1 - E_1' \quad , \quad (F-2)$$

$$P_3 = E_1 - W_3 - Y_2 - E_2 - W_5 - Y_3 - E_3 - W_6 - Y_1 - E_1' \quad , \quad (F-3)$$

$$P_4 = E_1 - W_2 - Y_3 - E_3 - W_4 - Y_2 - E_2 - W_1 - Y_1 - E_1' \quad , \quad (F-4)$$

$$P_5 = E_1 - W_2 - Y_3 - E_3 - W_6 - Y_1 - E_1' \quad . \quad (F-5)$$

The following set of closed loops are also obtained from the signal flow graph:

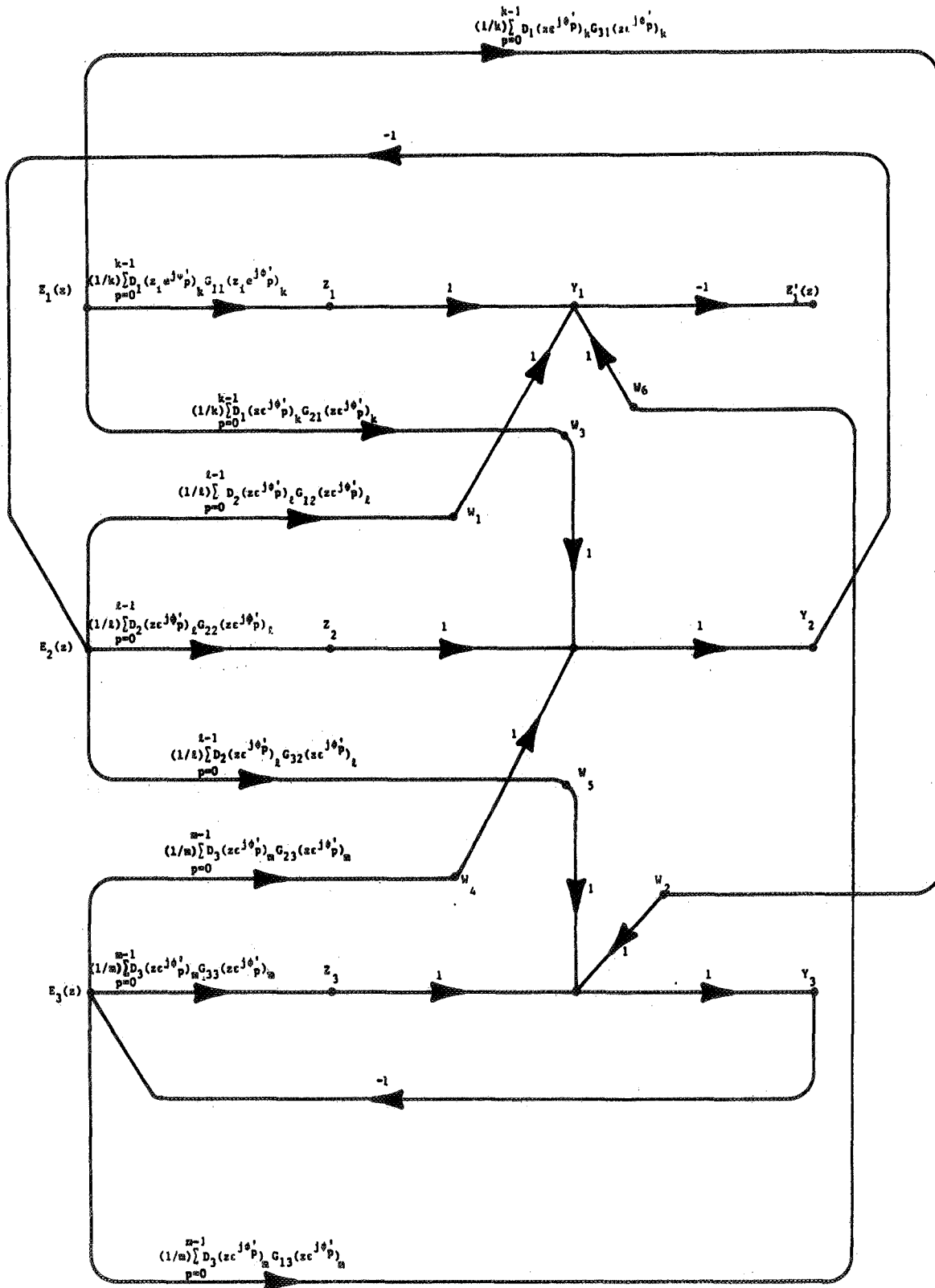


Figure F-1. Signal flow graph for three input-
Three Output System opened at $E_1(z)$.

$$L_1 = E_2 - Z_2 - Y_2 - E_2 \quad , \quad (F-6)$$

$$L_2 = E_3 - Z_3 - Y_3 - E_3 \quad , \quad (F-7)$$

$$L_3 = E_2 - W_5 - Y_3 - E_3 - W_4 - Y_2 - E_2 \quad , \quad (F-8)$$

where L_1 and L_2 are non-touching loops. The cofactors, Δ_i , for each of the above paths are obtained by eliminating the signal flow graph nodes which touch on the path under consideration, determining the remaining loops, and applying Mason's determinant formula [16]. The cofactors are:

$$\Delta_1 = 1 - (L_1 + L_2 + L_3) + L_1 \cdot L_2 \quad (F-9)$$

$$\Delta_2 = 1 - L_2 \quad , \quad (F-10)$$

$$\Delta_3 = \Delta_4 = 1 \quad , \quad (F-11)$$

$$\Delta_5 = 1 - L_1 \quad . \quad (F-12)$$

The system determinant is

$$\Delta = 1 - (L_1 + L_2 + L_3) + L_1 \cdot L_2 \quad (F-13)$$

The total open-loop transfer function may then be written

$$\frac{E_1'(z)}{E_1(z)} = - \frac{(P_1 \Delta_1 + P_2 \Delta_2 + P_3 \Delta_3 + P_4 \Delta_4 + P_5 \Delta_5)}{\Delta} \quad (F-14)$$

If it is assumed that the system is low-pass with respect to the slow-rate sampling frequency, we may write

$$\begin{aligned} \frac{E_1'(z)}{E_1(z)} = & (1/k) D_1(z)_k G_{11}(z)_k \\ & - \left\{ (1/k) D_1(z)_k G_{21}(z)_k \cdot (1/l) D_2(z)_l G_{12}(z)_l \right. \\ & \cdot (1 + (1/m) D_3(z)_m G_{33}(z)_m) + (1/k) D_1(z)_k G_{31}(z)_k \\ & \cdot (1/m) D_3(z)_m G_{13}(z)_m \cdot (1 + (1/l) D_2(z)_l G_{22}(z)_l) \\ & - (1/k) D_1(z)_k G_{21}(z)_k \cdot (1/l) D_2(z)_l G_{32}(z)_l \\ & \cdot (1/m) D_3(z)_m G_{13}(z)_m - (1/k) D_1(z)_k G_{31}(z)_k \\ & \left. \cdot (1/m) D_3(z)_m G_{23}(z)_m \cdot (1/l) D_2(z)_l G_{12}(z)_l \right\} \\ & \Delta \end{aligned} \quad (F-15)$$

where

$$\Delta = (1 + (1/l)D_2(z)_l G_{22}(z)_l) \cdot (1 + (1/m)D_3(z)_m G_{33}(z)_m) \\ - (1/l)D_2(z)_l G_{32}(z)_l \cdot (1/m)D_3(z)_m G_{23}(z)_m \quad . \quad (F-16)$$